Leibniz Institut
für Naturstoff-Forschung und Infektionsbiologie
Hans-Knöll-Institut

Hyperspectral imaging using intracellular spies: quantitative real-time measurement of intracellular parameters *in vivo* during host-pathogen interaction

Dissertation

to fulfill the requirements for the degree of

„Doctor rerum naturalium" (Dr. rer. nat.)

Submitted to the Council of the Faculty of Biology and Pharmacy of the Friedrich Schiller University Jena

MSc. Cell and Molecular Biology,
MSc. Microbiology
Sara Mohebbi
Born on 25.11.1982, Tehran

Reviewers

Prof. Dr. Hans-Peter Saluz (intern)
Friedrich Schiller University Jena and Leibniz Institute for Natural Product Research and Infection Biology, Department of Cell and Molecular Biology, Jena, Germany

Prof. Dr. Peter Zipfel (intern)
Friedrich Schiller University Jena and Leibniz Institute for Natural Product Research and Infection Biology, Department of Infection Biology, Jena, Germany

Prof. Dr. Maria D´Erme (extern)
Sapienza University, Department of Biochemical Sciences, Rome, Italy

Date of defense

26.09.2016

دل گرچه درین بادیه بسیار شتاف
یک موی ندانست ولی موی‌شکافت
اندر دلِ من هزارخورشید بتافت
آخر به کمالِ ذرّه‌ای راه نیافت
ابن سینا
ه.ش ۴۱۶ـ ۳۵۹

Although my senses were searching the desert fatiguelessly;
discovering nothing although finding a lot;
my soul was illuminated by a thousand suns;
but could never ever touch the perfection of a single atom.

Avicenna, c.980 –1037, Iran.

To my parents

Table of Contents

1 Summary

Through the interactions between host cell and infectious particles, programmed death of the host is one of the events that depends on the infection condition can be modulated via different mechanisms. The ubiquitous fungus *Aspergillus fumigatus*; an important opportunistic human fungal pathogen, is a widespread microorganism that based on the host's immune deficiency can cause variety of diseases, from respiratory allergic reactions to invasive aspergillosis and even death. The organism has been appeared to be capable of manipulating the host's immune system by either induction or inhibition of apoptosis. This ability seems to be related to the morphology of fungus that can change the fate of host cell. Nevertheless, still yet there are many unknown facts and elusive details about the mechanism behind that makes the necessity for further analysis and creating the alternative methods of investigation.

Hyperspectral imaging is a technique based on combining the classical spectroscopy and conventional digital image processing. It offers very powerful means for real-time measurements from various data points within one and the same sample. Initially, hyperspectral imaging was established for remote sensing satellites and geospatial analysis. Recently, it has been applied in food-processing, cancer diagnostics, astronomy, chemical science and biology. The technique is also well-suited for the quantitative real-time analysis of mixed overlapping fluorescence signals transmitted from several sources within one sample. Therefore, in the framework of pathogen-host cell interaction studies, a modified commercial fluorescence microscope equipped with hyperspectral imaging technology was applied and adopted to perform the kinetic studies of several intracellular, infection-related events in parallel, like the measurement of pH in phagolysosome and cytosol, apoptosis or cell death in response to *Aspergillus fumigatus* infection.
Using an improved HSI construction, the assays were conducted to track the real-time emission of different fluorescent dyes in a single living cell upon infection.
The labeled microorganisms including fungal conidia as intracellular "spies" were used to record the cell events during apoptosis upon infection. Remarkably, it was observed that the ability of melanin to modulate the apoptosis fate was directly linked to its capability of inhibiting the intra-cellular acidification and modulation the acidic pH. By comparing different species of *Aspergillus* and its mutant strains, it is shown that this property is not only

limited to *A.fumigatus*, but it also exists in the species which contain DHN-melanin i.e. *Aspergillus clavatus* and Δ*abr2* mutant.
The intracellular pH post-infection and during apoptosis was quantified and the pattern of intracellular pH changes upon infection was determined.
Additionally, in the single cell level, some different fungal (i.e. *Aspergillus clavatus*, *Aspergillus flavus* and *Lichtheimia brasiliensis*) were examined to evaluate the controls.
The presented data were highly reproducible and the statistical analysis show identical results.
The outcome would be versatile opportunities to benefit novel pharmaceuticals cell therapies i.e. in non-invasive therapeutic approaches and scheming fate of apoptosis in tumor treatments. The state of art modifications of HSI method has made it applicable as an alternative detection technique, compatible for the single cell analysis.

2 Zusammenfassung

Durch die Wechselwirkung der Wirtszelle und der infektiösen Partikel hebt sich der programmierte Zelltod als der Vorgang, der basierend auf der Infektionsart durch unterschiedliche Mechanismen angepasst werden kann, hervor. *Aspergillus fumigatus* ist ein ubiquitär vorkommender Schimmelpilz, wichtiger opportunistischer humanpathogener Pilz. Dieser weitverbreitete Mikroorganismus kann je nach Immunschwäche des Wirts eine Vielfalt von Erkrankungen verursachen, wie Atemwegserkrankungen, allergische Reaktionen, invasive Aspergillose und sogar Tod. Der Organismus scheint in der Lage zu sein, das Immunsystem des Wirts durch entweder Induktion oder Inhibierung der Apoptose zu manipulieren. Diese Fähigkeit scheint mit der Morphologie des Pilzes zusammenzuhängen, die das Schicksal der Wirtszelle beeinflussen kann. Dennoch gibt es viele unbekannte Faktoren und schwer fassbare Details bezüglich dieser Mechanismen, so dass weitere Analysen und alternative Untersuchungsmethoden notwendig sind.

Hyperspectral imaging ist eine Technik, die die klassische Spektroskopie mit der konventionellen digitalen Bildverarbeitung kombiniert. Es ermöglicht leistungsfähige Echtzeitmessung diverser Datenpunkte in ein und derselben Probe. Ursprünglich war hyperspectral imaging für Fernerkundungssatelliten und räumliche Analysen bestimmt. In letzter Zeit wurde es in Bereichen wie Lebensmittelverarbeitung, Krebsdiagnostik, Astronomie, Chemie und Biologie angewandt. Die Technik ist auch für quantitative Echtzeitmessung von vermischten, überlappenden Fluoreszenzsignalen, die aus mehreren Quellen innerhalb einer Probe stammen, geeignet. Demnach wurde ein modifiziertes, kommerzielles, mit der hyperspectral-imaging-Technologie ausgestattetes Fluoreszenzmikroskop verwendet, um kinetische Untersuchungen zu mehreren intrazellulären, infektionsbezogenen Ereignissen gleichzeitig durchzuführen, wie z.B. pH-Messungen in Phagolysom und Cytosol, bei Apoptose oder Zelltod als Reaktion auf eine *Aspergillus-fumigatus*-Infektion.

Mittels einer verbesserten HSI-Konstruktion wurden die Analysen durchgeführt, um in Echtzeit die Emission der verschiedenen Fluoreszenzfarbstoffe in einer einzelnen lebenden Zelle nach der Infektion zu verfolgen. Die markierten Mikroorganismen, inkl. Pilzkonidien, dienten als intrazelluläre „Spione“, um die Zellereignisse während der Apoptose nach der Infektion aufzuzeichnen. Bemerkenswerterweise wurde beobachtet, dass die Fähigkeit von Melanin, das Schicksal der Apoptose zu ändern in direktem Zusammenhang mit seiner Fähigkeit, die intrazelluläre Versauerung und die Einstellung des sauren pH-Wertes zu

verhindern, steht. Vergleiche zwischen verschiedenen *Aspergillus*-Spezies und den DHN-Melanin-mutanten Stämmen zeigen, dass diese Eigenschaft nicht einschließlich für *A.fumigatus* gilt, sondern in allen Spezies, die Melanin beinhalten, d.h. *Aspergillus clavatus*, existiert.

Der intrazelluläre pH-Wert nach der Infektion sowie während der Apoptose und das Muster der pH-Änderung in diesen Phasen wurden bestimmt. Zusätzlich wurden auf der Einzelzellebene mehrere Pilze (*Aspergillus clavatus*, *Aspergillus flavus* und *Lichtheimia brasiliensis*) untersucht, um die Kontrollen zu evaluieren und die Ergebnisse zu bestätigen. Die vorliegenden Daten waren sehr reproduzierbar. Die Ergebnisse bieten vielseitige Möglichkeiten, von neuen Medikamenten in der Zelltherapie zu profitieren (z.B. innovative Behandlungskonzepte und die nicht-invasive Methoden für Tumorerkrankungen und Apoptose) und die hochmodernen Modifizierungen der HSI-Methode machte sie anwendbar als eine alternative Detektionsmethode, besonders geeignet für Analysen der Einzelzellen.

3 Graphical abstract

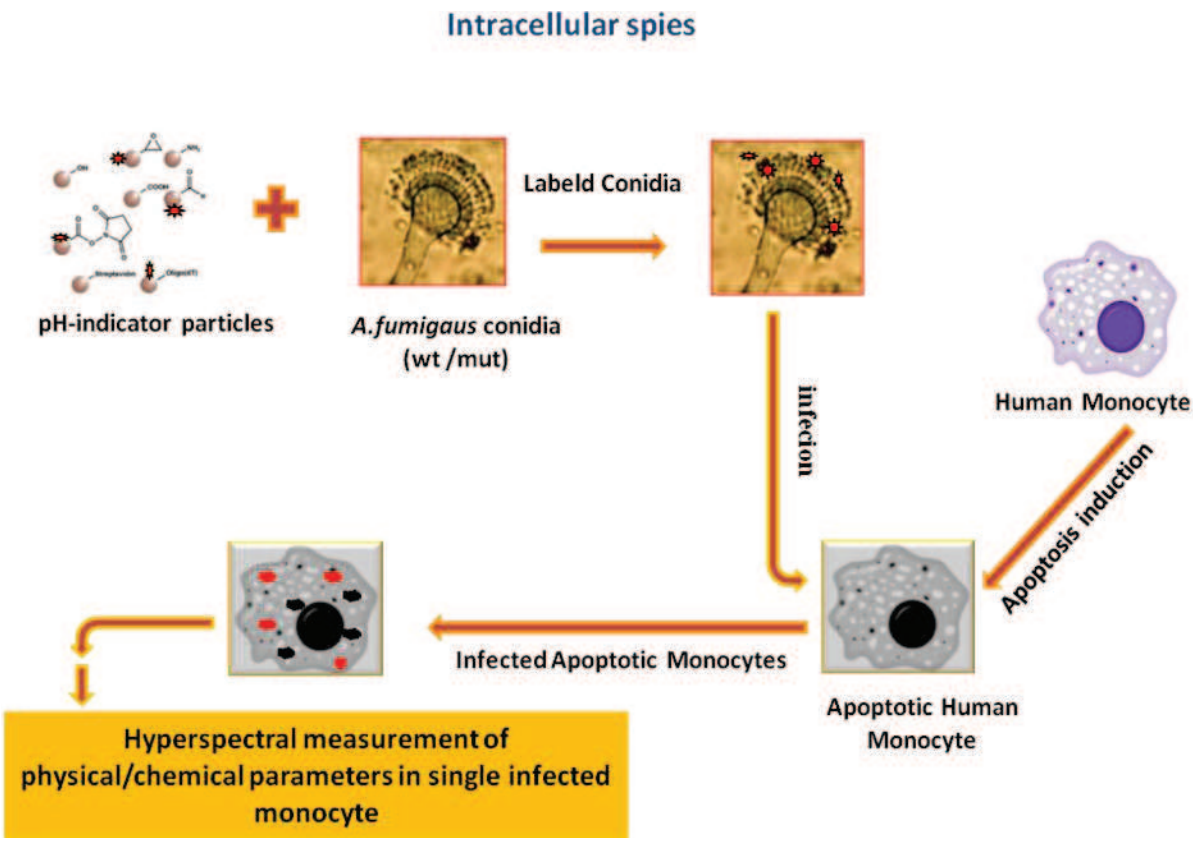

Graphical Abstract. The brief outlook of the project

4 Introduction

4.1 *Aspergillus fumigatus*: a saprophyte fungus and opportunistic pathogen

Fungal pathogens cause a broad range of diseases that depends on the immune status of their host, varying from allergic reactions to invasive and lethal infections. *Aspergillus* species as ubiquitous fungi, ecologically tend to inhabit on soil, water, vegetation and starchy products (Frisvad and Larsen, 2016). They have an imperative influence on the global carbon and nitrogen reproduction chain (Latge, 1999). In the nature, aspergilli initiate to produce conidia on decaying organic material. The conidium is gray-green, rather small (with 2-3 µm diameter), hydrophobic and totally resistant to the environmental stress (**Fig.** 1). The formation and development of conidiophores involves dynamic alteration in morphogenesis of fungus and its cellular polarity (Chi and Craven, 2016).

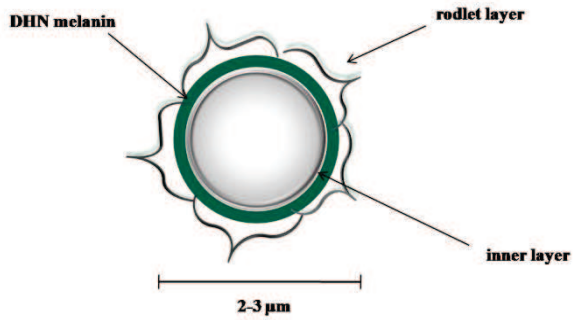

Figure 1. The schematic image of an *A.fumigatus* conidium. The cell wall consists of three divided sub layers: the outer part (rodlet layer) is formed via *rodA* and *rodB* to mask and protect the conidia from host's immune system. The intermediate layer consists of a dense pigment coat of 1,8-dihydroxynaphthalene (DHN)-like pentaketide melanin, which is adjacent to the broad electron translucent inner layer.

The protective cell wall of conidium is formed by three sub-layers and has essential role in host cell or environmental interactions. It is rigid but also dynamic and mostly is consisted of polysaccharides (Gastebois et al., 2009). In cell wall, the outer layer is called rodlet layer and the invasiveness of *A.fumigatus* conidia is indebted to it. The rodlet layer is formed by *rodA* and *rodB* and is responsible for masking and protecting the conidia from host's immune system (Thau et al., 1994).The middle layer of cell wall, is dense pigment layer of 1,8-dihydroxynaphthalene (DHN)-like pentaketide melanin, which is adjacent to the electron translucent inner layer (Bernard and Latgé, 2001), (Langfelder et al., 2003).

Throughout one sporulation huge amounts of conidia are produced which easily speared by the air flow and localized in new plants, animal and human hosts (Hohl and Feldmesser, 2007) (**Fig.** 2).

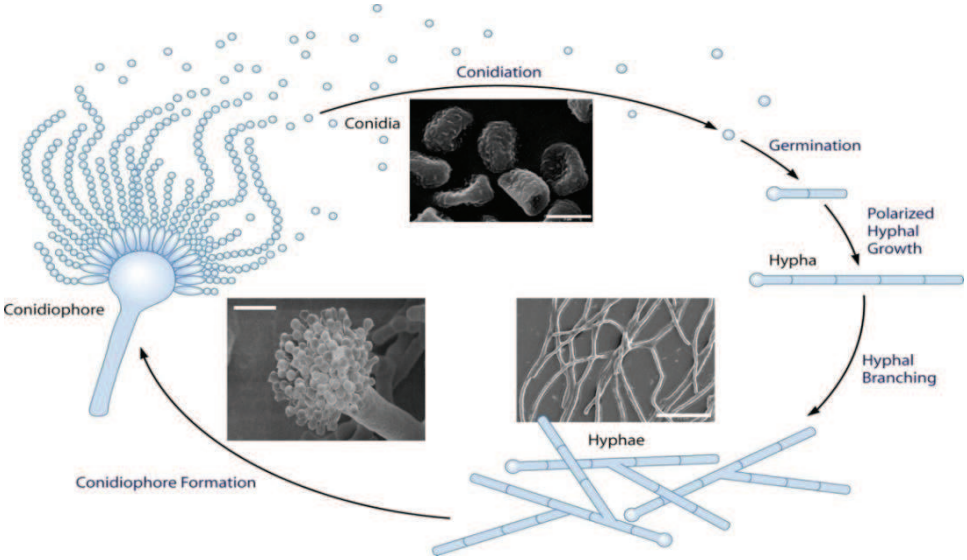

Figure 2. Life cycle and metamorphosis of *A.fumigatus*. During asexual cycle, conidium germinates through a polarized growth form the haploid hyphal cells. Conidium is further elongated to form conidiophores which are the origin of phialides and form the conidia. By the time the rodlet layer cell wall of conidia are completed, the conidia will detach from the chain and flow into the air (Shapiro et al., 2011), (Latge, 1999).

The genus includes around 344 species (Samson et al., 2014) which are mostly saprophytes. Among the pathogenic species such as *Aspergillus clavatus*, *flavus, fumigatus*, *niger*, *nudilans*, etc. *Aspergillus fumigatus* is one of the most prevalent fungi (Heinekamp et al., 2015) which in the fungal kingdom shows a close relevance to Penicillium species due to the ability of representing a group of prenylated indole alkaloids (Hohl and Feldmesser, 2007). The fungus grows in a hyphal vegetative form and reproduces either in sexual or asexual way (O'Gorman et al., 2009). It undergoes asexual reproduction via generating asexual conidiospores or mitotic division of haploid cells. Also the sexual reproduction is accomplished through heterothallic mating between two mating-type loci. There is a correlation between the nature of heterothallic mating and virulence in *A.fumigatus* (Ene and Bennett, 2014) (**Fig.** 3).

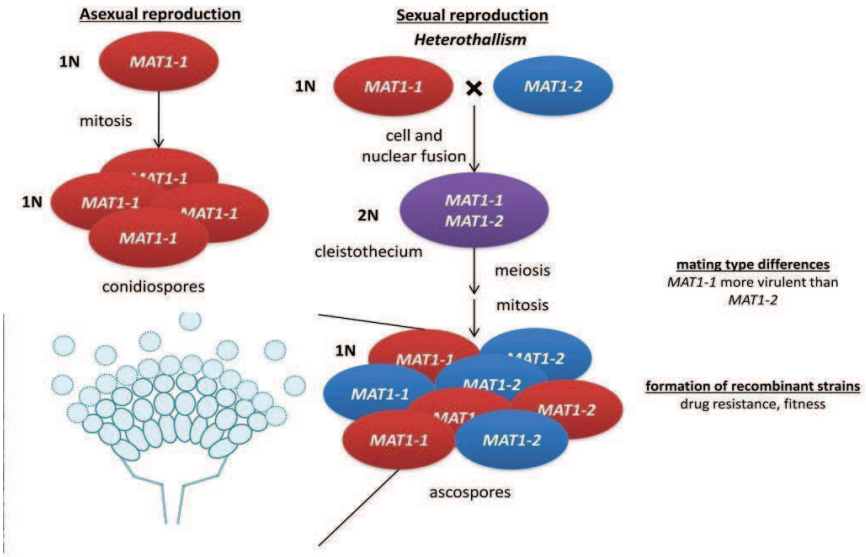

Figure 3. Comparing sexual and asexual reproduction in *A.fumigatus*.
Via asexual reproduction mitotic division will result in the haploid cells and form the conidiospores whereas sexual reproduction occurs between two species, when fictionalized MAT- cells (which are present in equal ratios in the nature) in two types undergo heterothallic mating to produce the recombinant cleistothecia. By meiosis division afterwards large numbers of ascospores will be produced (Dyer and Paoletti, 2005), (Ene and Bennett, 2014).

A.fumigatus is a thermo-tolerant fungus that can bear with the temperature over 50 $^{\circ}$C in the hyphal form and 70 $^{\circ}$C in the conidial form (Latge, 1999). In recent years, it has been shown that the *RodA* within hydrophobic proteinaceous layer assists the conidia to hide their immunogenic structures (Aimanianda et al., 2009). In addition, the other important factors that have been known to be involved in *A.fumigatus* virulence are melanin, gliotoxin and the components which engage zinc and iron along with different signaling pathways (Latge, 1999).

In *A.fumigatus* virulence among immunocompromised patients, Gliotoxin (GT) is the most effective factor which induces apoptosis through Bak-dependent mitochondrial apoptosis (Geissler et al., 2013). GT is an epipolythiodioxopiperazine (a class of fungal toxin) with a reactive disulfide bridge (Müllbacher et al., 1986). It can elicit the oxidative stress and is secreted during the hyphae formation. These abilities make it an important substance for invading the lung (Kupfahl et al., 2008).

Approximately several hundreds of its conidia are daily being inhaled by an healthy human and eliminated via the first line of innate immune defense (Hospenthal et al., 1998). In immunocompromised individuals *Aspergillus* is considered as the cause of allergic symptoms,

or by further localization in the respiratory tract or presence in blood and brain, causes severe infections which is so-called invasive aspergillosis (Dagenais and Keller, 2009).

During last decades *A.fumigatus* has been named as one of the most common airborne pathogen which can invasively attack the patients with suppressed immune system (i.e. organ transplants, burned patients, leukemic and HIV^+ patients) (Saral, 1991), (Brakhage and Liebmann, 2005) and develops secondary infections with the possibility of turning to fatal infectious cases specially among long-term hospitalized patients (Ahmad Sarji et al., 2006). Even nowadays in some clinical cases, the optimization of therapeutic agents and transplant medicines against malignancies caused by *A.fumigatus* are complicated (Wuren et al., 2014). In an healthy individual the inhaled conidia that are mostly localized inside the nose and lungs, are vanished by macrophages and neutrophils whereas in immunocompromised patients the conidia germinate and maintain the infection and invade the host tissues (Feldmesser, 2006).

4.1.1 Immune responses against *A.fumigatus* infection

Against infectious microbes, the primary defense of immune system is eliminating them from the blood via phagocytosis. The function includes the engulfment of the microorganism into a compartment called “phagosome” and it involves the plasma membrane in the site of infection which provides actin filaments to fuse the microbe (Aderem and Underhill, 1999). After the internalization of the infector organism by recruitment of actin monomers the oligomers are formed to surround and engulf it rapidly (Miao et al., 2015).
The first interaction between immune system and the entered microorganism also causes the further increase of macrophages numbers (Philippe et al., 2003). Once a microorganism is engulfed to the cell, the phagosome within a multipart process gets mature and turns into lysosome where the various enzymatic reactions powered by GTPases activity digest the infectious particles and eliminate them from the blood (Kornfeld and Mellman, 1989).

There are two immune reactions which occur after *A.fumigatus* infection:

- The polymerization of actin monomers involving phosphatidyloinositol 3-kinase activity and initiation the phagosytosis
- Formation of a mature phagolysosome from initial phagosome and digestion of conidia from the respiratory tract.

Once the conidia are inhaled, upon the internalization in the respiratory tract and alveolus, the phagocytosis initiates by the alveolar macrophages that are the most abundant phagocytic cells in the lung. Dissimilar to the immune-defeated patients who often develop the infection

in their lung by germinating the conidia and formation of mycelium (Ibrahim-Granet et al., 2003).

4.1.2 Melanin, its molecular characteristics and role in pathogenesis

Melanin is an ambiguous polymer which is produced by various organism in many different structures (Hill, 1992). The term melanin has been driven from Greek word *mèlas* which means black. Fungal melanin is a gray-green biopigment that is essential for the survival and virulence in fungal species (Tsai et al., 1998). Many organisms in nature are capable of producing melanin to take the advantages of its various functions.
Generally, in fungi the pigments are mostly attached to the cell wall and located in the outer layer (Pihet et al., 2009). Melanin is also known for its specific protective functions against environmental stress like UV irradiation, elevated temperature, lytic enzymes secreted from microbes and oxidative stress reactions (Nanis G. Allam, 2012). Besides its defensive character against the host cells responses, it has been shown that the conidia require melanin as a major structural component. Since it properly forms the conidial cell wall, it is expressed on the surface to provide a better adhesion.

In *A.fumigatus* the main pigment is DHN-melanin and is formed by a 19-kb DNA fragment that contains a cluster of six genes (*ALB1*, *AYG1*, *ARP1*, *ARP2*, *ABR1* and *ABR2*) (**Fig.** 4). (Pihet et al., 2009). It is localized on the outer layer of conidial cell wall and it has a direct interaction with the host cell (Cagas et al., 2011). Besides this genes, the cluster also contains the gene *pksP* which encodes a polyketide synthase and is essential for the formation of a pigmented conidium (Langfelder et al., 1998). During the metabolic and enzymatic processes many free radicals are generated and accumulated in the organism and further will be eliminated by the help of antioxidant enzymatic reactions (Olszewska-Słonina et al., 2007). Although melanin itself is known as a free radical substance, interestingly it also can bind to this radical molecules and perform as an antioxidant agent (Cunha et al., 2010). In the dynamic oxidation-reduction reactions between hydroquinone-quinone in the cell wall the melanin polymer operates as physiological redox buffer: it traps the unpaired electrons and binds them to metal ions to neutralized the generated oxidants (Jacobson, 2000). Hence, during the treatments against fungal diseases the presence of melanin can reduce the susceptibly of fungus against fungicides. It is capable of binding to anti-microbial peptides like caspofungin and amphotericin B and reducing their effectiveness (van Duin et al., 2002).

In *A.fumigatus* genome, if the mutation causes the lack of DHN melanin, the morphologic result will be white smoothed layer conidia (Langfelder et al., 1998). In case of such change

in the nature of wild-type melanized conidia, the melanin-free mutants show the lower survival rate inside monocytes (Amin et al.) as well as less virulence in host cells (Jacobson, 2000).

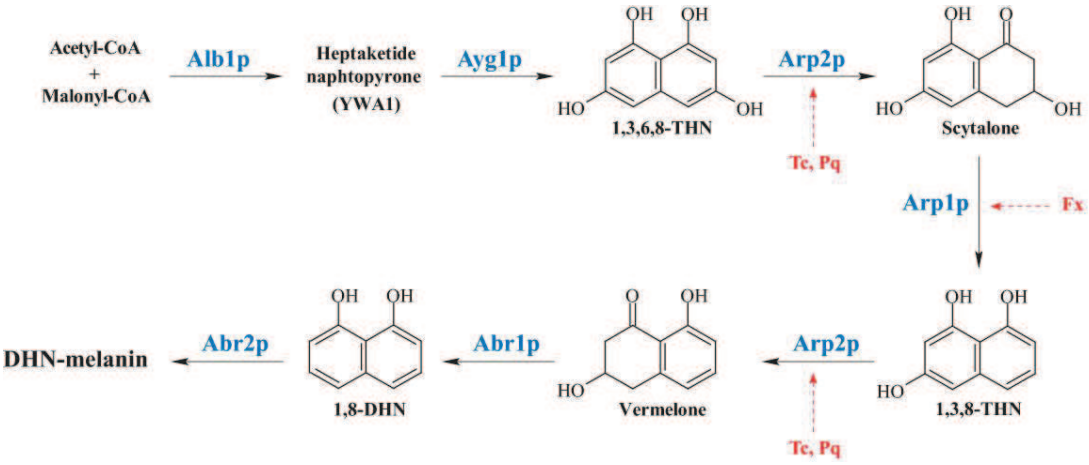

Figure 4. The biosynthesis pathway of DHN-melanin. Formation the DHN-melanin is through the cluster of six genes. The mutation in *ALB1* gene will generate the white melanin (also named *pksP*). The mutation in the other intermediated genes in the cluster will produce melanin with different colors (*Abr2, Arp1* and *Ayg1*: → brown, red and yellow, respectively) (Pihet et al., 2009), (Jahn et al., 1997).

4.1.3 Characterization of *A.fumigatus* mutants

Considering the similarities and differences of fungal pathogenesis, evolving the hypotheses on function of melanin and its interaction with the host cell seems necessary. Within the melanin synthesis pathway, different genes are responsible for the formation of intermediate molecules (Jahn et al., 1997) and in the case of mutation, their outcome would be different **(Fig.** 4). Although the regulation of DHN-melanin biosynthesis pathway has been not completely understood (Slesiona et al., 2012), it is already known that how different mutants of white, yellow, red and brown color are generated by introducing classical mutagenesis. For example, in the case of mutation at *pksP* gene which is essential for the conidial pigmentation and formation, the resulted conidia are white and smoothened in the surface, also more fragile when exposed to H_2O_2 (Langfelder et al., 1998).

In comparison to the white mutant, color mutant conidia that have deletions in any of certain six-gene cluster, show a better resistance to hydrogen peroxide and enhanced virulence in insect hosts regarding the more effective microbial invasion during infection (Rementeria et al., 2005), but the same virulence as wild-type in mice (Sugareva et al., 2006).

In one study (Jackson et al., 2009) the insect models were used to show that the color mutant *A.fumigatus* cause the higher rate of mortality in the infected insects compared to the wild-type. This is due to the pathogen-associated molecular patterns (PAMPs) and the self-damage of host's innate immune system that seems to be inevitable in the absence of completed form of melanin. In general, mutation in melanin pathways is the main cause for an enhanced virulence potential in color mutants. As far as the natural characteristic of melanin in quenching the reactive oxygen radicals will be lost over the mutation and the chance of immune system for the fungal resistance becomes lower (Tsai et al., 1998).

The *abr2* genes for *"Aspergillus brown 2"* that with abr1 is increased during conidiation and up regulated upon hyphal competency, has homology to the products of yA gene (laccase) studied in *Aspergillus nidulans* (Upadhyay et al., 2013). Regarding the fact that DHN gene cluster is only expressed during the conidiation (not in form of vegetative hyphae) and *abr2* is expressed so late in the pathway, necessity of *abr2* for the formation of the dark pigment is obvious. Then the deletion of *abr2* will change the pigment from green-gray to a brown color and the reduction of general conidial ornamentation (Sugareva et al., 2006).
The *arp1* for *"Aspergillus reddish-pink 1"* shows resemblance with hydroxynaphthalene reductases, polyketide synthases and scytalone dehydratases in DHN-melanin pathway of brown and black mold (Tsai et al., 1999). The *arp1* is also responsible for the flaviolin molecule. Flaviolin which is accumulated in *arp1*-disrupted strains (Osiewacz, 2002), is an autoxidation product of 1,3,6,8 tetrahydroxynaphthalene and is involved in monooxygenase and transferase activity (Berman et al., 2000).

Unlike *abr2* and *arp*1, *ayg1* gene for *"Aspergillus yellow 1"* has a role in polyketide shortening and is required for synthesis of 1,3,6,8-THN. Blockage of the 1,3,6,8-THN, alters the completion of conidial color. By deleting the *ayg1* gene, yellow pigmented conidia will be produced (Tsai et al., 1999). Interestingly, by the mutation of the *ayg1* the 1,3,6,8-THN will not be accumulated in the culture. It is interpreted that deletion of *ayg1* will prevent the synthesis of 1,3,6,8-THN and flaviolin (Teutschbein et al., 2010), (Tsai et al., 1999). The presence of these genes together in the biosynthetic pathway suggests that formation of DHN-melanin is more complex than a simple conidial pigmentation (Tsai et al., 1999).
However, for synthesis of both common types of melanin (DOPA and DHN-melanin), the secretion and activity of laccase enzymes are essential (Sapmak et al., 2015). Also recently, in a plant pathogenic fungus from *Leotiomycetes* class, two key enzymes (Bcpks 12-13) have been identified that are required for conidial melanogenesis showing DHN melanin, at least in

some cases, has been developmentally regulated and dispensable via a non-linear metabolic pathways (Schumacher, 2016).

4.2 Apoptosis

Although some components of apoptosis event have been described many years ago, the term of apoptosis was first proposed in 1972 when Kerr et al. described the morphological transformation and various features of a cell during its intentional death (Kerr et al., 1972). Apoptosis is a planned cells suicide having been observed in prokaryotes, plants, reptiles and mammals. The cell suicide is an active molecular-based and genetic-related mechanism which has been highly conserved along the evolution and plays a key role in establishing the homeostasis, securing the development and adoption to the environmental stress (Alberts et al., 2002), (Hochman, 1997). The event proceeds until the morphology and biochemical characters of the cell dramatically are changed (Thornberry and Lazebnik, 1998).

Deregulation of apoptosis and malfunction during its process causes several of the most common diseases such as Parkinson's, malignant neoplastic disease and rising tumors (Nilsson et al., 2003). During apoptosis various morphological changes occur. Chromatin becomes condensed along with aggregation the apoptotic bodies as the results of defragmentation and dissolving the nucleolus (Holmgren et al., 1999). DNA turns gradually fragmented and plasma membrane blebs (Fackler and Grosse, 2008). Apoptosis starts by activation of the cysteine aspartate-specific proteases family (caspases) from several possible entries like mitochondria (mitochondrial pathway) or plasma membrane (receptor pathway) (Fulda and Debatin, 2006). Caspases at first place are expressed as zymogens (inactive pro-enzymes) and once their members receive the death signal, are cleaved by proteolysis and get activated (Creagh et al., 2003). Regarding the apoptosis-relative functions, caspases are generally dividable in two categories:

- Initiator caspases (mitochondrial pathway): including caspases -2,-8, -7 and -9 in mammals that are coupled to pro-apoptotic signals. Caspases -2,-8, -9 are apical caspases and their activation requires the executioners. The mitochondrial pathway is triggered by the cellular stress, environmental changes and toxins .The members are responsible for the apoptosis signal transition and stimulation of the caspases cascade. The mitochondrial pathway is started by the release of many apoptotic factors such as apoptosis inducing factor (AIF), inhibitor of apoptosis protein (IAP), cytochrome C, second mitochondria-derived activator of caspases (DIABLO) (Saelens et al., 2004).

- Effector (executioner) caspases (extrinsic pathway): like caspases -3,-6, -7 that executes apoptosis. The pathway is triggered by death receptor engagement and the members are responsible for proteolytic cleaving the apoptotic substrates and cellular proteins like Aspartate residues (Cullen and Martin, 2009), (Degterev and Yuan, 2008) (**Fig.** 5).

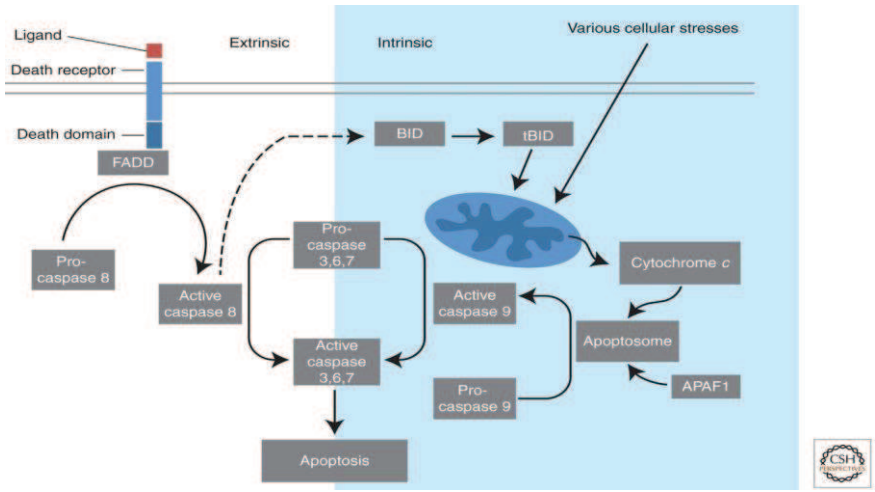

Figure 5. Extrinsic vs. intrinsic pathways of apoptosis. Apoptosis signaling pathways can be initiated extrinsically via receptor ligation and stimulation for example by the recruitment of Fas-associated death domain (FADD) or receptors of the tumor necrosis factor (TNF), etc. On the other hand it can be also started intrinsically at the mitochondria by stress signals and releasing the apoptotic factors for example under UV irradiation, bacteria, staurosporine, cytochrome c, etc. (McIlwain et al., 2013).

4.2.1 Different stages of apoptosis

Apoptosis is governed by various pro- and anti-apoptotic signals that compete with each other and integrate until the cell chooses between the final death signal or life cycle responses (Kravchenko-Balasha et al., 2009).The structural changes arise mainly within two steps. First, the nuclei and cytoplasm get condense to the point falling apart into many fragments named apoptotic bodies. Then the fragments discrete from epithelial surfaces and undergo phagocytosis mostly by macrophages (Kerr et al., 1972).

In programmed cell death, there are different stages which are finely diverse: Early apoptosis, late apoptosis, death and finally necrosis. Certainly, apoptosis should be considered as a different phenomenon with necrosis, which is a toxic degradative process where the cell enters the death mode and occurs after cell death (Elmore, 2007). It has been shown that in adherent cells, apoptosis generally occurs and progresses slower than floating cells like

monocytes (it needs more than 48 h to complete the 4 stages) (Desjardins and MacManus, 1995).

4.3 Intracellular pH during phagocytosis and mitochondrial-mediated apoptosis

Mitochondria are responsible to maintain the electrochemical gradients in cells which accomplished by pumping protons from the matrix towards their inner membrane. The electrochemical gradients at first place, is created by efflux of hydrogen ions from matrix to the inner membrane space and also it is established by ΔpH components. By this means, the charge is built up and the status from charge to discharge will be formed based on the changes in protons ingredient through the matrix (Konforti, 1999).

Maintaining homeostasis is one of the main challenges for a phagocytosis cell whereas by this activity, extensive amount of acid is generated which is enough to acidify the entire cell and its environment. Also, intracellular pH gradient affects the proteins activity and therefore contributes to cell directional migration and motility (VanHook, 2015).Then keeping the balance between the proton gradient and the amount of acids in the corresponding compartments is very crucial since the phagocytes i.e. neutrophils and monocytes, are responsible for various activities including cell migration, scavenging, microbicidal functions, etc., that all are pH dependent (Coakley et al., 2002).

The alteration in the cellular pH appears to be associated with the initiation or progression of mitochondria-derived apoptosis pathways (Matsuyama and Reed, 2000). In the cell death, several compartments will be affected leading to different causes such as DNA fragmentation, the membrane permeability and cell shrinkage. The toxins are accumulated and the ions gradient alters resulting the necrosis afterwards (Park, 1995).

During apoptosis cytosol and its organelles are acidified. It is believed that the lysosome is the most acidic compartments during apoptosis and the release of lysosomal protons is the reason for cytosol acidification (Nilsson et al., 2003). It seems that the extensive acidification in cytosol during apoptosis is one of the most important reasons for the necrosis and cell degradation (Park, 1995). Although the importance of this excessive acidification during apoptosis has not been well-defined yet, it is believed it might facilitate the initiation of caspases and assist them to activate (Nilsson et al., 2003). Several theories have been mentioned to explain the mechanism of apoptotic cell acidification. Most of them suggest the plasma membrane Na^+/H^+ antiporter, along with the reversed proton pumping of mitochondrial membrane, modulate pH (Liu, 2000).

4.4 *A.fumigatus* and its role in apoptosis as an infectious microorganism

There is a fine link between the importance of caspases-3 in/during apoptosis in monocytes and the anti-apoptotic properties of *A.fumigatus* when it is engulfed through phagocytosis. In the case of infection with pigmented conidia, in macrophages and epithelial cells sustained level of anti-apoptotic proteins belong to Bcl family. Also DHN-melanin showed in such cases has the ability to reduce the release of cytochrome C from mitochondria followed by preventing the inflammatory cytokines and limiting apoptosis prompting activation of the corresponding effectors i.e. caspases 3 and 7 (Féménia et al., 2009), (Heinekamp et al., 2013). Moreover the melanized conidia appear to have an inhibitory effect on extrinsic and intrinsic apoptotic pathway. The wild-type is capable of modulating the caspases and even preventing the caspases initiation in macrophages (Volling et al., 2011). Up to now, our knowledge about the actual role of melanin during apoptosis and also the inner-cell condition during apoptosis in the presence of melanin is limited.

4.5 Intercellular events during apoptosis upon interaction with other fungi different from *A.fumigatus*

To provide the candidates for negative/positive controls, among pigmented microorganisms, some fungi that contain pigments were randomly selected. The information about the characteristics of these fungal pigments upon their abilities to modulate of host's pH or apoptosis is very limited.

4.5.1 *Aspergillus clavatus*

The fungus lives on soil and decomposing materials. Also it has been considered for its potential anti-microbial activity (Saravanan and Nanda, 2010) and anti-fungal peptide secretion (Skouri-Gargouri et al., 2010). *A.clavatus* produces sprouting grains being ingested mostly by ruminants including cattle and the further toxication followed by paralysis and tremors is lethal (Botha et al., 2014). It is also known as entomopathogenic fungus and has the ability to invade the guts of insects and collapse the cells (Seye et al., 2009). The conidial pigment of A.clavatus is (DHN)-like pentaketide melanin (unpublished data, HKI fungal collection). Up to know, still there are many unknown facts about this fungus.

4.5.2 *Aspergillus flavus*

In recent years the prevalence of *A.flavus* in certain hospitals has shown a higher frequency than *A.fumigatus* (Hedayati et al., 2007). It is an airborne ubiquitous fungus which at the second place after *A.fumigatus* is the cause for human invasive aspergillosis (Abbas, 2005),

(Hedayati et al., 2007). It completes its life cycle mostly in the soil and in tropical lands becomes more widespread. The fungus includes two distinguished strains: strain S, which produces small sclerotia (less than 400 μm in diameter) but in greater quantities; and strain L, standing for large sclerotia (over 400 μm in diameter) (Cotty, 1989). The conidiophores appear in various shapes and pigmentations. The pigment generally is greenish-yellow since in the cluster of *pks* any alteration will result in different metabolite. It has been observed that the green color is due to the inactivation of cluster 27 pks which causes the formation of sclerotia (the resistant structures) due to asparasone synthesis (Cary et al., 2014), (Calvo and Cary, 2015). Also, it can produce reddish pigments since in many spices the pigment is made up of ferric-based molecules or even mainly consisted of iron atom, molecules of aspergillic acid or its isomers which are responsible for the yellowish touch. These sub-group is popular for aflatoxin secretion and food contamination (Assante et al., 1981), (Abbas, 2005).

4.5.3 *Lichtheimia brasiliensis*

The fungus belongs to the Mucorales order and has been recently introduced as a novel species within the genus Lichtheimia. It comprises 46 strains in total of six species and first was isolated and reported from soil samples in Brazil (Schwartze et al., 2012). *L.brasiliensis* is known as a non-pathogenic member in the genus though the other species are the common cause for mucoromycosis (Skiada et al., 2011). In the genus, thermo-tolerance is the essential factor for categorizing and distinguishing *Lichtheimia* its optimal growth temperature is at 35-37 ºC, and cannot grow at 42 °C, whereas those species that prefer higher temperature, typically are of clinical importance as secondary human pathogen (Hoffmann et al., 2007). Dissimilar to the most of members in *Lichtheimia'*s genus, it represents the most basal species (Schwartze et al., 2014). The pigment is called sporopollenin and is generated from of carotenoids degradation. It is known to be a common pigment in the phylum *Zygomycota* (Kwon-Chung, 2012).

Up to now there is not much information available about this fungus (Jena Microbial Resource Collection (JMRC) Jena, Germany).

4.6 Human monocytes (Mono Mac 6 cell line)

Monocytes are the heterogeneous leukocyte population which are circulating in peripheral blood (Geissmann et al., 2003). They originally are driven from progenitors in the bone marrow (Shi and Pamer, 2011). In any bacterial, viral or fungal infection, recruitment of these cells is essential for initiating, maintaining and resolving the immune responses since they can effectively contribute to inflammatory conditions and remove the pathogens from blood

stream. These cells mostly are responsible for reloading the dendritic cells and macrophages. By differentiating, they encounter any infectious material or inflammatory cytokines. Also they have different markers that dependent on their function (i.e. recognition pathogens, inflammatory responses or scavenging activities) could be divided in different subsets (Yang et al., 2014). The monocytes half-life is variable from one to three days. They are able to migrate into tissue and turn to the resident macrophages (Nahrendorf et al., 2007). In the absence of sufficient stimuli from immune system, monocyte undergoes apoptosis. Caspase-3 appears to play the central role in determining programmed death of monocytes (Fahy et al., 1999).

Mono Mac 6 (MM6) that is the case study in this project is a human monocyte cell line with a strong ability in phagocytosis. The cells are independent from the age of cell culture, and show the features of mature blood cells with the same abilities such as IL production or CD 14 antigen expression (Neustock et al., 1993). Also the value of their adhesion properties to the other cells are remarkably high (Erl et al., 1995).

4.7 Hyperspectral Imaging technique (HSI)

Hyperspectral Imaging at first place in 1980s was proposed by Goetz for observation and remote sensing of the Earth and ever since has become established as a significant technique (Goetz et al., 1985).The technique is designed based on the combination of classical spectroscopy and conventional digital image. Such adaptation creates an absolutely proper tool for all kind of real-time measurements. In biology the main principle is grounded on making the measurement from various data points within an individual sample to acquire laboratory-like spectra (Di Napoli et al., 2014) (**Fig.** 6a, b).

In the early years of emerging HSI technique, in accordance with the instrumental capacity of the time, it appeared too costly and bulky to be applied for any purposes other than astronomy, generating geospatial maps by satellites or military activities (Iqbal et al., 2014). But ever since, during last decades and along with the expense and space reduction of HSI cameras design and data base storage it has been used broadly in applied science and industrial experiments. In parallel with the market demands, it was applied for food-processing and experiments in quality controls in food industry (Gosnell et al., 2016). Gradually with the development of environmental or mineralogical sensing, it was applied in biological assays, pharmaceuticals and chemical imaging purposes (Di Napoli et al., 2014). The prefix “hyper” stands for the large number of wavelength bands or fluorescent dyes that can be differentiated by this technique. Typically these numbers are much greater than the 3

bands of RGB cameras and in our study they are about 35. In contrast to conventional fluorescence microscopy, in which the recorded wavelength is based on positioning the band-pass filters within the optical path, in HSI the images obtain an entire spectrum from each point of interest within the sample and a complete fluorescence emission spectrum will be recorded.

4.7.1 The main scanning methods in hyperspectral measurements

For the hyperspectral measurements, there are several scanning methods:

- **Whiskbroom scanner**: It collects HSI data by point scanning. The instance for its application is spectral laser scanning microscopes which use whiskbroom scanner by scanning the sample with a one-channel-spectrometer in two dimensions (Lu and Fei, 2014).
- **Push broom scanner**: It performs line scanning. The application is based on measuring a series of points forming a line that is being scanned only in one dimension. This method is suitable for linear measurements with no need for spatial scanning (Knetsch et al., 2009).
- **Wavelength scanner** (tunable filters or FTIR): It acquires images over time (Daly et al., 2000). They are full data cube snapshot imagers, without any need for scanning (the newest sub method of HSI) (Wagadarikar et al., 2009). Such novel devices which are just being developed and emerging in the market. Their advantage is their larger arrays of detector elements (Kriesel et al., 2012). The range of solutions using imaging spectrometers has strongly increased due to the availability of two-dimensional CCD arrays. These devices deflect the light radiance from each pixel of an image to produce various extended spectral bands, therefore each pixel in the image contains the entire spectrum, thus providing a highly resolved image with detailed information (Li et al., 2008).

4.7.2 The features and benefits of HSI

The greatest benefit of HSI which makes it a better option than classical fluorescent microscopy is the ability of precise measurements in simpler ways although the outcome data is more advanced and accurate than in confocal microcopy. Applying HSI, there is no need for narrow band filters and also for the application, no advanced knowledge is required for selecting the emission filter corresponding to the applied dyes.

Post-processing of the obtained spectra allows all information from the data set to be recorded (Lu and Fei, 2014). Therefore if the experiment is conducted based on measurements of mixed fluorescence signals of different compounds or compartments, HSI would be one of the best experimental method options. Since it measures the transmitted signals from all different sources within one single sample (Vo-Dinh, 2004).

As another example for advantages of HSI, one could mention the possibility of massive data acquisition, which is done by computer-based spectral measuring technique. With such technique, the constituent values could be separated and analyzed individually. For example, the multiple overlapping fluorescent labels are discriminated by minimal use of optical filters. This feature represents a powerful tool to detect the distribution of one or more chemical or biological compounds in the area of interest. The samples that are analyzed by HSI, include a broad range of fluorescent labels that spectrally overlap (Pike et al., 2014). The samples also could be mounted on any microscopic slides, suspended in buffer solutions or cultured in media. Irrespective of the size of sample, HSI enables the applicant to measure the spatial relationships between the various spectra in any sectional region, and elaborate the spectral-spatial models for a very accurate segmentation of the outcome image, for example in any compartments in a tissue or between some molecules within a cell (Bertani et al., 2013).

Although HSI technique requires the extensive capacity for storing the large amount of data and also it requires informatics, data processing and analysis which are usually costly, but the privilege of using the combined filters simultaneously with no need for changing them is not even negligible but also appealing.

Moreover the real-time detection and data acquiring from various spots in one sample at the same time plus the ability for long term measurements under the constant conditions, makes it a preferable tool when compared to other technique i.e. Fluorescence-activated cell sorting (FACS) analysis (which is limited to a high numbers of cells) or other microscopic systems like light or confocal microscopy (that their results are dependent on the high resolution of images).

Even in compared to the conventional color microscopy that works based on capturing the light in three spectral windows, hyperspectral system is able to record an entire data section of the electromagnetic spectrum at each pixel.

Thus, although the method itself is not new, still yet many novel studies in different fields of biology with a variety of approaches have been published that are basically conducted on HSI (Chen et al., 2016), (Decan et al., 2016),(Peña et al., 2016), (Turra et al., 2015).Such various

applications verify the feasibility of the technique and its capacity for adjustment to different platforms of investigation.

The most important concerns in HSI are associated with the designing and developing the suitable instrumentation that meets all requirements of application. Also the calibration and exploitation of spectral data is a crucial point that must be taken into account. Last but not the least, the improvement of efficiency, expanding the algorithm along with the miniaturization of the structure have been always a concern (Serranti and Bonifazi, 2014), (Serranti et al., 2012).

a.

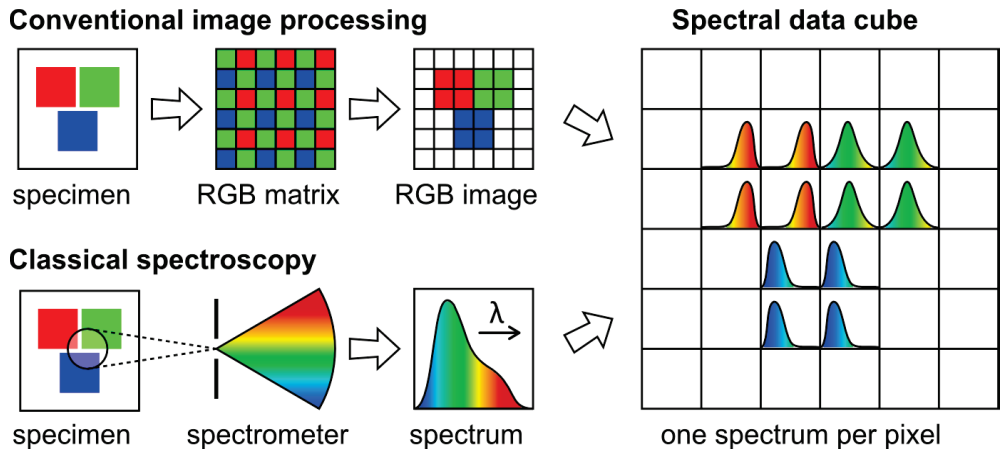

b.

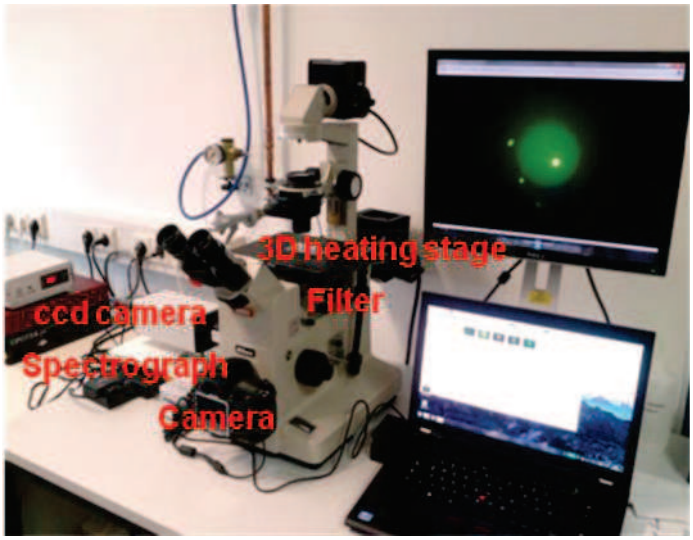

Figure 6. Scheme of Hyperspectral Imaging principle (HSI). **a**. Combination of classical spectroscopy with conventional image processing has led to HSI technique with no need for scanning the samples. The spectral data cubes include a set of data pixels that are layered on top of one another.

Therefore, each pixel in the cube consists of an entire spectrum (Bioucas-Dias et al., 2012).Typically in hyperspectral imagery, the spatial information is collected in the X-Y plane and spectral information represented in the Z-direction (Vo-Dinh, 2004). **b**. The set of hyperspectral device

5 Aims of This Research

In the research framework of pathogen-host cell interactions, I aim to perform kinetic studies on several intracellular events during infection. For instance: measuring pH in phagolysosome and cytosol during apoptosis upon infection with *Aspergillus fumigatus*. I expect to perform a quantitative analysis based on the guidelines of hyperspectral imaging (HSI) in the single-cell studies. I consider the hyperspectral image acquisition as a methodical solution to verify the cell event during apoptosis.

The main goal for this project is conducting novel protocols that use ‘’bio-spies’’ i.e. *Aspergillus fumigatus* conidia as the intracellular pH reporters, by the means of a principally commercial fluorescence microscope which has been modified to HSI tool.

Since it has been shown that *A. fumigatus* conidia could interfere with the acidification of phagolysosomes in macrophage (Volling et al., 2011), then I intend to extend this finding to human monocytes as a model system and apply HSI to quantify the pH changes in the cell compartments. I also aim at exploring any possible relation between the ability of DHN-melanin molecule in *A. fumigatus* to modulate pH. Therefore, I need to support the results by examining pigments of different nature from various classes of microorganisms and quantify the intracellular pH in an apoptotic human monocyte.

Also I aim to show the pattern of intercellular pH alteration along with the fate of apoptosis through long-term measurements.

Up to know there has been no report published on adaptation the HSI technique to provide quantitative analysis of host cell-fungi interaction in single cell level.

6 Materials and Methods

6.1 Materials

6.1.1 Chemicals

The chemical substances mentioned in the method section, mainly were purchased from Life technology (Darmstadt, Germany), Sigma-Aldrich (Darmstadt, Germany), Zeiss (Jena, Germany), Carl Roth GmbH (Karlsruhe, Germany) and Roche (Mannheim, Germany).

6.1.2 Instruments

The Instrument used for this project, are listed in the table below

Table 1: List of equipment and hardware

Instrument	Manufacturers
Analytical Balance	Sartorius (Göttingen, Germany)
Centrifuge 5415 R	Eppendorf (Hamburg, Germany)
Centrifuge 4K15C	Sigma-Aldrich (Steinheim, Germany)
Centrifuge Universal 32 R	Hettich Zentrifugen (Tuttlingen, Germany)
CO_2 Incubator	Joan/Thermo Scientific (Schwerte, Germany)
FACS Calibur™	Becton Dickinson (Heidelberg, Germany)
Filter Cassette DM510 (excitation EX450-490, emission BA520)	Nikon (Germany)
Filter Cassette DM580 (excitation EX510-560, emission BA590)	Nikon (Germany)
Filter Cassette #49913 (beam splitter ZT640rdc, excitation ZET635/20×, emission ET655lp)	Chroma Technology Corp, (Vermont, USA)
Fluorescence Microscope BX-51M	Olympus (Hamburg, Germany)
Heating Stage	Minitüb GmbH (Tiefenbach, Germany)
Hyperspectral Microscope Nikon Diaphot TMD (Inversed fluorescence microscope, custom built C-mount adapter)	Nikon (Germany)
Light Microscope Axiovert 25	Carl Zeiss Microimaging (Göttingen, Germany)
Magnetic Stirrer/Heater	IKA Labortechnik (Staufen, Germany)
Microscope Camera	Olympus (Hamburg, Germany)
Microscope Full-frame SLR Camera	Nikon (Niederschöna, Germany)

Microscope Sensicam 680KU Camera, equipped with a highly sensitive Electron Multiplying Charge Coupled Device (EMCCD)	PCO (Kelheim, Germany)
pHmeter CG840	Schott (Mainz, Germany)
Thermomixer 5436	Eppendorf (Hamburg, Germany)
Ultrasonic Gemie 2™	Carl Roth GmbH & Co (Karlsruhe, Germany)
Water Bath	GFL (Burgwedel, Germany)

6.1.3 Consumables

Table 2: List of labware, consumables and accessories

Tool	Manufacturer
Bottle Top Filteration	VWR®
Cell Culture Flasks	BD Falcon™ (Dresden, Germany)
Cell Strainer (40µm)	BD Falcon™ (Dresden, Germany)
FACS Tubes	BD Falcon™ (Dresden, Germany)
Falcon Tubes (15ml/50ml)	BD Falcon™ (Dresden, Germany)
µ-Slide VI $^{0:4}$, cell in focus	Ibid GmbH (Martinsried, Germany)
Microscopy Chamber	Ibid GmbH (Martinsried, Germany)
Microscope Slides and Coverslips	Carl Roth GmbH & Co(Karlsruhe, Germany)
Multiwell™ 6 Well	BD Falcon™ (Dresden, Germany)
NanoDrop	Thermo Scientific (Schwerte, Germany)
Petri Dish	Carl Roth GmbH & Co (Karlsruhe, Germany)
Pipette Filter Tips	Starlab (Ahrensberg, Germany)
Pipette Tips	Sarstedt (Nümbrecht, Germany)
Serological Pipettes	BD Falcon™ (Dresden, Germany)
Test Tubes	Eppendorf (Hamburg, Germany)
Thoma Counting Chamber	Carl Roth GmbH & Co(Karlsruhe, Germany)
Vaccum Filteration-system	TPP (Switzerland)

6.1.4 Culture media

To cultivate fungal strains, Aspergillus minimal medium (AMM) was used. To prepare the AMM; the corresponding material listed in Table 3 were mixed, autoclaved and after adjusting pH 6.3-6.5, 15g/l autoclaved Difco Agar was added to the mixture. Trace elements were mixed, heated to boil, turned to deep purple and after adjusting pH by KOH and then added to the medium.

Table 3: List of culture media

Culture Medium	Ingredients	Concentration
Aspergillus Minimal Medium (AMM) (Pontecorvo et al., 1953)	KH_2PO_4 KCl $NANO_3$ $MgSO_4*7H_2O$ Glucose 20%	0.76g 0.26g 3g 0.26 5g
Complete Medium (per liter of minimal medium) (Barratt et al., 1965)	Difco malt extract Bacto-peptone glucose agar	2% 1% 2% 2%
Hunter's Trace Elements for AMM (Hill and Käefer, 2001)	$ZnSO_4$-$7H_2O$ $MnCl_2$-$4H_2O$ H_3BO_3 $FeSO_4$-$7H_2O$ $CuSO_4$-$5H_2O$ $CoCl_2$-6H2O $(NH_4)MO_7O_2$-$4H_2O$ EDTA (Disoduim salt) H_2O	2.2g 0.5g 1.1g 0.5g 0.16g 0.16g 0.11g 6g 100ml

6.1.5 Buffers and reagents

Table 4: List of buffers and reagents

Name	Ingredients	Concentration
Annexin Binding Buffer pH 7.4	NaCl HEPES $CaCl_2$	140 mM 10 mM 2.5 mM
Bafilomycin A1	In PBS	100 nM
Chloroquine	In PBS	20 μM
Hank's Balanced Salt Solution (HBSS)	NaCl KCl Na_2HPO_4 Glucose KH_2PO_4 $CaCl_2$ $MgSO_4$ $NaHCO_3$	0.137 M 5.4 mM 0.25 mM 0.1g 0.44 mM 1.3 mM 1.0 mM 4.2 mM
Live Cell Imaging Solution	NaCl KCl $CaCl_2$ $MgCl_2$ HEPES pH	140 mM 2.5 mM 1.8 mM 1 mM 20 mM 7.4

0.9%NaCl/0.1%Tween20	NaCl Tween20	9 g/l 1 ml/l
Propidium Iodide (PI)	PI in sodium citrate buffer	2 mg/l
PBS pH 7.4	NaCl KCL KH_2PO_4 Na_2HPO_4	8 g/l 0.2 g/l 0.2 g/l 1.15 g/l
PBS/0.1%Tween20 pH 7.4	NaCl KCL KH_2PO_4 Na_2HPO_4 Tween20	8 g/l 0.2 g/l 0.2 g/l 1.15 g/l 1 ml/l
Staurosporine	In DMSO	1.5 M

6.1.6 Kits

Table 5: The list of kits

CellTitre-Ble® Assay Kit	Promega (Mannheim, Germany)
pH Calibration Buffer Kit	Life technology (Darmstadt, Germany)

6.1.7 Software

Table 6: List of applied software

Camera Control ver.2.8	Nikon GmbH (Niederschöna, Germany)
Image J	Image processing and analysis in Java (open source)
Microsoft Office 2007	Microsoft Deutschland GmbH
Pco. Imaging	PCO AG (Kelheim, Germany)
R	Ver. 3.2.3

6.1.8 Fungal strains

Table 7: List of fungal strains

Strain	Genotype/Phenotype	Reference
***Aspergillus fumigatus* ATCC 46645**	Wild- type	ATCC
***pksP* mutant**	Encodes a non-functional *pksP* gene/white	(Langfelder et al., 1998)
Δ*abr2*	*abr2*::*hph*,Hyg^R/Brownish	(Sugareva et al., 2006)
Δ*arp1*	*arp1*::*hph*,Hyg^R/Reddish	J.Schmaler-Ripcke, Jena
Δ*ayg1*	*ayg1*::*hph*,Hyg^R/yellowish	V.Sugareva, Jena
Aspergillus clavatus	wild-type, melanized	Molecular and Applied Microbiology dept.(MAM), Jena
Aspergillus flavus	wild-type, siderophore pigment/ yellowish green	MAM dept., Jena
Lichtheimia brasiliensis	wild-type, carotenoid pigment/ Brownish	11615, Jena Microbial Resource Collection (JMRC) dept., Jena

All of the strains were cultivated for 5 days on AMM Petri dish at 37ºC, 5% CO_2, freshly harvested and used. Swollen conidia were prepared by incubation conidia in RPMI 1640 medium supplemented with 10% heat inactivated fatal calf serum. Inactivated conidia were prepared by autoclaving the conidial suspension at 121ºC for 30 min.

6.2 Methods

6.2.1 Cell cultivation

The human monocyte cell line (MM6) in suspension was maintained in RPMI 1640 no phenol red Medium (Life technology, #11835-030) supplemented with 10% (v/v) heat-inactivated fetal calf serum (FCS), MEM non-essential amino acid 100× and 10 mg/ml gentamicin. The incubations were carried out at 37 ºC in a humidified incubator with 5% (v/v) CO_2. Upon reaching 80% confluence per 175 cm^2 surface area, cells were washed with PBS buffer and passaged at a 1 to 6 ratio two times per week. Cells were frequently assayed for mycoplasma contamination using VenorGeM mycoplasma Detection Kit (Biochrom AG, Berlin, Germany) according to the manufacturer's instructions.

6.2.2 Cell viability

The viability of cells was determined before each assay by using a CellTitre-Blue ® (Promega, Mannheim, Germany) assay according to the manufacturer's instructions.

6.2.3 Fungal culture and conidial suspensions

A. fumigatus ATCC 46445 wild-type strain, the *pksP* melanin-free mutant (Jahn et al., 1997) derived from ATCC 46645, along with *abr2* (brownish), *arp1* (reddish) and *ayg1* (yellowish) (HKI fungi collection, Jena) were propagated on *Aspergillus* minimal medium (AMM) (Litzka et al., 1996) agar plates at 37 ºC.
A.clavatus and *A.flavus* were cultured on AMM enriched by malt extract agar plates incubated at 37 ºC.
On day 5 of the culture, the Wild-type conidia were harvested by rinsing the culture plates with 10 ml 0.9 % (w/v) NaCl solution supplemented with 0.1% (v/v) Tween 20 and carefully scratched with a rubber policeman. The suspensions were filtered through a cell strainer with 40µm pore size (BD Bioscience, Heidelberg, Germany).
The conidial suspensions were incubated in RPMI 1640 no phenol red, without FBS for 3 h at 37 ºC, and then washed 2 times with sterile phosphate-buffered saline (PBS) supplemented with 1% (v/v) Tween 20. Spore concentration was calculated according to the classical method by using a Thoma chamber and microscopic enumeration.
The *A.fumigatus* mutants were harvested with ddH_2O and incubated in the same condition as the wild-type.

Lichtheimia. brasiliensis culture was arranged by JMRC Dept, HKI, Jena; {growth on SUP medium (Wostemeyer, 1985)}: 30 mmol l^{-1} potassium dihydrogen phosphate, 5 mmol l^{-1} di-potassium hydrogen phosphate, 55 mmol l^{-1} glucose, 1 mmol l^{-1} magnesium sulphate, 20 mmol l^{-1} ammonium chloride, and 0.5% yeast extract) at 37 °C for 7 days (Schwartze et al., 2014). On the day 7 of culture, *L. brasiliensis* conidia were harvested using sterile fresh PBS and washed three times accordingly. The spore concentrations were determined microscopically in a Thoma counting chamber and diluted to the concentrations with PBS.

6.2.4 Labeling conidia with flurecein-5-isothiocyanate (FITS)

To calculate the amount of conidia per cell based on the described method (Sturtevant and Latgé, 1992), conidia were harvested and added to 1ml sterile 0·9% NaCl solution, were filtered to separate conidia from mycelium. The conidial suspension was centrifuged and the fresh conidia immediately were resuspended in 0.1M carbonate buffer (pH 9.3) and at 1×10^8

/ml with 0.1 mg/ml FITC (Sigma-Aldrich, Steinheim, Germany) was rotary incubated for 1h at 37 ºC under light protection. The conidia were washed three times with PBS/0.1% Tween20 at 5000×g for 10min, resuspended in 1ml PBS and counted. The result of calculation Multiplicity of infection (MOI) was recorded to apply for all measurements.

6.2.5 Phagocytosis and ingestion assay

To ensure that conidia have been absorbed by MM6 host cells, the rate of ingestion was determined based on the technique which has been selectively derived from Phillippe et al.'s techniques (Philippe et al., 2003). 2×10^6 cells/well were centrifuged at 900× g, 4 ºC for 5min and washed. They were plated in 6-well plates and after 6 h of incubation at 37 ºC with 5% CO_2, were seeded with freshly FITC labeled conidia in the ratio of 1:1 up to 1:5. After 3, 6, 12 and 24 h post infection (p.i.), the cells were washed with pre-warmed media to eliminate unbound conidia. Phagocytosis was stopped by washing ice-cold PBS. Before the counting, the cells were fixed with 4% (v/v) Rotfix (Roth, Germany) for 15 min at room temperature (RT) followed by three times BPS washing. The cells were transferred on microscopy glass slides, cover slips were mounted onto the slides and three random fields containing more than 100 cells/field of view from three experiments were considered for determination the ratio of successfully engaged conidia.

6.2.6 Colocalization of pH sensitive beads and conidia

To trace the cell events after taking up the labeled conidia, two type of fluorescent pH sensitive beads where used to introduce to the cells along with the conidia: pHrodo® Red Zymosan BioParticles® Conjugate Ex/Em 560⁄585 (Life technologies, Darmstadt, Germany), and also pHrodo® Green Zymosan BioParticles® Conjugate Ex/Em 509⁄533 (Life technologies Darmstadt, Germany). Per each well, 25µg of particles were added to 20 ml RPMI1640-no phenol red, 3.75 ml pvp and 750 µl DMSO. The mixture was placed in the shaker at -8 ºC for 30 min followed by the sonication for 5 min. The homogenized solution was added to the 2×10^6 cells/well, including fresh medium.

6.2.7 pH detector labels

To generate red-labeled spies, freshly harvested conidia were washed with PBS/1% (v/v) Tween 20. To make a sufficient conjugation with dyes, the conidia were resuspended in the buffer solution pH 6.00±0.02 (Roth, Germany). 1 mg vial of Red succinimidyl (NHS) pHrodo™ ester, MW= ~650 (Life technologies, Darmstadt, Germany) was added to 150 µl anhydrous DMSO (10 mM dye concentration) and mixed with 0.1 M fresh sodium

bicarbonate buffer (pH= 8.3), making the concentration of 10.2 mg/ml as stock solution. It was immediately diluted in DMSO to final concentration of 1 mM pHrodo™ working solution. 1×10^8 conidia were added to the working solution and after 40 min light-protected incubation at RT, the conidia were first washed with 10× Hank's balanced salt solution (HBSS) (Life technologies, Darmstadt, Germany). Next, they were washed once with 1:10 diluted DMSO, and then with HBSS as the last washing step. The pH calibration was done based on the manufacturer's protocol (Life technology, Darmstadt, Germany).

To prepare green-labeled spies, a vial of 1mg amine-reactive pHrodo™ STP ester, MW= ~750 (Life technologies, Darmstadt, Germany) was diluted with 150 µl no hydrous DMSO to generate the stock solution of 8.9 mM. By adding 0.1 M fresh sodium bicarbonate buffer to reach pH 8.3 and diluting it in DMSO to the concentration of 1 mM, the working solution was prepared. 1×10^8 conidia were immediately resuspended in pHrodo™ working solution. The incubation time was optimized to 60 min at RT and the remaining steps were carried out similar to the red fluorescent labeling steps. The pH calibration was accomplished based on the manufacturer's protocol (Life technology, Darmstadt, Germany).

6.2.8 Apoptosis induction

To induce the mitochondria-mediated apoptotic pathway (intrinsic apoptosis initiation), Staurosporine (STS) was used (Deshmukh and Johnson, 2000). Cells were cultured in a FCS-free medium and after 24 h of incubation, 1×10^6 cells were transferred to 6-well plates in the volume of 1 ml/well. STS with the concentration of 1.5 µmol was added to each well and after 4 h of incubation the cells were washed with PBS buffer and resuspended in fresh media.

6.2.9 Multi labeled samples

After 24 h of incubation at FCS-free medium, monocytes were washed and the nuclei were stained with 1 µg/ml DAPI in PBS for 15 min at RT. For the apoptosis-related assays, after the induction and 4 h further incubation, cells were washed once with cold PBS and colored with AnnexinV. The cells were again labeled with pHrodo™ Green AM conjugate and were infected with labeled conidia. For the assays with non-apoptotic cells, except the steps of induction and labeling with AnnexinV, the rest of treatment were the same. After transferring the final samples in to the 6-well plates and keeping incubation time for the 15 min, 40 µl of samples were loaded into the µ-slide VI $^{0.4}$ microchannel (ibidi GmbH, Martinsried, Germany) (**Fig.** 7c).

6.2.10 Measuring real-time pH during apoptosis

Since in this study all of the labels were pH sensitive, the intensity of transmitted signal from each label was representing the pH condition of the source of interest. After induction apoptosis and keeping 4 h of incubation time, apoptotic cells were resuspended in Live Cell Imaging Solution (LCIS) (Life technologies, Darmstadt, Germany). 10 µl of pHrodo™ Green AM probe (Life technologies, Darmstadt, Germany) added to 100 µl Powerload™ concentrate (Life technology, Darmstadt, Germany) and the resulting mixture was diluted into 10 ml of LCIS. The cells were centrifuged, washed and added to the mixture probe. After 30 min incubation at 37 ºC, cells were washed again with LCIS and injected into the micro channels. The hyperspectral measurement was carried out every 15 min. The pH calibration was accomplished using calibration kit provided by the manufacturer (Life technologies, Darmstadt, Germany).

By using different apoptosis indicators, the induced cells were sorted out. Since blebbing the plasma membrane and formation of apoptotic bodies confirm apoptosis (Elmore, 2007), at this stage induced cells were mounted on glass slides covered by cover slips and sealed with freshly opened nail polish. The changes in the nucleus, cell shrinkage and deformities were observed under ×1000 magnification (Customized Nikon Diaphot TMD microscope).
The progress of apoptosis in different stages (from early apoptosis to necrosis) was investigated by modified apoptosis assay (Rieger et al., 2011). Therefore, following the induction of apoptosis, cells were resuspended in Annexin-binding buffer (140 mM NaCl, 10 mM HEPES, 2.5 mM $CaCl_2$, pH 7.4). To label the induced but not necrotic cells, 10 µl of AnnexinV conjugate Ex/Em 650/668 (Life technologies, Darmstadt, Germany) was added to each well and incubated for 15 min at RT. To determine necrotic and dead cells (and exclude them from further analysis) 4µl of propidium iodide (PI) (Sigma-Aldrich, Germany) (that in advanced, has been diluted 1:10 in Annexin binding buffer to yield the concentration of 2mg/ml per well) was added to the wells, incubated for 15 min RT in the dark. Cells were washed accordingly with 500 ml Annexin binding buffer, and two more times with PBS. Finally they were injected into the micro channel.

6.2.11 Inhibition of intracellular acidification during apoptosis upon melanin presence

To check the outcome of preventing phagosomes-lysosome merging during apoptosis upon infection and also to study the effect of phagosomes-lysosome acidification, two assays have been performed.
First, after induction apoptosis the cells were treated with chloroquine as the chemical agent

which is capable of reducing enzyme activities in acidic compartments like lysosome (Bhat and Hickey, 2000) . For, 1×10^6 monocytes per well were induced by STS and treated with 20µM chloroquine (Sigma-Aldrich, Germany), incubated for 4 h in FCS free RPMI 1640 no phenol red at 37 ºC. After washing with PBS, the cells were seeded by either the wild-type or *pksP* mutant labelled conidia.

In addition, the effect of a further phagosomal acidification inhibition with Vacuolar ATPase (V-ATPase) inhibitor was examined. To study the effect of melanin towards the inhibition of V-ATPase during apoptosis, bafilomycin A1 was selected as it is a substance with the ability of preventing lysosome from degradation and maintaining the internal pH of this organelle (Fass et al., 2006).

1×10^6 monocytes per well were induced with STS, and then treated with 100 nM bafilomycin A1 (Sigma-Aldrich, Germany), incubated with RPMI 1640 no phenol red, no FCS for 4 h at 37ºC. The cells where washed with PBS and finally infected with either wild-type or *pksP* mutant labelled conidia.

6.2.12 Measuring the intracellular pH during apoptosis upon infection with other fungal samples: *A.clavatus, A.flavus* and *L. brasilliensis*

To declare that if only melanin has such influence on apoptosis upon interaction with the host-cell, two other species from the *Aspergillus* genus were selected based on their pigments structure. Additionally a non-pathogenic pigmented fungus (*L. brasilliensis*) from a different genus was selected to provide a reliable control. Although regarding the different colors of pigments (*A.clavatus:* gray*, A.flavus:* yellowish green and *L. brasilliensis* brownish) for each assay, the standard curves were individually generated. Labeling along with measurements was carried out likewise to the mentioned procedures.

6.2.13 Modifying the hyperspectral microscope

For this study, the HSI microscope was specifically designed and based on the requisite demands of project, was modified gradually. The settings for HSI microscope was adjusted in the visible objects mode. The unit was built up by a camera attached to an imaging spectrograph which with 80µm wide provided a spectral resolution up to 7nm. With 50% efficiency of light transmission, the internal reproduction scale was 1:1. Two C-month interface were connected to the objective lens as well as the camera which is a PCO *Sensicam* 680KU supplied by a sensitive Electron Multiplying Charge Coupled Device (EMCCD) sensor to be applicable in low light condition. The sensor physically is able to cool down to -11 ºC and it comprises 1004 × 1002 pixels. The HSI unit is attached to the side port of

inverse fluorescence microscope Nikon Diaphot TMD camera with a custom-built C-mount adapter (**Fig**. 7a). The spectra transmitted from conidia or host cell (**Fig**. 7b), were acquired via recording a narrow line of 200 × 2 μm^2 in sample within a circular object field of 450 µm. For each 1µm distance along this line, five binned pixels were acquired and this provided a spatial resolution of 0.2 µm per pixel. The fluorescence is excited by a Nikon epi-fluorescence attachment TMD-EF supplied by a mercury arc lamp. For splitting the excitation channels from emission, different interference filter sets were used.

To detect pHrodo Red, the filter cassette DM580 (excitation EX510-560, emission BA590) was used. Also, the filter cassette DM510 (excitation EX450-490, emission BA520) was used to detect pHrodo Green and DAPI. Annexin was detected by using a Chroma filter cassette #49913 (beam splitter ZT640rdc, excitation ZET635/20×, emission ET655lp).

The samples were injected to the microchannel flow chamber (**Fig**. 7c) to keep the numbers of cells fixed under the focused and made it possible to exchange and refresh the media when there was a need. The temperature of chambers was controlled by a heating stage and mostly adjusted to 18-20 ºC. Microscopic images were taken by a full-frame SLR camera (Nikon D600) attached to the front camera port of the microscope. For the single cell measurements, by observing one-dimensional line, a two-dimensional image was acquired (**Fig**. 7b). The signal intensity distribution reflects the fluorescence emission in space (vertically) and wavelength (horizontally). The region of interest within the sample contained the fluorescence emission from the selected spot labeled with different dyes and evidently resulted the compact information within emitted spectra.

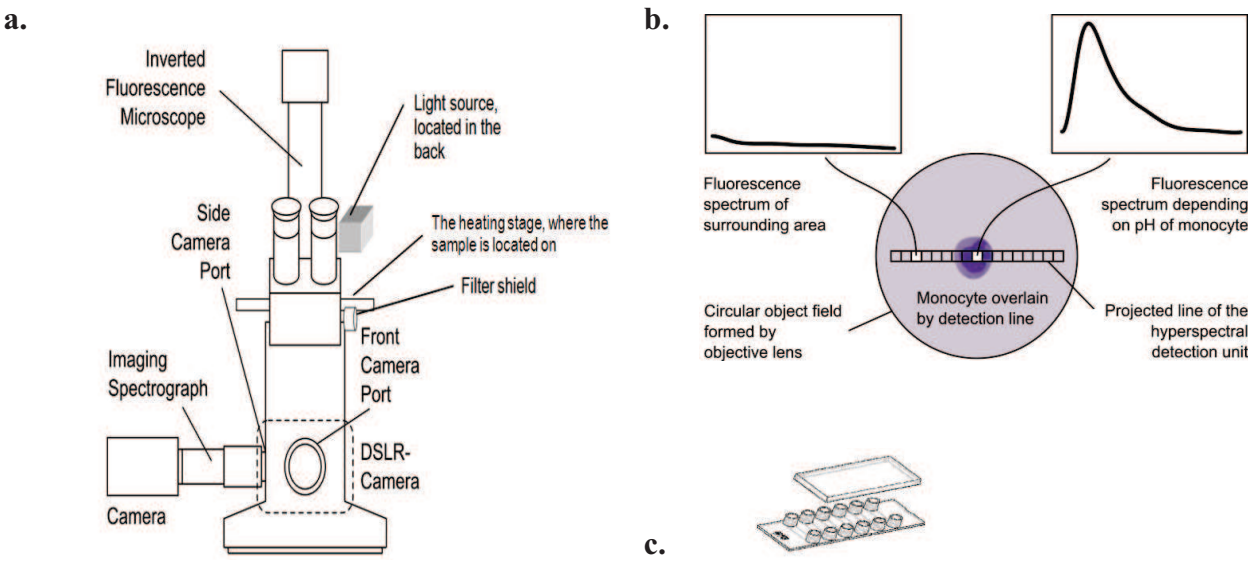

Figure 7. Hyperspectral imaging unit. **a.** HSI detector attached to the side camera port of an inverted microscope. This combination comprises the imaging spectrograph with sensitive monochrome camera. The fluorescence light source is located in the back of camera segment and is adjustable to

give an ample light intensity **b. The Different spectral responses at the distinct positions within the detected line**. The sample (here was an infected monocyte) was placed in the objective field spectra, and then the multiple spectra from the image of cell (the conidium or their background) were simultaneously acquired. **c**. **Microchannel.** The samples were loaded to the channel to minimize the media evaporation.

6.2.14 Processing images and data analysis

The recorded spectra, were processed using a Java-based program developed by the National Institute of Health; Image processing and analysis in java (*Image J* software) that converts the data pixels which have been generated from the images into quantified digits (http://imagej.nih.gov/ij/).

When the hyperspectral image is acquired, there will be columns of digits that needed to be summarized and converted into graphs. For, all the digits in order of their appearance were transferred to the Excel. As the figure in bellow shows, based on the purpose of experiment (showing the entire spectrum and measuring the highest peak or following the shifts between spectra in the time frames) (**Fig**. 8) the data points of interest were selected vertically or horizontally. These data generate the preliminary graphs.

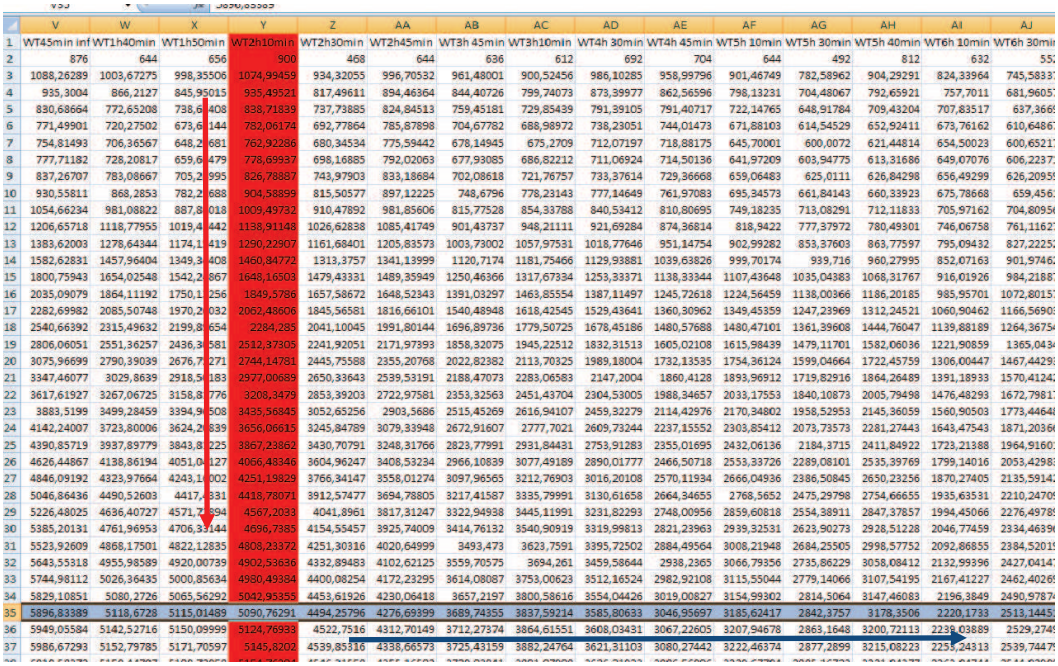

	V	W	X	Y	Z	AA	AB	AC	AD	AE	AF	AG	AH	AI	AJ
1	WT45min inf	WT1h40min	WT1h50min	WT2h10min	WT2h30min	WT2h45min	WT3h 45min	WT3h10min	WT4h 30min	WT4h 45min	WT5h 10min	WT5h 30min	WT5h 40min	WT6h 10min	WT6h 30mi
2	876	644	656	900	468	644	636	612	692	704	644	492	812	632	55
3	1088,26289	1003,67275	998,35506	1074,99459	934,32055	996,70532	961,48001	900,52456	986,10285	958,99796	901,46749	782,58962	904,29291	824,33964	745,5833
4	935,3004	866,2127	845,95015	935,49521	817,49611	894,46364	844,40726	799,74073	873,39977	862,56596	798,13231	704,48067	792,65921	757,7011	681,9605
5	830,68664	772,65208	738,6 408	838,71839	737,73885	824,84513	759,45181	729,85439	791,39105	791,40717	722,14765	648,91784	709,43204	707,83517	637,3665
6	771,49901	720,27502	673,6 144	782,06174	692,77864	785,87898	704,67782	688,98972	738,23051	744,01473	671,88103	614,54529	652,92411	673,76162	610,6486
7	754,81493	706,36567	648,2 681	762,92286	680,34534	775,59442	678,14945	675,2709	712,07197	718,88175	645,70001	600,0072	621,44814	654,50023	600,6521
8	777,71182	728,20817	659,6 479	778,69937	698,16885	792,02063	677,93085	686,82212	711,06924	714,50136	641,97209	603,94775	613,31686	649,07076	606,2237
9	837,26707	783,08667	705,2 995	826,78887	743,97903	833,18684	702,08618	721,76757	733,37614	729,36668	659,06483	625,0111	626,84298	656,49299	626,2095
10	930,55811	868,2853	782,2 688	904,58899	815,50577	897,12225	748,6796	778,23143	777,14649	761,97083	695,34573	661,84143	660,33923	675,78668	659,456
11	1054,66234	981,08822	887,8 018	1009,49732	910,47892	981,85606	815,77528	854,33788	840,53412	810,80695	749,18235	713,08291	712,11833	705,97162	704,8095
12	1206,65718	1118,77955	1019,4 442	1138,91148	1026,62838	1085,41749	901,43737	948,21111	921,69284	874,36814	818,9422	777,37972	780,49301	746,06758	761,1162
13	1383,62003	1278,64344	1174,1 419	1290,22907	1161,68401	1205,83573	1003,73002	1057,97531	1018,77646	951,14754	902,99282	853,37603	863,77597	795,09432	827,2225
14	1582,62831	1457,96404	1349,3 408	1460,84772	1313,3757	1341,13999	1120,7174	1181,75466	1129,93881	1039,63826	999,70174	939,716	960,27995	852,07163	901,9746
15	1800,75943	1654,02548	1542,2 867	1648,16503	1479,43331	1489,35949	1250,46366	1317,67334	1253,33371	1138,33344	1107,43648	1035,04383	1068,31767	916,01926	984,2188
16	2035,09079	1864,11192	1750,1 256	1849,5786	1657,58672	1648,52343	1391,03297	1463,85554	1387,11497	1245,72618	1224,56459	1138,00366	1186,20185	985,95701	1072,8015
17	2282,69982	2085,50748	1970,2 032	2062,48606	1845,56581	1816,66101	1540,48948	1618,42545	1529,43641	1360,30962	1349,45359	1247,23969	1312,24521	1060,90462	1166,5690
18	2540,66392	2315,49632	2199,8 654	2284,285	2041,10045	1991,80144	1696,89736	1779,50725	1678,45186	1480,57688	1480,47101	1361,39608	1444,76047	1139,88189	1264,3675
19	2806,06051	2551,36257	2436,3 581	2512,37305	2241,92051	2171,97393	1858,32075	1945,22512	1832,31513	1605,02108	1615,98439	1479,11701	1582,06036	1221,90859	1365,043
20	3075,96699	2790,39039	2676,7 271	2744,14781	2445,75588	2355,20768	2022,82382	2113,70325	1989,18004	1732,13535	1754,36124	1599,04664	1722,45759	1306,00447	1467,4429
21	3347,46077	3029,8639	2918,5 183	2977,00689	2650,33643	2539,53191	2188,47073	2283,06583	2147,2004	1860,4128	1893,96912	1719,82916	1864,26489	1391,18933	1570,4124
22	3617,61927	3267,06725	3158,8 776	3208,3479	2853,39203	2722,97581	2353,32563	2451,43704	2304,53005	1988,34657	2033,17553	1840,10873	2005,79498	1476,48293	1672,7981
23	3883,5199	3499,28459	3394,9 508	3435,56845	3052,65256	2903,5686	2515,45269	2616,94107	2459,32279	2114,42976	2170,34802	1958,52953	2145,36059	1560,90503	1773,4464
24	4142,24007	3723,80006	3624,2 839	3656,06615	3245,84789	3079,33948	2672,91607	2777,7021	2609,73244	2237,15552	2303,85412	2073,73573	2281,27443	1643,47543	1871,2036
25	4390,85719	3937,89779	3843,8 225	3867,23862	3430,70791	3248,31766	2823,77991	2931,84431	2753,91283	2355,01695	2432,06136	2184,3715	2411,84922	1723,21388	1964,9160
26	4626,44867	4138,86194	4051,0 127	4066,48346	3604,96247	3408,53234	2966,10839	3077,49189	2890,01777	2466,50718	2553,33726	2289,08101	2535,39769	1799,14016	2053,4298
27	4846,09192	4323,97664	4243,1 302	4251,19829	3766,34147	3558,01274	3097,96565	3212,76903	3016,20108	2570,11934	2666,04936	2386,50845	2650,23256	1870,27405	2135,5914
28	5046,86436	4490,52603	4417,4 331	4418,78071	3912,57477	3694,78805	3217,41587	3335,79991	3130,61658	2664,34655	2768,5652	2475,29798	2754,66655	1935,63531	2210,2470
29	5226,48025	4636,40727	4571,7 394	4567,2033	4041,8961	3817,31247	3322,94938	3445,11991	3231,82293	2748,00956	2859,60818	2554,38911	2847,37857	1994,45066	2276,4978
30	5385,20131	4761,96953	4706,3 144	4696,7385	4154,55457	3925,74009	3414,76132	3540,90919	3319,99813	2821,23963	2939,32531	2623,90273	2928,51228	2046,77459	2334,4639
31	5523,92609	4868,17501	4822,12835	4808,23372	4251,30316	4020,64999	3493,473	3623,7591	3395,72502	2884,49564	3008,21948	2684,25505	2998,57752	2092,86855	2384,5201
32	5643,55318	4955,98589	4920,00739	4902,53636	4332,89483	4102,62125	3559,70575	3694,261	3459,58644	2938,2365	3066,79356	2735,86229	3058,08412	2132,99396	2427,0414
33	5744,98112	5026,36435	5000,85634	4980,49384	4400,08254	4172,23295	3614,08087	3753,00623	3512,16524	2982,92108	3115,55044	2779,14066	3107,54195	2167,41227	2462,4026
34	5829,10851	5080,2726	5065,56292	5042,95355	4453,61926	4230,06418	3657,2197	3800,58616	3554,04426	3019,00827	3154,99302	2814,5064	3147,46083	2196,3849	2490,9787
35	5896,83389	5118,6728	5115,01489	5090,76291	4494,25796	4276,69399	3689,74355	3837,59214	3585,80633	3046,95697	3185,62417	2842,3757	3178,3506	2220,1733	2513,1445
36	5949,05584	5142,52716	5150,09999	5124,76933	4522,7516	4312,70149	3712,27374	3864,61551	3608,03431	3067,22605	3207,94678	2863,1648	3200,72113	2238,03889	2529,2745
37	5986,67293	5152,79785	5171,70597	5145,8202	4539,85316	4338,66573	3725,43159	3882,24764	3621,31103	3080,27442	3222,46374	2877,2899	3215,08223	2255,24313	2539,7447

Figure 8. Spectral data selection. Based on the aim of analysis, showing the entire spectrum in one measurement (vertically) or collecting the continuous data points from the spectra (horizontally), the data were selected.

The HSI unit is operated by proprietary software of the camera manufacturer, named *pco.camware* (Kelheim, Germany).To reduce the background signals and noises, the data was smoothed using the spline approximation. A spline is usually applied in modeling arbitrary functions and the one which was used here for analyzing the fluorescence spectra, is a (hybrid) polynomial function. It is a piecewise that is distinct by multiple sub-functions and is a polynomial on each of the sub-domains which are belonged to it (Dierckx, 1993).

To convert and save the plots in R, the version 3.2.3 of R program with the standard plotting function of the base package was used (https://cran.r-project.org/src/base/R-3/). Each plot comprised of two y axis and one x. Fist, after the importing data from Excel, the second y axis showing pH values was plotted through the integral formula: 7-7.2e-4 * x + 9.35e-8 * x^2 - 6.39e-12 * x^. Then to show the time points, the x axis was plotted manually. Finally to show the signal intensity the other y axis was plotted based on the original values generated by the microscope.

7 Results

7.1 Rate of residing wild-type and mutant conidia in monocytes is different

The wild-type conidia appeared to have different tendency to phagocytosis compared to the *pksP* mutant conidia. To calculate, cells in each well were seeded with FITS-labeled conidia and the successfully bound conidia, were transferred to the standard counting chamber. The data clearly showed that the internalization of *pksP* mutant conidia in MM6 monocytes was ~ 25% more than the wild-type (**Fig.** 9). However regardless of the type of conidia, for the healthy cells it usually took around 7-8 h to digest the conidia (**Fig.** 12). This difference in the rates of phagocytosis by MM6 monocytes, has been also observed in human neutrophils (Tsai et al., 1998) and THP-1 monocytes (Thywißen et al., 2011).

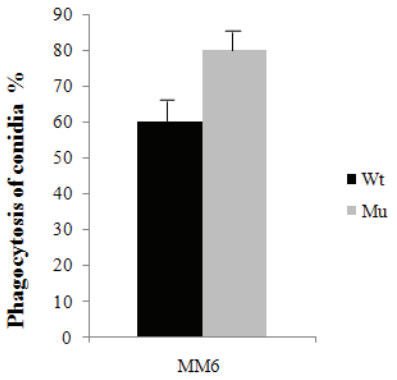

Figure 9. Determining the percentage of incorporated conidia with MM6 monocytes. Conidia were labeled with FITS, incubated 4 h in the cell culture and counted. Data represent the mean value and standard deviation (SD) from six experiments.

7.2 The intensities of fluorescent signals correspond to different pH values

The schematic figures (**Fig**. 10a, b) show the principle of the pHrodo dyes. Generally when the probes or the labeled infectious particles are taken to the cell, dependent on the stage of digestion (from early phagosomes to the final phagolysosome) pH will be gradually decreased. The signal that is associated with each phagocytosis stage, causes a unique curve which determining the pH value. Highly dependent on the color range of fluorescent dye, the wavelength of excitation and emission become different. However, the exclusive benefit of pHrodo probes is that the Ex/Em happens at the same area of color wavelength, therefore there is no need to use different filters to detect each probe (**Fig.** 10c).

Although the products have been basically designed for labeling the bacterial samples, by reconstruction and modifying the original protocol, its application could be used to coat different samples.

a. **b.**

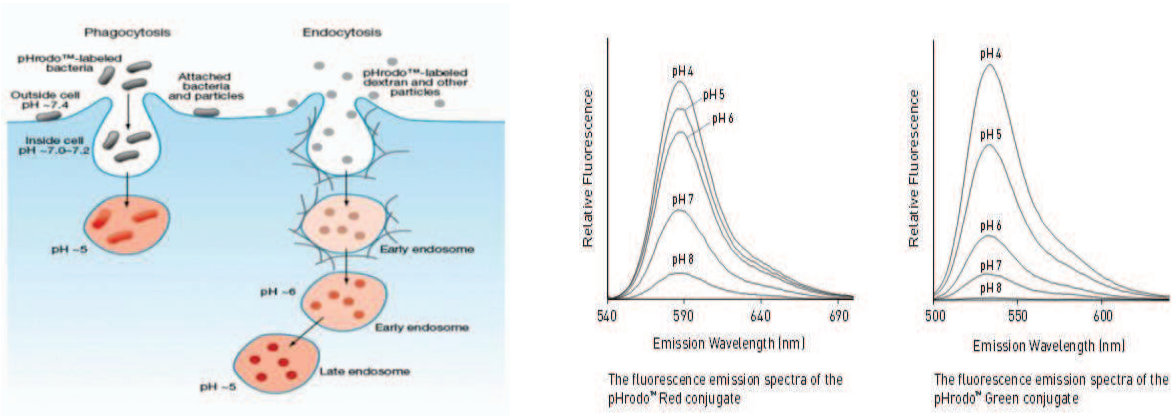

c.

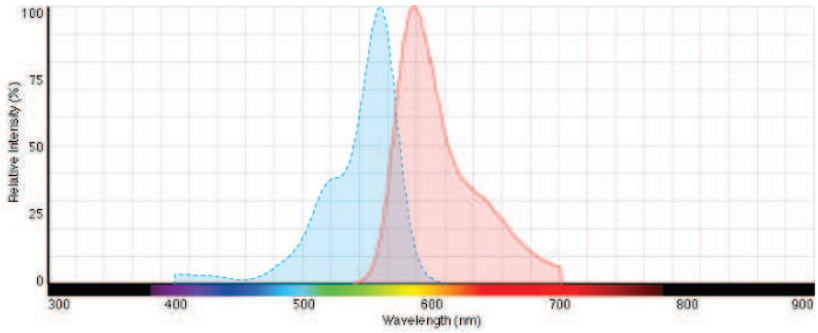

Figure 10. The principle of schematic pH sensitive labels. a. Cells are seeded with the microorganisms (or biomolecules) that have been labeled with pHrodo™ dye. The probes are highly sensitive to the changes of pH (the lower pH causes the brighter fluorescence and also the stronger signal). When the probes are non-specifically attached to the targets, the fluorescent signal will not be generated. As soon as the engulfed microorganisms have moved into the vesicles i.e. phagosomes, pH decreases and the particles will fluoresce brightly. **b. The spectra corresponding to each pH value.** Labeling in different pH condition, will result in different spectra. **c. The EX/Em range of the probe.** If the spectra overlap, the same filter can be used for detecting the sample. (Pub. no. MAN0009581, detailed protocol is available online at www.lifetechnologies.com/manuals).

Through the calibration of pH, all of the pH-sensitive dyes were measured at different pH condition 5 times and the average of each was determined as the final value. The images of labeled samples show the difference between neutral to very acidic conditions (Image 1).

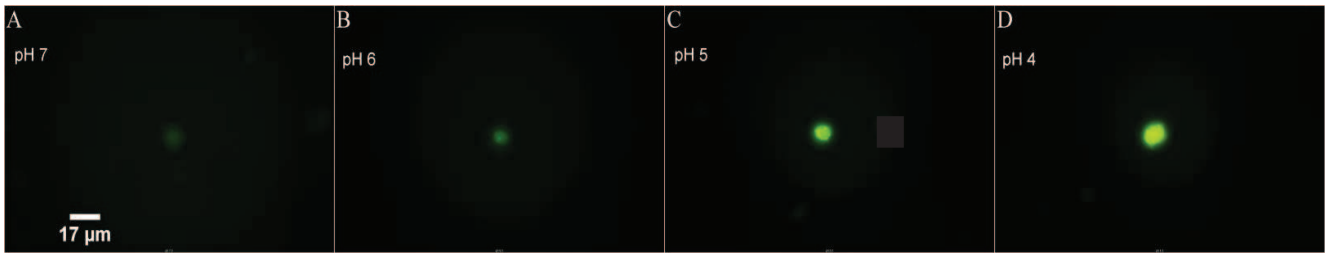

Image 1. The color intensity is reflecting the pH 4 – 7. To label monocytes, the pHrodo green pH-sensitive fluorescent dye was used at different pH buffers. The more acidic condition (D) caused the more intense color while in neutral pH the monocyte is hardly seen (A).

To determine the signal intensity of each pH value, the average of 5 measured signals was calculated and following elimination of background signals, the standard curve for each pH value was determined (**Fig.** 11).

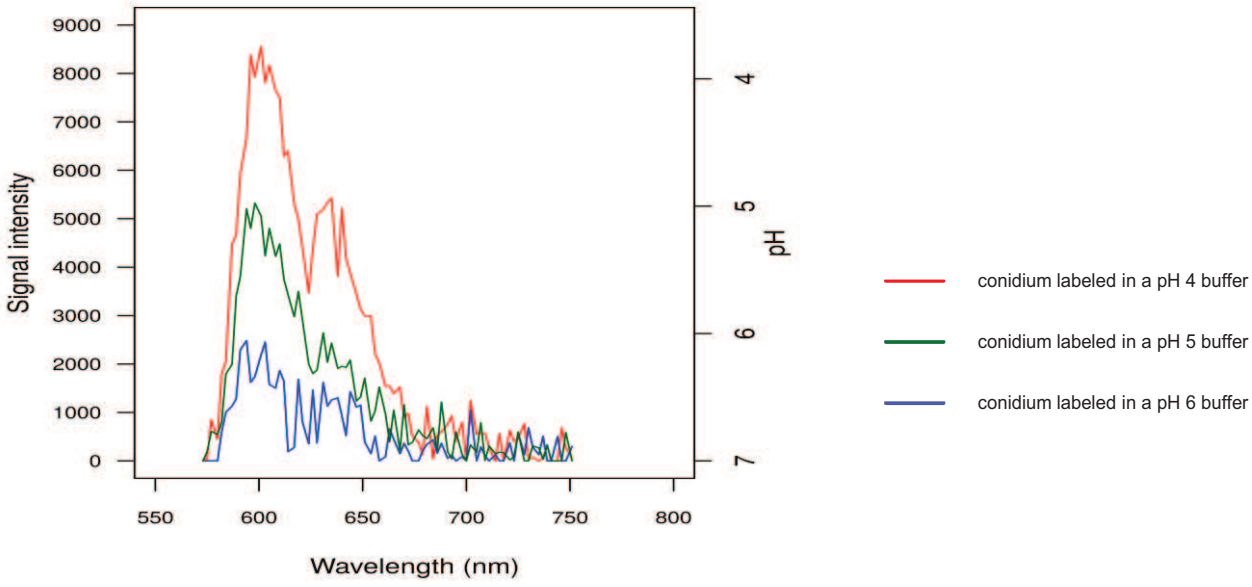

Figure 11. Standard curves for pHrodo Red fluorescent dye. Each curve corresponds to a certain pH value and is derived through averaging 5 measurements. The shift from each spectrum to the other is due to the change of pH values. The lower pH causes the higher signal and at the neutral pH no signal was detectable.

7.3 Determining the impact of *A. fumigatus* infection on monocytes

It was observed that within 4 h after infection with active and intact conidia, producing the hyphae will be initiated, making the host cell shrinks after 4 h p.i. due the hyphae formation (Serbina et al., 2009).Therefore to avoid of germlings, the conidia were heat-deactivated in advance. However, the heat- deactivation did not show any effect on the rate of phagocytosis of the conidia.

When the cells were infected with wild-type conidia, pH dropped within 1 h p.i. to 5.4, and it reached to 4.7. At 2 h p.i. it started to recover steadily and reached to pH 6.2. Finally, at 7 h p.i. the cell showed shrinkage (**Fig.** 12a). Interestingly, a different pattern was observed when the cell was infected with *pksP* mutant conidia (**Fig.** 12b). The first drop of pH appeared at 45 min p.i. and was stronger compared to wild-type conidia. It followed by a slight recovery to a pH of about 5.6. Then from this time onwards, pH stayed constant around 5.8 when the last signal was detected at 8:30 h p.i. The results are plotted together in **Fig.** 12c.

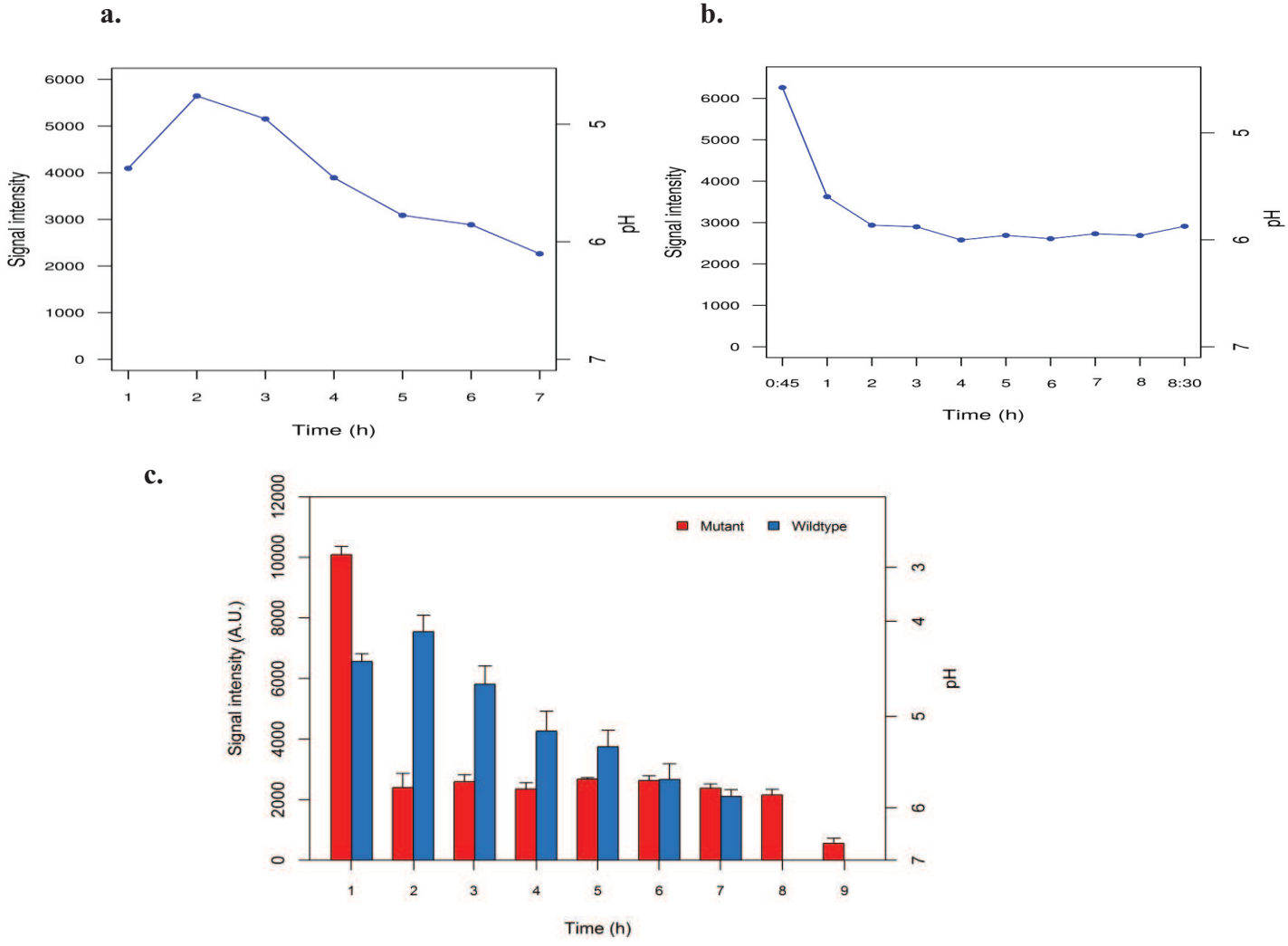

Figure 12. Monocytes infected with labeled wild-type conidia and *pksP* mutant conidia. The

highest peak representing the lowest pH (~pH 4.7) was observed 2 h p.i. After this time point, pH started to recover and finally reached to ~ 6.2. 7 h p.i. when the germination of conidia was initiated. **b.** The first signal of pH drop to ~ 4.4 was observed 45 min p.i. The pH slightly recovered, rose to ~ 5.8 and stayed constant. 8 h p.i. the cell shrank. **c.** The results from wild-type and mutant infection over 9 h are plotted together. Data present the mean value ± SD of three experiments.

7.4 *A.fumigatus* modulates apoptosis by adjusting intercellular pH trough digestion of melanin

Based on the results from previous study on apoptosis inhibition in macrophages by *A.fumigatus* (Volling et al., 2007) and regarding the fact that melanin can inhibit apoptosis in the host cell (Guobin et al., 1999), the role of *A. fumigatus* conidia on apoptotic cells with focus on intracellular pH was studied. As it has been shown before, apoptosis is generally accomplished within 4 h p.i. and during this time, the cells gradually display physiological malformation due to the appearance of apoptotic particles. Therefore, 4 h of induction was selected as the time point of introducing the infection. After the engulfment of conidia to the host cells, by measuring the spectra of pH changes, it was observed that pH was lower when the cells were apoptotic in contrast to the non-apoptotic cells. **Fig.** 13, shows the differences between the effect of melanized conidia and *pksP* white mutant conidia on both apoptotic and non-apoptotic cells. The spectra related to the uptake of wild-type or *pksP* mutant conidia were detected in the comparable pH value 6 h p.i. After 10 h, the mutant conidia showed a significant pH drop in the cell, whereas at this time point the spectrum for wild-type conidia was in the same range as before.

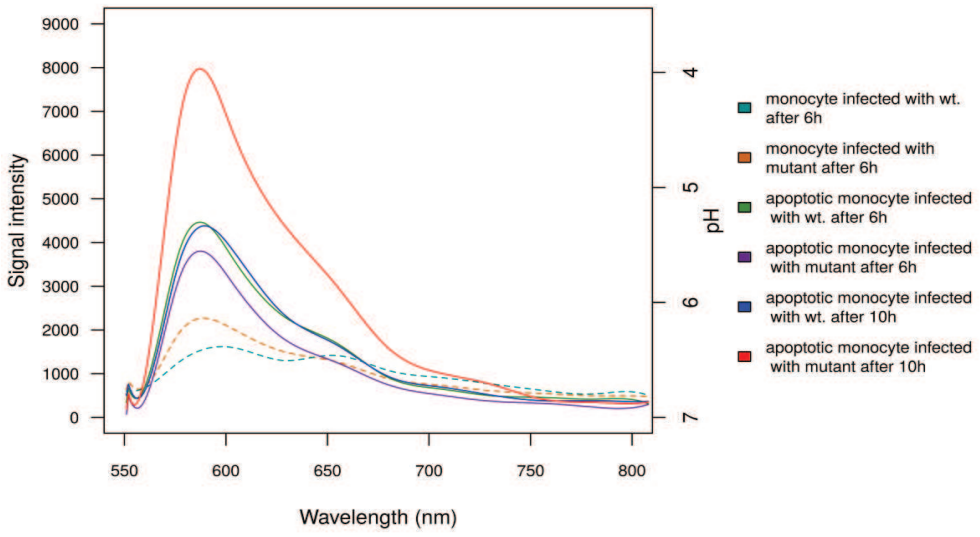

Figure 13. The entire spectra of intracellular pH upon *A. fumigatus* infection, in apoptotic and

non-apoptotic monocytes. Each spectrum shows pH at given time points (6 h and 10 h post infection). The dashed lines are the spectra of pH in wild-type (wt.) and mutant infection in non-apoptotic monocyte at 6 h p.i. when their pH appeared approximately in the same values (6.3 to 6.5). The constant lines represent the wild-type/ mutant infections in apoptotic monocytes. The most acidic pH (less than 4) was recorded 10 h p.i. from the mutant infection whereas at the same time point the monocyte infected with wild-type showed a higher pH around 5.3. Regardless of the type of infection, the signals in non-apoptotic cells were generally less intense than in apoptotic cells. 10 h p.i., the apoptotic cells infected with melanin-free *pksP* mutant conidia were far more acidic compared to cells containing wild-type conidia.

To study the possible correlation between cytosol acidification in an apoptotic monocyte and *A. fumigatus* infection, the labeled conidia were used as intracellular spies to report pH from their apoptotic host cells. First by comparing two single apoptotic monocytes which have been infected either by melanized conidia or white *pksP* mutant conidia, the effect of melanin on recovering the pH was determined. When the apoptotic monocyte had been infected with wild-type conidia, the cell apparently could survive and endure apoptosis while it was gradually recovering from acidic pH. In contrast, when the apoptotic monocyte had been seeded by melanin-free *pksP* mutant conidia, the cytosolic pH did not recover (**Fig**. 14 a, b).

a. **b.**

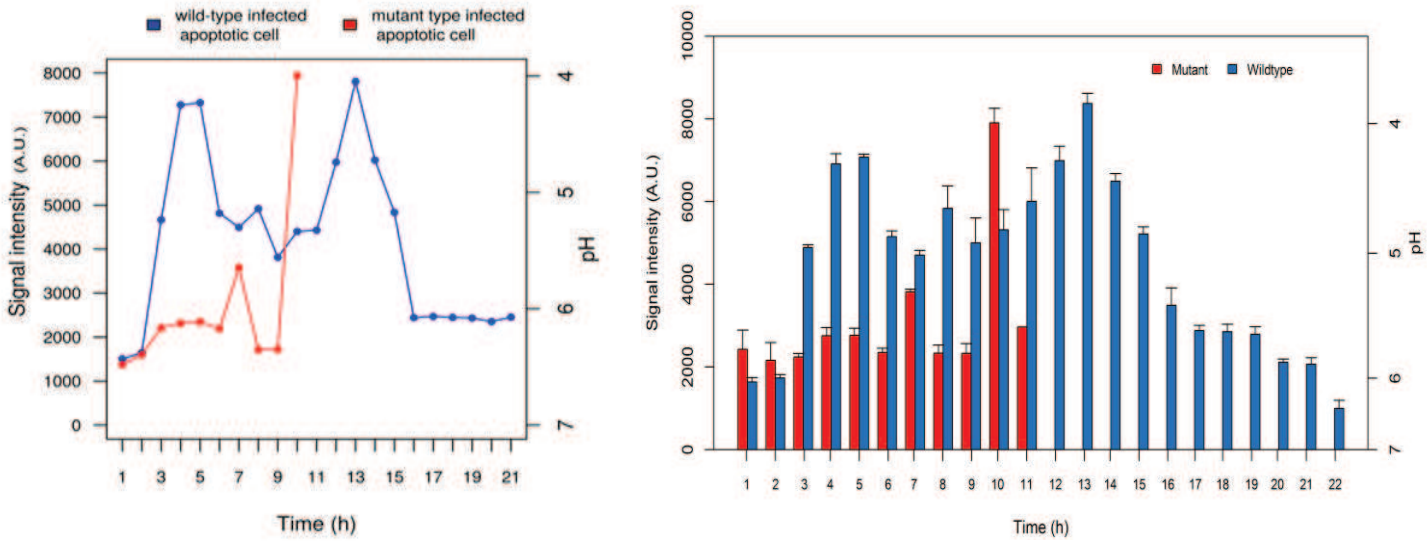

Figure 14. Monitoring the pH changes during *A.fumigatus* wild-type/mutant infection in an apoptotic monocyte. a. The behavior of pH in the apoptotic monocyte which is infected with labeled wild-type *A. fumigatus* conidia, in comparison to the apoptotic monocyte infected with labeled-*pksP* mutant conidia over 22 h. Red fluorescent pHrodo was used for labeling. Although in the mutant infection the apoptotic monocyte couldn't survive more than 9 h p.i., the apoptotic monocyte

infected with wild-type continued the life cycle along with gradual pH recovery. **b**. Data present the mean ± SD from three experiments.

Measurements of pH in apoptotic infected cells always showed a second peak representing the pH drop. Indeed, after this second pH drop, the type of infection (wild-type vs. mutant) had determined the fate of cell. The acidified pH in mitochondria is the certain consequence of the mitochondria-mediated apoptosis (Matsuyama and Reed, 2000), (Tait and Green, 2010). To investigate more, in addition to the labeled conidia, a second pH-sensitive dye which directly labeled the phagoysosme in cytosol was applied. By this means, the changes of phagolysosmal pH where the conidia have been already digested also could be identified. The signals from the cytoplasmic pH showed the same patterns as the signal from labeled conidia. Also the highest signals from the first and the second pH fall, were appeared around the same time that the signals related to the phagocytosis and digestion of conidia were recorded. Within this time frame of 35 h of measurements, the phagolysosome pH reached to 4 and the cell remained apoptotic during the entire time (**Fig.** 15a, b).

a.

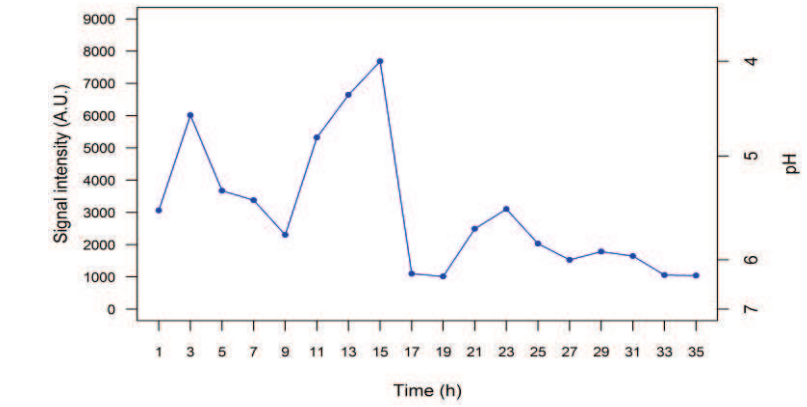

b.

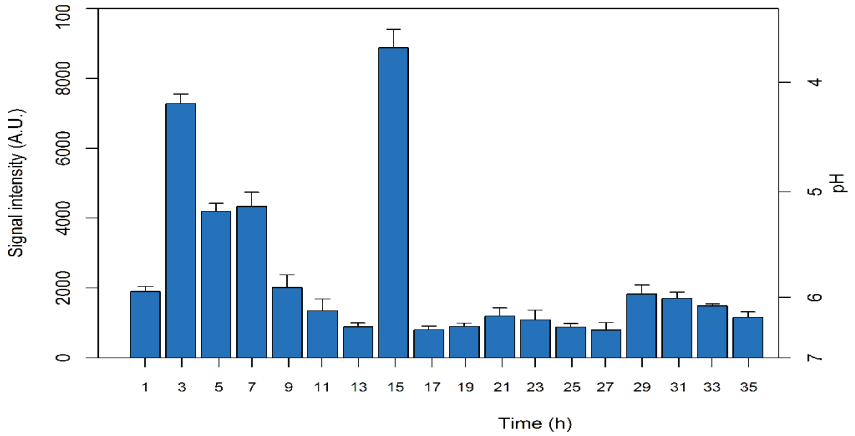

Figure 15. Measuring phagolysosome pH changes as a sign of apoptosis process in an *A.fumigatus*-infected apoptotic monocyte. a. In parallel with tracking the signals from conidia, the

phagolysosome was labeled with the Green fluorescent pHrodo. By switching the corresponding filters; different signals from each pH source were detectable. To detect mitochondrial pH, filter cassette DM510 for detecting green pHrodo was used. At time point 15 h post infection, the highest peak (representing the lowest cytosolic pH) was observed, which was correlated to the continuation of apoptosis and consequential acidic pH (Kim et al., 2003).The peak was identical to the second peak detected from wild-type conidia in **Fig.** 14**. b.** Data represent the mean ₊ SD from three experiments.

7.5 Melanin properties will be altered in different *A.fumigatus* mutants

Next, to provide the experimental controls, the intermediate *A.fumigatus* mutants were studied (image 2).

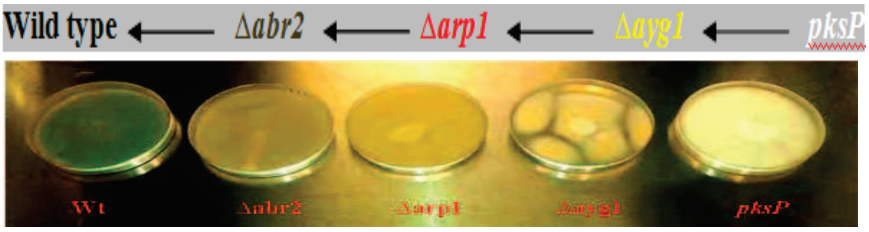

Image 2. Different morphologies in *A.fumigatus* due to the presence of melanin mutants. In melanin synthesis pathway, mutations will cause the formation of different intermediate molecules that produce different pigments with different colors and properties.

Applying the same method as mentioned in the previous chapter, the mutant conidia were labeled and introduced to an apoptotic monocyte. Interestingly, in comparison to the wild-type and *pksP* white mutant infection, pH showed in-between changes in the infected host cells. The darker pigmented conidia caused the lower pH when the cell had been acidic (**Fig**. 16-18).

So it was hypothesized that any circumstance which has modulated pH, a common substance should be present as the main effective factor. The melanin molecule is the best candidate to be addressed here, as it is responsible for the dark color of conidial pigments and its less complete structure is present in the lighter mutants. DHN-melanin that is located on conidial surface is generally produced by some fungi, including some of *Aspergillus* strains. The effect of melanin on host immune responses has been reported in many studies (Stanzani et al., 2005), (Miao et al., 2015).

In fact, the fungus has various strategies to suppress the host response in favor of establishing itself and spreading the virulence. These strategies include the uptake the conidia, reducing the phagocytosis rate and avoiding the complement system by binding to complement

regulators (Jahn et al., 2002), (Behnsen et al., 2008). By taking these facts into one account, it can be concluded that the longer life cycle which has been observed in apoptotic cell upon infection with darker mutants, is due to melanin and its ability to modulate pH while the light color mutants that contain only primitive forms of melanin molecule, did not show this ability.

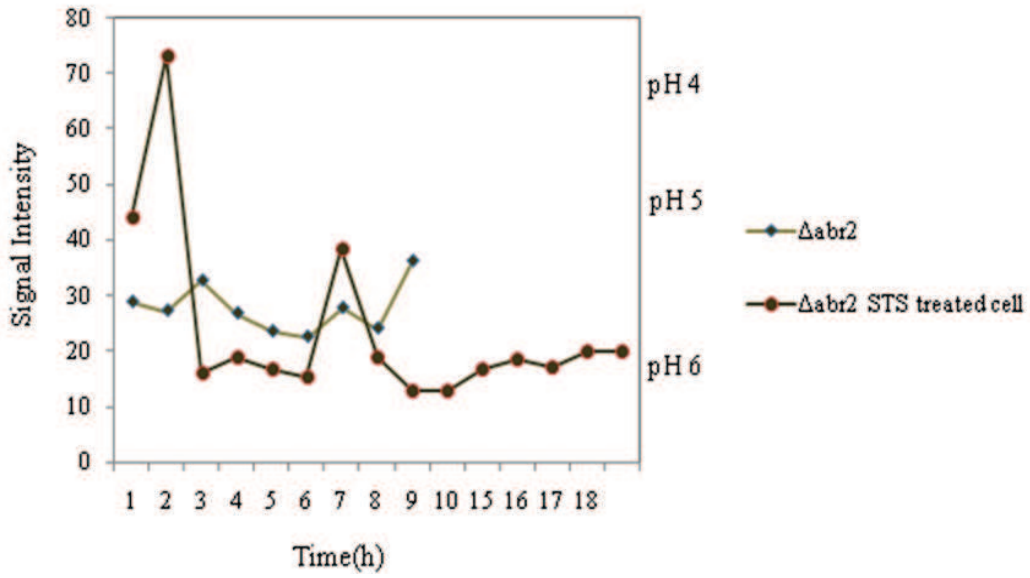

Figure 16. Intracellular pH of apoptotic and non-apoptotic monocyte infected with Δ*abr* (brown color) *A.fumigatus* mutant. Similar to the wild-type infection, the first drop of pH happened 1 h p.i. The lowest pH was observed within 2-3 h p.i. and then it was recovered to pH~ 5.5 and remained stable. The signal of pH was detectable up to 9 h. The cell was still alive at this moment but the shrinkage was started. The infection of apoptotic cell in the same condition with non-apoptotic cell appeared totally different. When the cell was undergoing apoptosis, the signal from the labeled conidia was detectable up to 15 h p.i. Also, from the second drop of pH (around 7-8 h p.i.) onward, pH was recovered to pH 6 and stayed constant.

Comparing the life time of surviving apoptotic cell infected with different mutants shows interesting results. It seems that among mutants, only the Δ*abr2* (brown mutant) could cause the cell to endure apoptosis for a longer period (**Fig**.16), whereas the two other (red and yellow) mutants similarly to the *pksP* white mutant, did not show such effect. Although in the infection with *A.fumigatus* red mutant, the final pH was around 5.4, and the life time of cell was 4 h shorter than the brown mutant infection (**Fig.** 17).

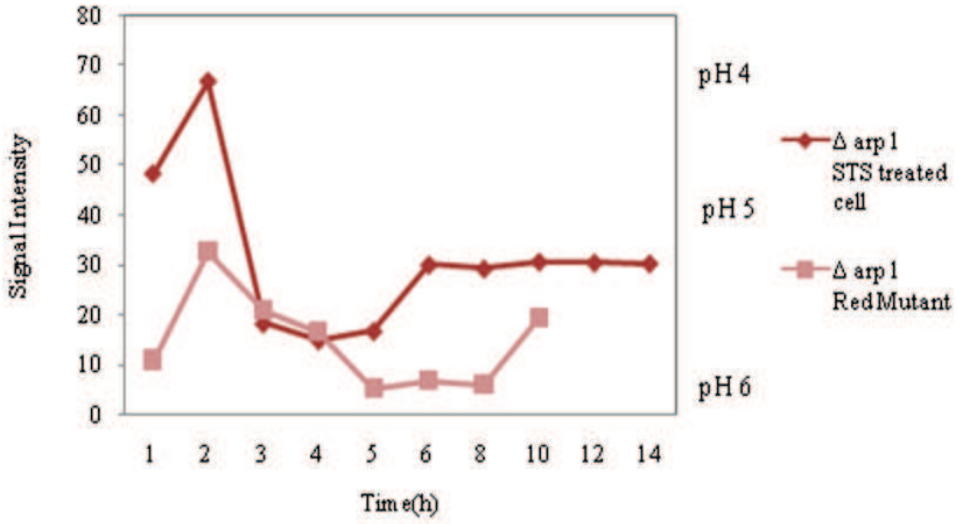

Figure 17.Intracellular pH of apoptotic and non-apoptotic monocyte infected with Δ*arp1* (red color) *A.fumigatus* mutant .The first drop of pH was observed at the same time (around 1h p.i.) in the both non-apoptotic and apoptotic monocytes. As expected, in apoptotic monocyte pH was more acidic at the beginning. In non-apoptotic infected monocyte, the pH signal was detectable up to 8 h, where the conidia were digested by the cell. In apoptotic infected cell, the pH signal was measurable up to 14 h. However, pH still was more acidic that compare to the wild-type or Δ*abr* infection. In contrast to the Δ*abr2* infection, the cell died faster.

Throughout the infection with the yellow mutant, pH showed the lowest value in compare to the darker mutants. The infection with yellow mutant did not show a significant difference neither in life time nor pH of apoptotic cell. In fact, the fate of cell was almost similar to when it was infected with *pksP* white mutant.

The observed difference or similarities in the results from examined mutants were addressed to the presence of melanin. Consequently, in the absence of melanin the mutant conidia did not interfere with apoptosis and therefore the cell remained in the acidic condition until entered the lethal phase.

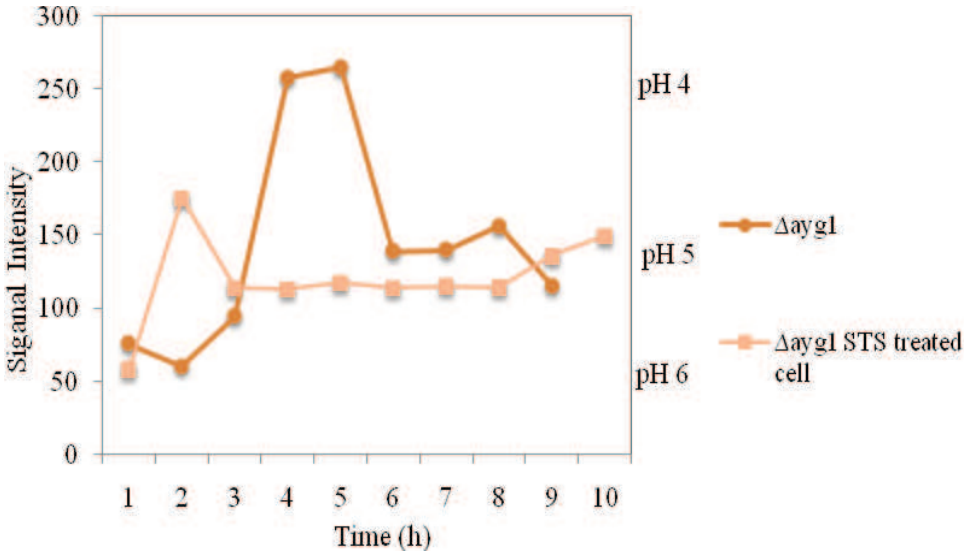

Figure 18.Intracellular pH of an apoptotic and non-apoptotic monocyte infected with Δ*ayg1* (yellow color) *A.fumigatus* mutant. In the both apoptotic and non-apoptotic cells, the pH remained acidic during the infection. The apoptotic cell could endure the infection up to 10 h, when pH decreased to ~ 4.8 and the cell shrank. Interestingly the life-time of the apoptotic cell was similar to the cell that had been infected with Δ*arp1* mutant (**Fig.** 17) rather than infection with Δ*abr2* (**Fig.** 16).

7.6 The inhibition of cell acidification is dependent on melanin but is not limited to *A.fumigatus*

A.clavatus has the similar pigment to *A.fumigatus* (HKI unpublished data bank). Therefore, it provides a reliable indicator in determining the effect of *A.fumigatus* on an apoptotic cell and its intracellular pH. Since the modulation of pH by *A.fumigatus* has been correlated to the melanin, it is expected that *A.clavatus* shows the same impact on the apoptotic cell.
Two different species from *Aspergillus* genus were selected to evaluate the effect of their pigments in comparison with *A.fumigatus* conidia.
When the apoptotic cell has been infected with *A.clavatus*, the effect of its conidia on pH was similar to the *A.fumigatus* wild-type. The apoptotic cell endured apoptosis and from 11 h p.i. onwards, the pH started gradually increasing (**Fig.** 19).

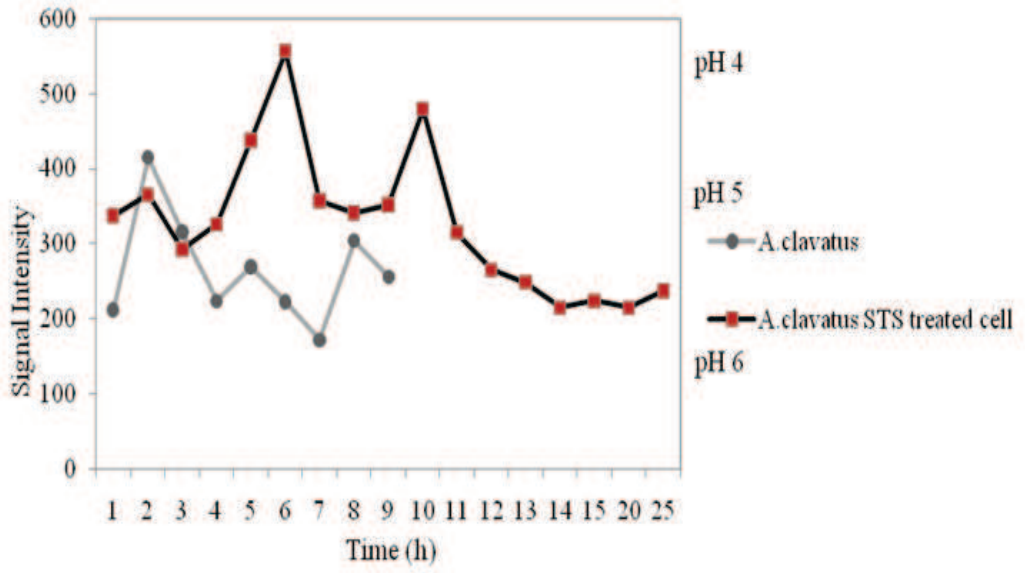

Figure 19. Intracellular pH of apoptotic and non-apoptotic monocyte infected with *A.clavatus*. Comparing two graphs of pH in non-apoptotic vs. apoptotic cell, indicates the effects of melanin on apoptosis. Once the apoptotic cell has been infected with *A.clavatus*, despite the acidic condition which normally is the phenomenon of ongoing apoptosis, pH was gradually recovered and the cell could bare the stress for much longer time (26 h) which is comparable to the result from *A.fumigatus* wild-type infection.

Expectedly, when the apoptotic cell had been infected with a fungus that its pigment has different molecule than melanin, the outcome was different. *A.flavus* produces either yellowish to red pigments that their molecule is being formed through Aflatoxin secretion (Assante et al., 1981), or greenish-yellow pigments which is belong to *pks*-derived secondary metabolites (Cary et al., 2014). When the cell was infected with this fungus, after the first pH drop due to the initiation of phagocytosis, pH gradually returned to acidic condition and the cell would stay alive for 15 h p.i. But when the cell was apoptotic in advance, the infection showed no impact on the apoptosis fate including the pH. Moreover the cell life cycle reduced to half compared to the non- apoptotic cell (**Fig.** 20).

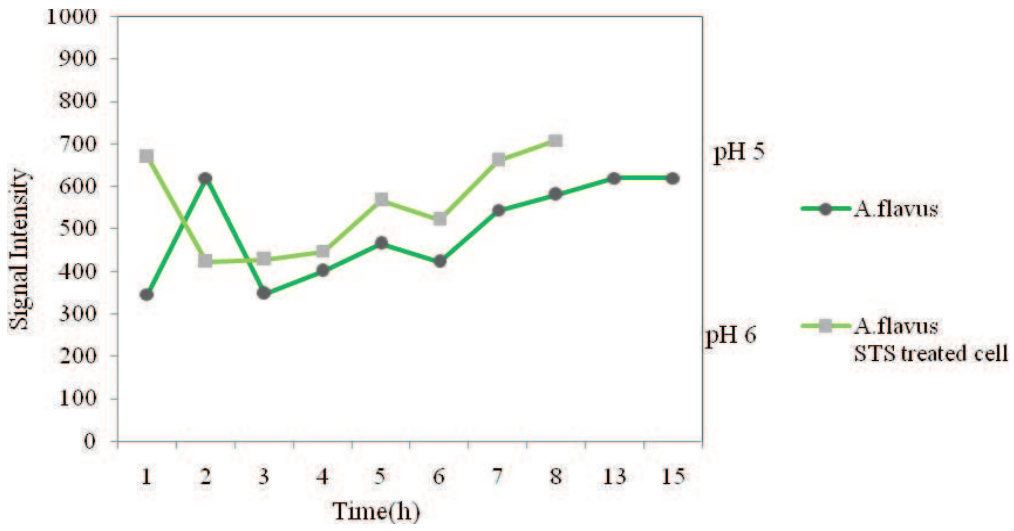

Figure 20. Intracellular pH of an apoptotic and non-apoptotic monocyte infected with *A.flavus*. For the period of the infection with *A.flavus*, despite the first pH drop due to the early minutes of engulfment, the monocyte did not show much acidic condition. The pH barely reached to lower than 5 but still the signal was detectable until 10 h p.i. In the apoptotic cell, following the second drop of pH, it gradually reduced until the cell is dead at 8 h p.i.

In comparison to the assayed *Aspergillus* spp., the non-pathogenic fungus *L.brasiliensis* was considered as an alternative choice for negative control. It contains different types of conidia (Sporangiospores) and is the most basal fungus among the other members of the genus (Schwartze et al., 2014). Since the fluorescence of the pigment is not so strong, the conidia were first labeled and then introduced to the cell. As it was predicted, the *L.brasiliensis* infection did interfere neither with apoptosis, nor the intracellular pH of an apoptotic cell (**Fig.** 21). The spectrum of pH, indicated on the preference of fungus for the basal environment. The infection slightly reduced the intracellular pH in a non-induced cell. In contrast, when the cell is apoptotic, the pigment did not appear to modulate the pH and the cell started the death phase.

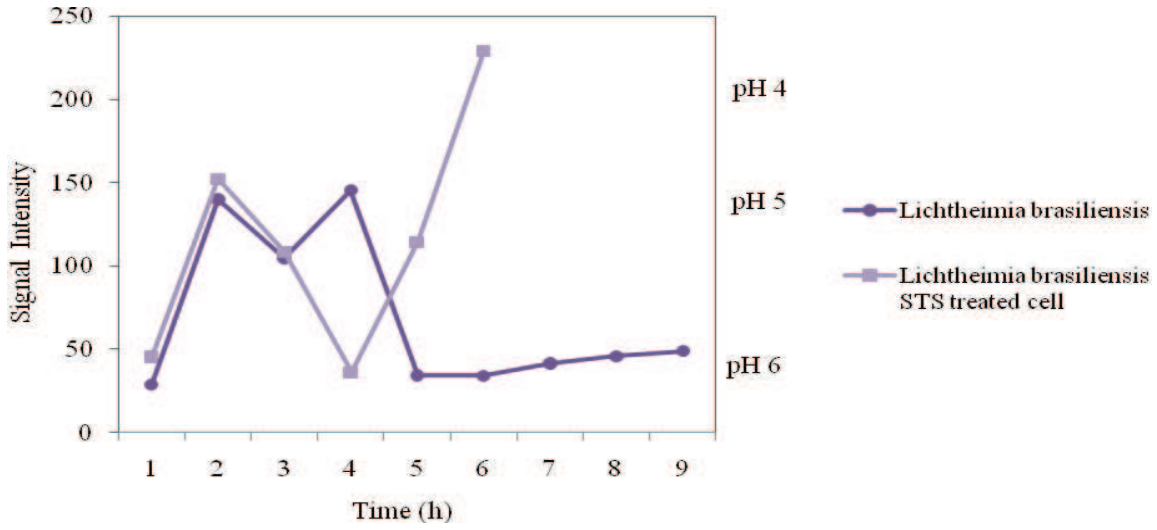

Figure 21. Intracellular pH in an apoptotic and non-apoptotic monocyte infected with *L.brasiliensis*. The first peak in both figures showing the acidic condition due to the engulfment of conidium to the host. Although the non-induced cell could survive more than 9 h post infection and the pH value remained constant around 6, apoptotic cell died after 6 h p.i. with the final pH was less than 4. *L.brasiliensis* prefers the basic pH, then the pH fall in induced cells is only related to the ongoing apoptosis and the pigment cannot modulate it.

7.7 Prevention of phagosomes-lysosome merging reverses the anti-apoptotic properties of melanin while perturbing V-ATPase shows no impact on it

When the conidia have been inhaled and localized to the respiratory tract, the first response of the lung cells towards the fungal particles is phagocytosis around alveoli of the lung . Next, conidia are bound into the phagocytes, endosomes are formed and then phagosomes merge with endocytic organelles, i.e. the lysosome establishing the highly acidic compartments to remove the fungal particles. By producing digestive enzymes, these compartments are responsible for eliminating the pathogens and preventing them from metabolic adaptation in host cells (Jahn et al. 1997). It has been shown that during infection with *pksP* mutant, the rate of phagosomal formation is five time more than melanized *A.fumigatus* since wild-type conidia appeared to reduce the formation of phagolysosomes effectively (Jahn et al., 2002). Interestingly, similar to the effect of *pksP* mutant infection, the same results have been obtained when the cell was treated with chloroquine since chloroquine is able to prevent the phagosomes- lysosome fusion. When the cell is exposed to chloroquine, the environment in the phagolysosomes will be preserved (Volling et al., 2011).To examine the impact of melanin on the acidic environment in light of its anti-apoptotic properties, apoptotic cells

were exposed to chloroquine. As expected, after stimulating the apoptotic cells with chloroquine, neither wild-type nor *pksP* mutant infection, reversed the acidic pH or rescued the cells (**Fig.** 22).

Volling et al. 2011 indicate that chloroquine appears to be an inhibitor of caspases-3 that maintains the cellular pH.Therefore, as infected apoptotic cells did not recover from the acidic pH after the treatment with chloroquine, it was concluded that phagocytosis of pigmented conidia and the correct localization of melanin within the phagolysosome is highly crucial for inhibiting apoptosis and acidification. Complementary but unlike to the effect of chloroquine, bafilomycin was used to establish pH in the phagosomes, preventing it from integration with lysosome by inhibiting the vacuolar ATPase (V-ATPase) and perturbing the phagosome acidification (Bowman et al., 1988). Interestingly, in the presence of bafilomycin, melanized *A.fumigatus* was not affected by the V-ATPase inactivation to modulate the acidic pH during apoptosis, whereas infection with *pksP* mutant did not recover the pH (**Fig.** 23).These results point it out that melanin needs to be successfully localised into the pahagolysosome, being capable of responding to the apoptosis signals but also it can impose this fusion when it has been prevented in advanced via V-ATPase inactivation.

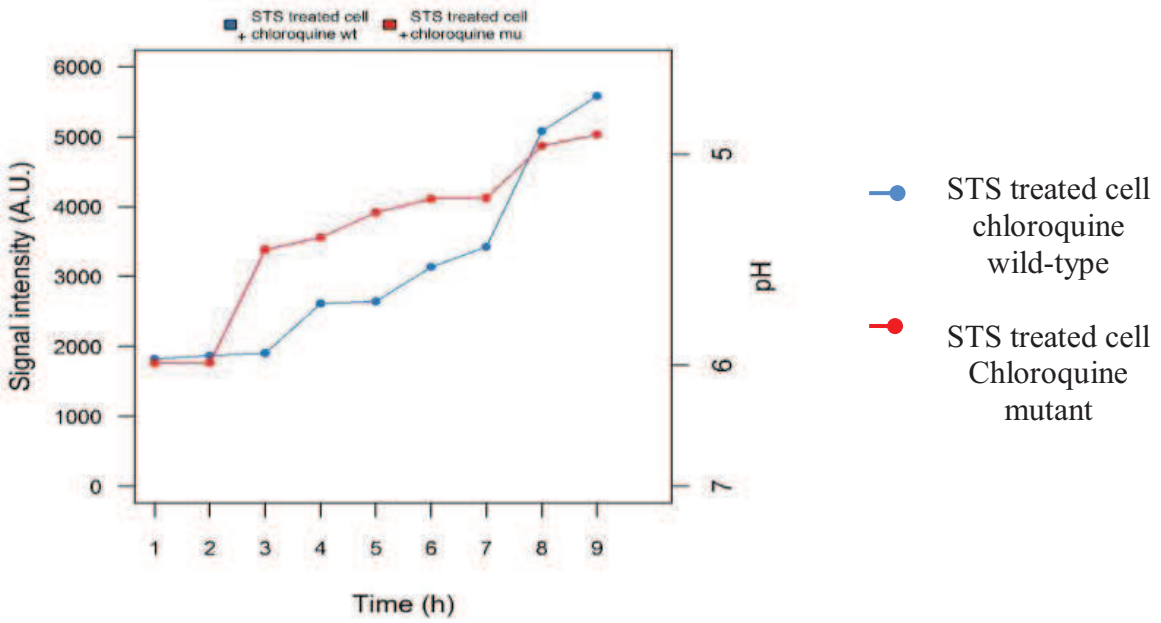

Figure 22.Effects of chloroquine treatment and inhibition of phagosomal acidification upon *A.fumigatus* infection in an apoptotic monocyte. The acidified pH of the apoptotic cell in the presence of chloroquine was maintained after the infection. *A.fumigatus* only interferes with pH if the phagolysosome stays intact.

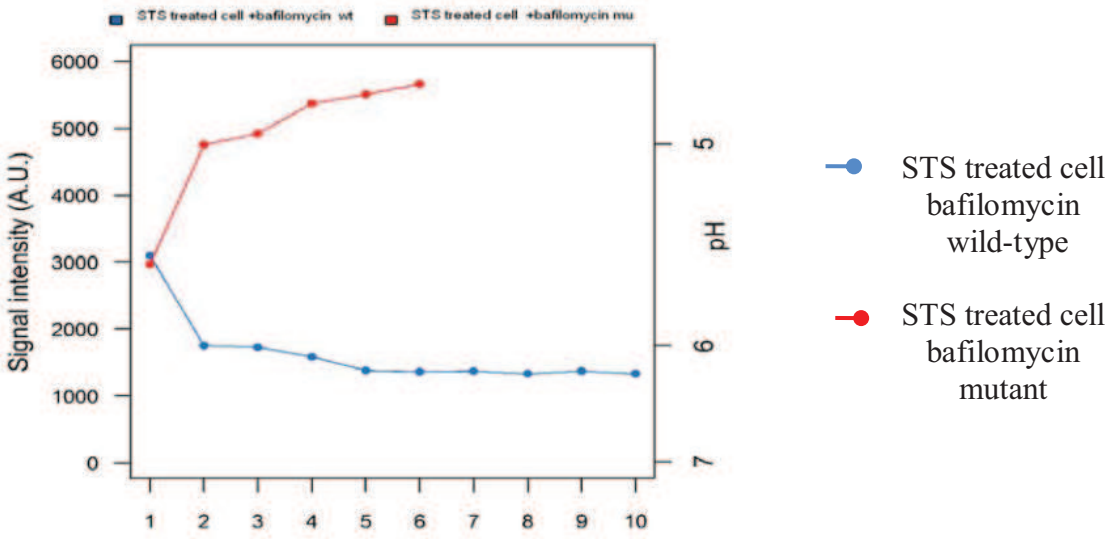

Figure 23. Effects of bafilomycin A1 treatment and V-ATPase inhibition in *A.fumigatus* infected apoptotic monocyte. Bafilomycin A1, effectively reduces the V-ATPase efficiency and regulates the cytokine responses (Ip et al., 2010). In the presence of bafilomycin, melanin infection was not affected by the substance and the intra-cellular acidification was inhibited by the conidia.Wild-type infection caused pH neutralization, while the *pksP* mutant was not able to recover the acidic pH.

7.8 Statistical figures

Although within a cell population the gene expression is ubiquitous, due to some molecular and non-genetic heterogeneity the experimental observations and analysis in the single cell level could show differences from one cell to another (Huang, 2009). Such variations are not avoidable since they are mostly derived from the natural biological variance. Also, in any circumstances that the external environment is slightly differed, the response to the same stimulus could not be different (Reiter et al., 2011).Thus, when a single cell is considered as an *in-vivo* case study, obtaining exactly the same values from each trial is not expected but the pattern of intracellular changes and cell fate decision should be in the same direction (Levsky and Singer, 2003).

Levesky and Singer interpreted the outcome in single cell analysis as ‘‘*an averaged cell*’’ which is a contrivance for showing the data beyond than the capacity of detection method. For this project, each experiment has been repeated at least three times in biological duplicates to provide reliable statistics. The pattern of pH changes and the cell fate in all experiments were identical, indicating that the data are reproducible.

Most notably, hyperspectral analysis due to its design provides the data series which include the entire spectral information of a target of interest in each pixel.Then the data all together are immediately available to the system in one collection (Wilson and Latifi, 2014). By that

means, through each measurement, the data-load itself comprises the statistics (Hernandez-Palacios et al., 2011). However, the results from the key experiments (**Fig.** 12a, b), (**Fig.** 14a) and (**Fig.** 15a) were supplementary graphed together in a way that each of figures shows three experimental replica together. As demonstrated here, despiteful the fact that cells of each replica are not standing in the exact time points against pH, they are significantly follow the same pattern that each pH value is expected to be achieved within the similar time frame.

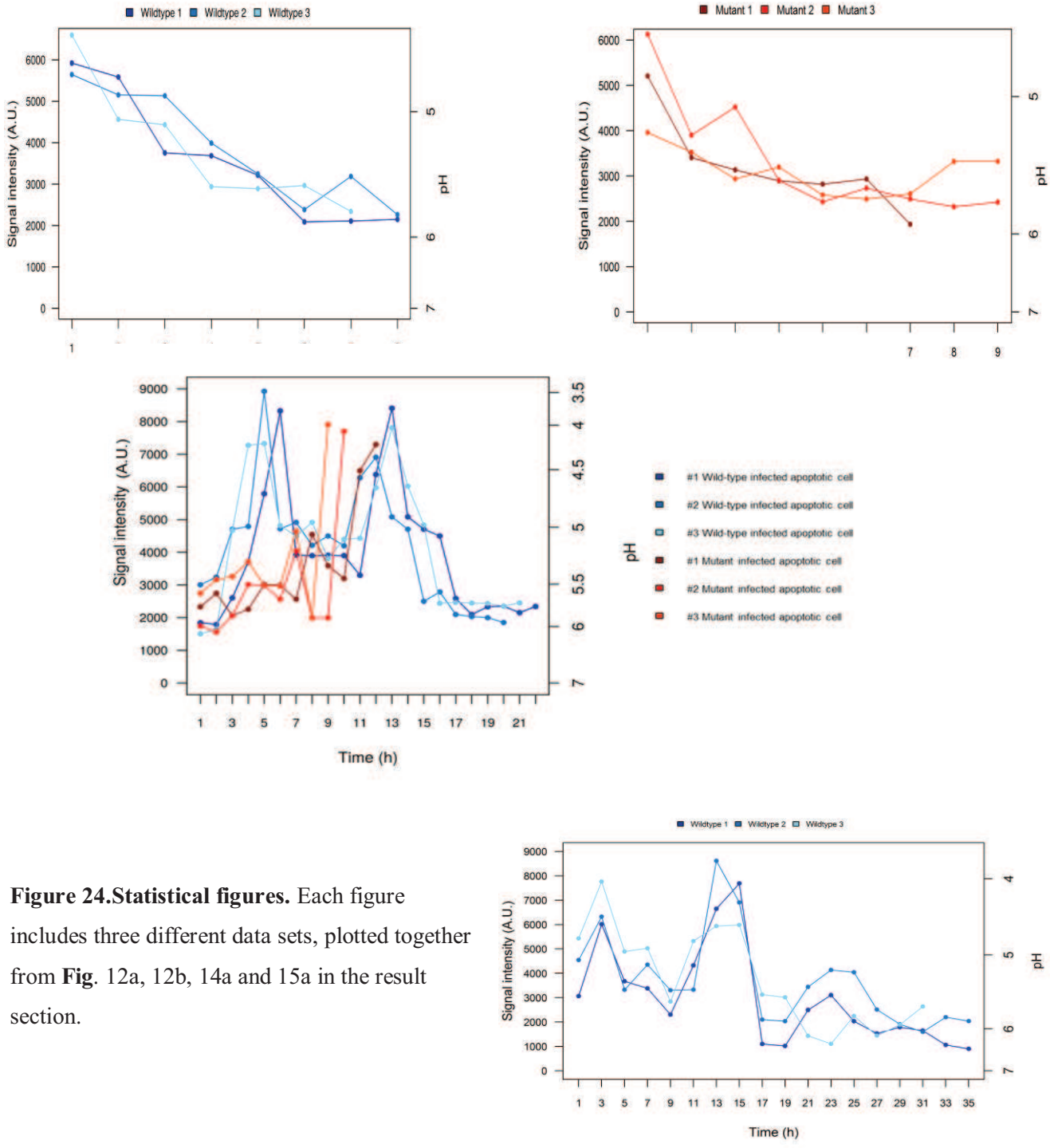

Figure 24.Statistical figures. Each figure includes three different data sets, plotted together from **Fig**. 12a, 12b, 14a and 15a in the result section.

7.9 Imaging the different stages of apoptosis and the alterations during infection

Along with the hyperspectral measurements, a series of fluorescence microscopic images were acquired from the cell events. Different apoptotic phases (early apoptosis, late apoptosis, necrosis and cell death phase) were imaged by STS-induced cells treatments with AnnexinV and propidium iodide (PI). The stronger fluorescence and brighter colour indicated advanced apoptosis, while ultimately turned to necrosis (Image 3). Within 4 h after apoptosis induction by STS, those apoptotic but not necrotic cells were selected for the experiments and the rest of cells were excluded.

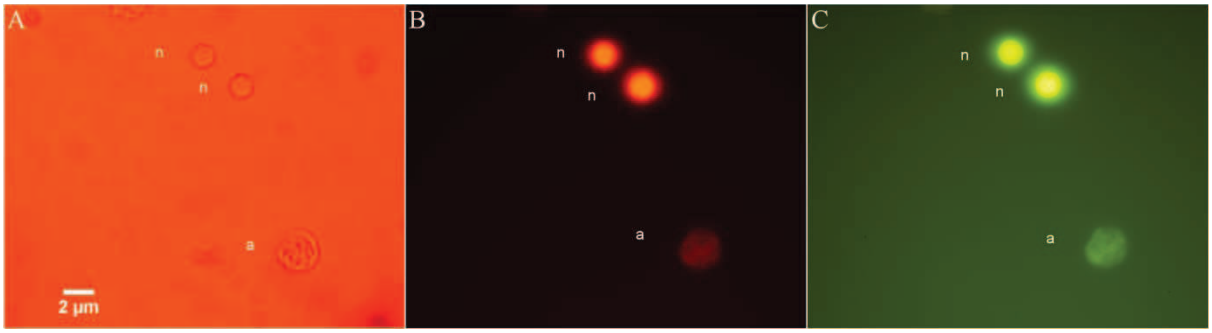

Image 3. Monocytes treated by STS and labelled with AnnexinV and PI.
5 h after STS treatment the apoptotic cells papered bright while the shinier cells are necrotic cells.
(A) White light, Chroma filter cassette 49913 (beam splitter ZT640rdc, excitation ZET635/20x, emission ET655lp) filter,
(B) Chroma filter cassette 49913, (C) Green filter cassette DM510 (excitation EX450-490, emission BA520).
a: apoptosis
n.: necrosis.

When the suitable monocyte (apoptotic but not necrotic) was detected, it was selected as the sample of target for the further treatments and analysis. This way, the already dying cells or the cells have not induced, were eliminated from the study. The target cells were injected to the new channel and the treatments with different probes or conidia were carried on accordingly. Since the different probes (apoptosis detectors and labelled conidia) did not overlap, the cell event after infection was detectable in parallel with apoptosis (Image 4).

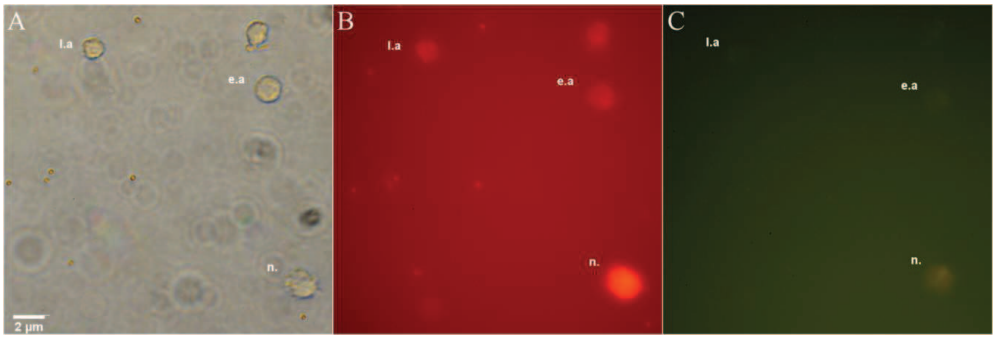

Image 4. Monocytes treated by STS and labelled with AnnexinV and PI.
5 h after the STS treatment, the apoptotic cells appeared relatively bright while the brightest cells were necrotic cells. (A) No filter, (B) Chroma filter cassette 49913 (beam splitter ZT640rdc, excitation ZET635/20x, emission ET655lp), (C) Green filter cassette DM510 (excitation EX450-490, emission BA520).
l.a: late apoptosis
e.a: early apoptosis
n.: necrosis.

Through the infection, along with hyperspectral measurements the images were recorded from the cells of interest.
The cells were infected with *A. fumigatus* wild-type and *pksP* mutant conidia and the further changes in colour intensity were imaged (Image 5). Although the monocytes infected with wild-type conidia (5 A) were still apoptotic as the corresponding label shows (5 C), no acidic pH was detected 7 h p.i. (5 B). In contrast, apoptotic monocytes infected with mutant conidia (5 D) with the same set up showed acidic pH condition (5 E) along with the ongoing apoptosis (5 F).

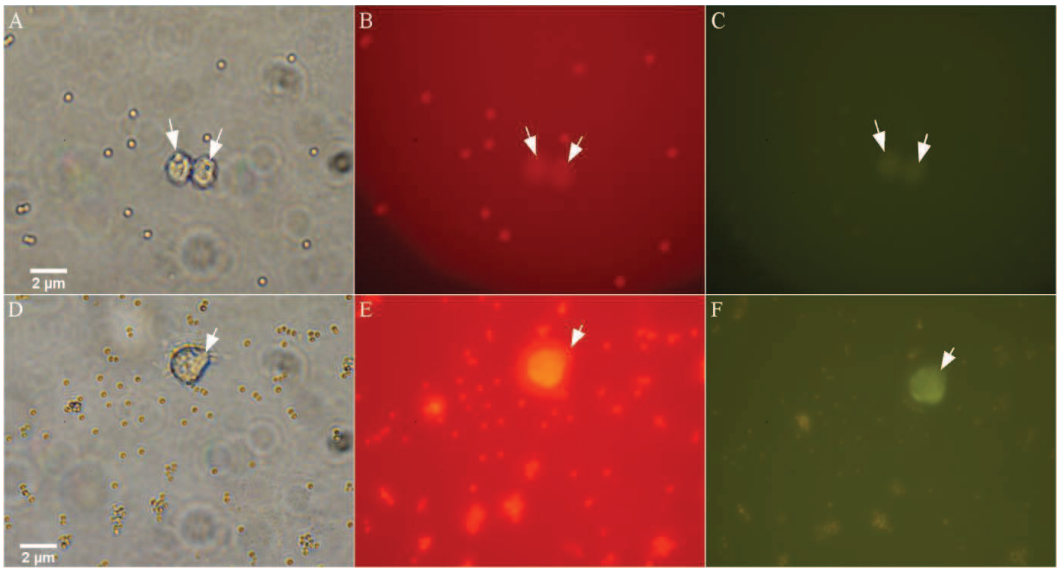

Image 5. Apoptosis-induced monocyte infected with *A. fumigatus* wild-type and mutant conidia. (A, B, C) Images are taken with different filters from the labelled apoptotic monocytes 7 h p.i. The cells were infected with wild-type conidia (labelled with pHrodo Red). To monitor apoptosis at different stages, the cytosols were labelled with pHrodo Green. After 7 h, when the pH returned to neutral (A), the conidia within the cells were hardly detectable (B). The slightly brightened spots in monocytes in image C, indicate that apoptosis has been sustained. (D, E, F) Images from apoptotic monocytes infected by *pksP* mutant conidia. The high intensity of red label in the image E shows the acidic condition reported from conidia, contrary to the infection with wild-type conidia at the same time point (image B). The bright flourscent detected in image F shows the acidic cytosol, as a result of mitochondrial-driven apoptosis (compared to image C). (A, D): No filter, (B, E): Chroma filter cassette 49913 (beam splitter ZT640rdc, excitation ZET635/20x, emission ET655lp), (C, F): Green filter cassette DM510 (excitation EX450-490, emission BA520). Arrows point out the location of the detected cells.

The general condition of cytosol in both cases of melanized wild-type and *pksP* mutant infected cells, at14 h p.i. displayed a significant differences between these two types of infection. The pH sensitive probe, in the apoptotic cell infected with wild-type conidia appeared to be less intense while in mutant infection the cytosol is extremely acidic (Image 6).

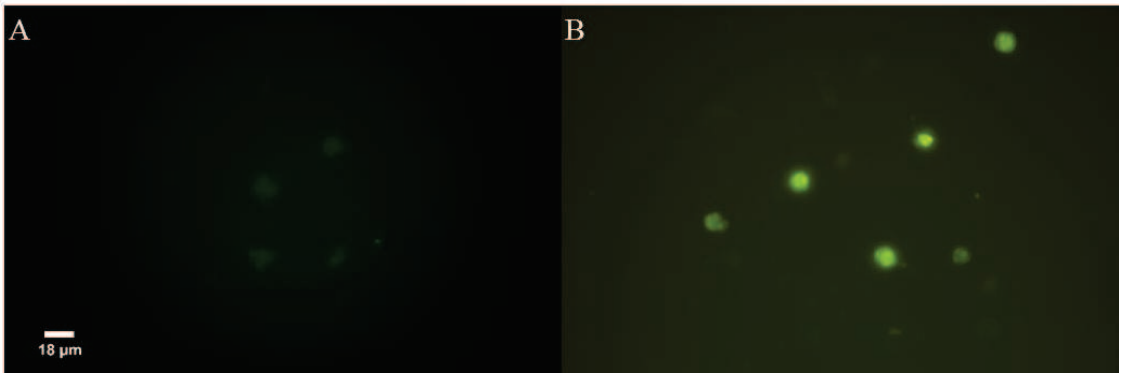

Image 6. The effect of *A. fumigatus* conidia, 14 h post infection on apoptotic monocytes. (A) Monocytes labeled with pHrodo Green, infected by wild-type conidia; visualized with green filter cassette DM510 (excitation EX450-490, emission BA520). The lighter spots represent the lower pH. As the image shows, the cell with wild-type conidia survived although the cytosolic pH was not neutral (as a sign of apoptosis). (B) Apoptotic monocytes labeled with pHrodo Green and infected by mutant conidia 8 h post infection. Cells were detected with Green filter cassette DM510 (excitation EX450-490, emission BA520). Cells were brighter representing more acidic pH. The shiny green spots displayed the cell necrosis.

7.10 Imaging the effect of other *Aspergillus* strains on apoptotic monocytes

To indicate on role of melanin in pH modulation during apoptosis, besides A.fumigatus wild-type and *pksP* mutant, two other pigmented species (*A.flavus* and *A.clavatus*) were studied and meanwhile, the images were taken. As it presented below, 19 h p.i., only those cells endured apoptosis that had been contained melanin. Among the cases bellow, only *A.fumigatus* wt and *A.clavatus* contain DHN-melanin. The images indicate the role of melanin in surviving the apoptotic cell (Image 7).

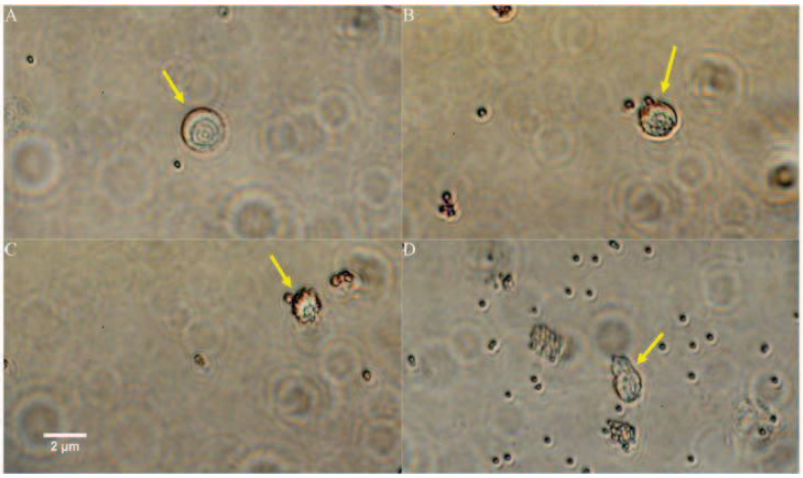

Image 7. STS treated monocyte upon different types of infection, 19 h p.i.

A) *A.fumigatus* wt
B)*A.clavatus*
C)*A.flavus*
D)*A.fumigatus pksP* mu

7.11 Imaging the effect of different *A. fumigatus* mutants on apoptotic monocytes

Colorful mutant conidia contain different intermediate molecules of melanin which it is determined by the type of mutation (Heinekamp et al., 2013). The more complete the melanin molecule is, the darker pigment will be produced (Langfelder et al., 2003). To compare the probable impact of different mutations through melanin pathway on melanin property, the interaction of different mutant conidia with apoptotic monocyte was examined.
The infection with colorful mutants was studied based on the same method used for the wild-type. It took around 1 h after the infection when the apoptotic cells started responding to the engulfed conidia regarding the changes in pH (**Fig**. 16-18) but till 5 h p.i. the cells seemed still intact (Image 8. A, B, C).
Among this group of mutants, the higher number of engulfed conidia was belonged to the *A.fumigatus* yellow mutant. It can be explained by the fact that yellow Δ*ayg1* mutant gene cluster, is the closest to *pksP* white mutant gene in melanin biosynthesis pathway. It has been shown before that *pksP* conidia are taken up in the higher range in compared to the wild-type (Tsai et al., 1998), (Luther et al., 2007). These facts together make an interesting summit since it was also observed that in modulating the host's pH; the impact of the Δ*ayg1* and *pksP* mutants was similar.

In the case of melanin properties, also the shared characters between wild-type and brown mutant Δ*abr2* were noticeable. Putting alongside the resulting pH from the wild-type infection (**Fig.** 14) and Δ*abr2* mutant (**Fig.** 16) provides an explanation for the similarity of their effect on the apoptotic host cell (Image 8A and 8D).
As the image in bellow demonstrates, 9 h p.i., the apoptotic cells that have been infected with red or yellow mutant shirked while in the case of brown mutant infection, the cell seemed to enduring apoptosis.

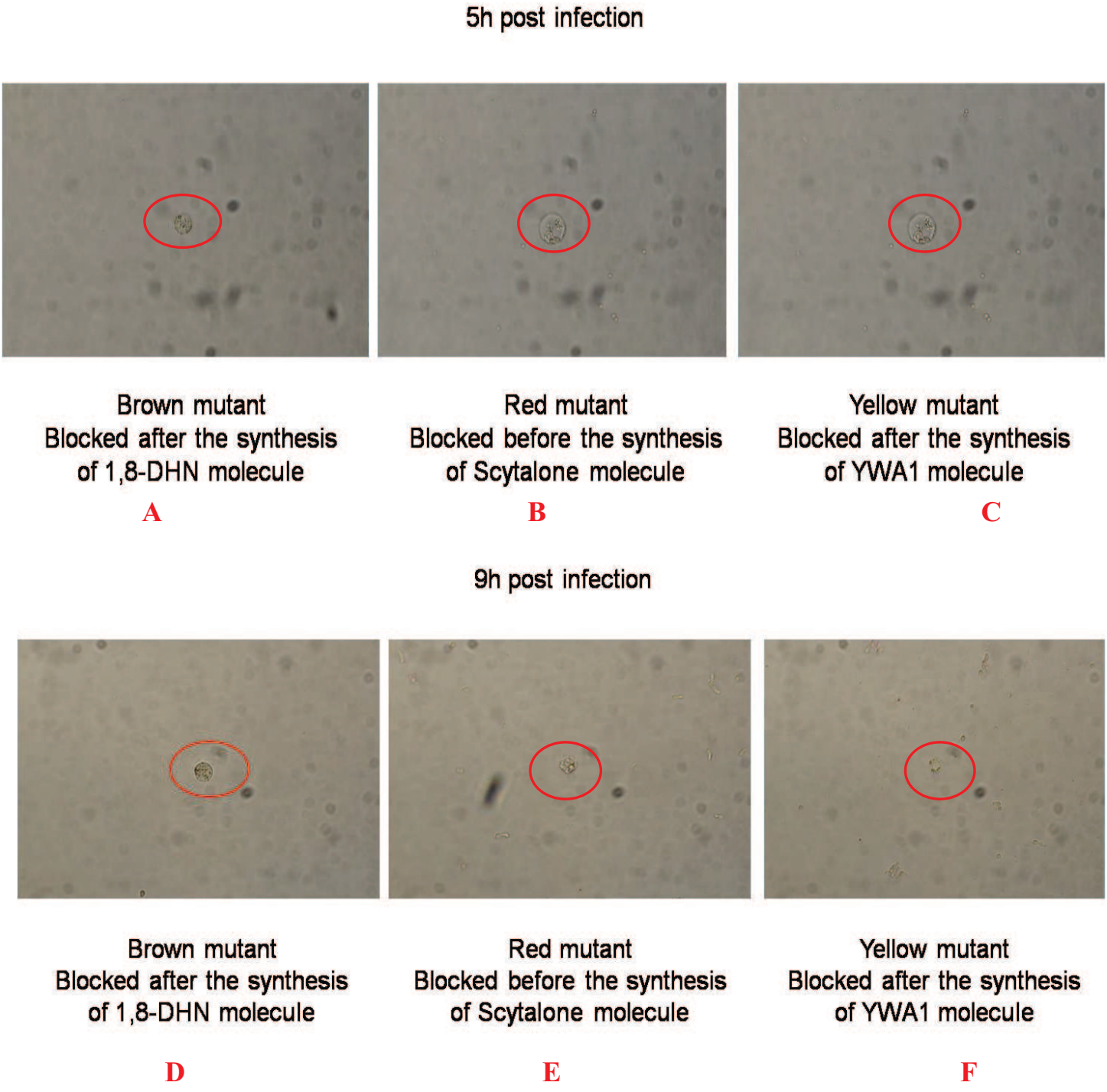

Image 8. Comparing the effects of different colorful mutants 5 h and 9 h post infection on apoptotic monocytes. A, B, C: The apoptotic monocytes that have been infected with different color *A.fumigatus* mutants were still alive 5 h p.i. **D, E, F**: 9 h p.i., only the cell that had been infected with the Δ*abr2* brown mutant (darker pigment, closer to melanin molecule) remained in shape and the two other cells shirked and deformed.

7.12 Imaging the effect of phagosomal acidification inhibition on apoptotic infected monocyte

When conidia are engulfed and fused to phagosomes, they will be gradually digested through the secretion of acidic enzymes in endolytic organelles specifically lysosomes (Luzio et al., 2007). As it is represented in **Fig.** 22, to analyse the importance of *A.fumigatus* effect on modulating the cytosol pH and also its survival in phagolysosomes, first the phagosomes and lysosome merging was prevented by chloroquine treatment. It has been assumed that if melanin was needed to recover pH during apoptosis, it should have been effectively located into phagolysosome. Observing the reversed effect when the cells were treated with chloroquine in compare to the untreated cells, indicated the facts that although melanin should be present in the cell for pH modulation, it has to be engulfed and located in the phagolysosome in advance, to be effectively functioning.
The image 9, demonstrates the cells from the **Fig.** 22. As it shows, in the presence of chloroquine, in wild-type infection apoptotic bodies have been formed and the cells are acidic. In the mutant infection9 h p.i., the cell is dead in this time point and no more signal is detectable.

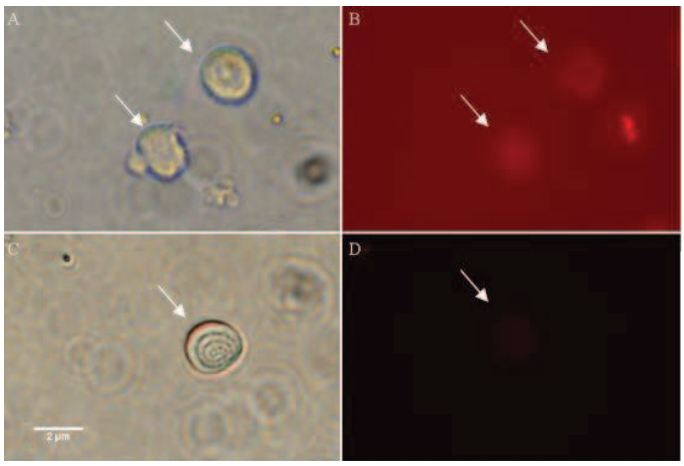

Image 9. (A, B): Apoptotic cell treated with chloroquine and infected wild-type, 9 h p.i.
(C, D): Apoptotic cell treated with chloroquine and infected with *pksP* mutant
(A, C): no filter, (B,D) Red filter casset

To study the effect of melanin when pH of phagosome has been stabilized during apoptosis, bafilomycin was used (Image 10). As the result from the same treatment in **Fig**. 23 shows, in compare to *pksP* mutant, the melanized conidia significantly nutralized the acidification up to a point that there was no signal to detect (B).

In compare, the *pksP* mutant infection in the apoptotic cell treated with bafilomycin did not mediate any cell event either with apoptosis (D) or with acidic pH (E).

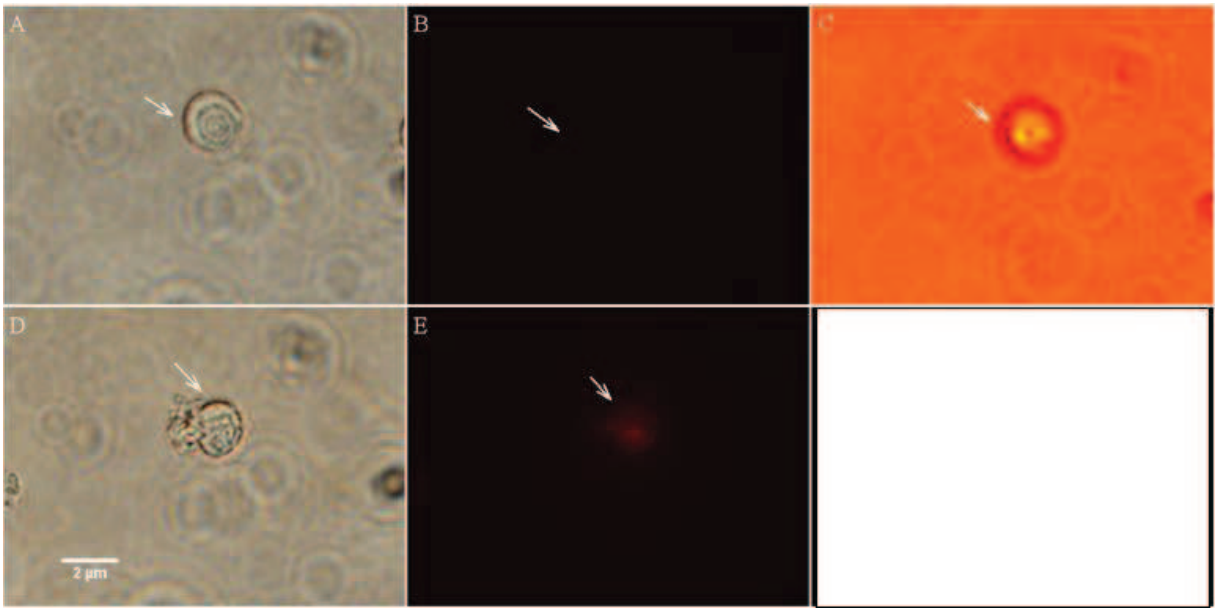

Image 10. (A, B, C): Apoptotic cell treated with bafilomycin infected with wild-type, (D, E): Apoptotic cell treated with bafilomycin infected with mutant.

(A, D): No filter
(B, E): Chroma filter cassette 49913
(C): While light, Chroma filter cassette 49913

7.13 FACS analysis

The two given examples bellow, describe that how FACS failed to present the exact amount of incorporated pH detector probes into apoptotic cells (**Fig**. 25). Also sorting the necrotic cells from induced ones using PI and Annexin V together, did not have any outcome for that the assays which required only induced cells containing the probes inside. When sorting out the sample of interest appears sophisticated but is highly necessary, it is predictable that using a method like FACS would not facilitate the study. Further, in the case of using different markers to detect the late stage of apoptosis from necrosis i.e. Annexin V and PI, these method is usually unable to differentiate between them (Ledda-Columbano et al., 1991).

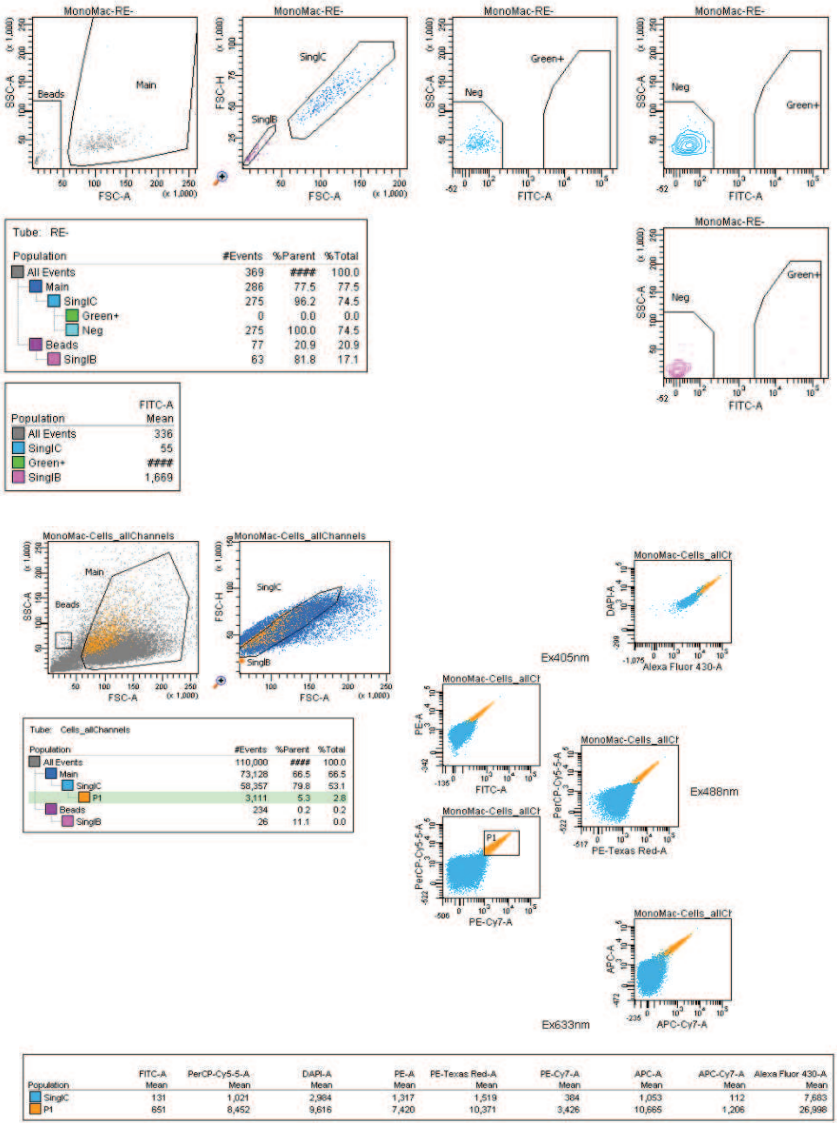

Figure 25. An example of the FACS analysis result on bio particles-conidia

8 Discussion

The intracellular phenomena following the interaction between host cells and infectious particles are determined by the nature of the pathogen and its ability to interfere with the different intracellular compartments and pathways. *A.fumigatus,* as the most prevalent airborne opportunistic pathogen, has multiple factors which determine its strategies for its virulence and adaptation to the host's environment i.e. versatile metabolism, thermo tolerance, secreting toxins and various metabolites including pigments. The fungus causes the morbidity and mortality in immunocompromised patients. It is capable of manipulating the human's immune system by modulating apoptosis and completing the cell fate (Eisenman and Casadevall, 2012). One hand, the fungus shows the anti-apoptotic properties which interfere with apoptotic cascades. On the other hand, when it is in the vegetative form, it appears to have pro apoptotic activity that by secreting its mycotoxin (gliotoxin), which suppresses the activity of T-cells, stimulates preferential death of monocytes and induces apoptosis among them (Stanzani et al., 2005).

Regarding the lack of knowledge about the details of *A.fumigatus* pathogenicity and its contradictory effects on apoptosis events, for the first time the influence of *A.fumigatus* melanin on pH of apoptotic human monocyte by the means of hyperspectral imaging in the single cell level was investigated. The monocytes are mostly in charge of eliminating the fungus from immune system. Although, their intracellular pH and fate of cell cycle during apoptosis upon infection are still unknown (Busca et al., 2009). In this study, the effect of *A.fumigatus* conidia on the fate of apoptosis in MM6 monocytes treated with STS was examined. This substance was selected as the inducer of mitochondrial-driven apoptosis since its function during A.fumigatus localization in the cell has been well established (Volling et al., 2011). Since Volling et al. revealed that the anti-apoptotic properties of this fungus dependent on the sustained activation of the PI3K/Akt pro-survival signaling pathway, it was hypothesized that this activity could be strappingly linked to melanin presence.

To examine this, a multimetric analysis at single cell level was required to generate quantitative data from real time measurements using a combination of identification markers. To achieve this, the experiments were designed based on hyperspectral imagery. Various pigmented microorganisms that their pigments were of a different nature than DHN-melanin, were chosen for this study. Here, it was demonstrated that *A.fumigatus* melanized conidia modulate the acidic pH in apoptotic cells, this being the reason why they could efficiently inhibit apoptosis. Also, for the first time, the intracellular pH in an apoptotic monocyte upon

melanin-interaction and the pattern of pH changes during infection in the cell undergoing apoptosis was determined.

8.1 Intracellular pH is one of the essential factors during apoptosis which could be altered through different mechanisms

The term apoptosis is suggested for a cell event in which an organized cell removal plays the opposite role to mitosis, with the aim of controlling the cell population. The cell suicide program mostly regulates the number of macrophages and monocytes to maintain homeostasis (Kerr et al., 1972). Via this important mechanism, unwanted cells or damaged tissue are removed without evoking any further inflammatory responses. Caspase activation plays the key role for apoptosis initiation, which is achieved via several mechanisms including the release of granzymes from T cells and natural killer cells or mitochondrial permeabilization trough the activation of death receptor pathway.

When the cell death takes place trough apoptosis, it imposed some changes in the protein expression and causes modifications in the post-translational interactions in the protein levels i.e. phosphorylation and proteolytic cleavage. Besides, the affected proteins could experience displacement to a new compartment and through the interaction with the substrates, they modulate the apoptosis machinery (Johansson et al., 2010). Apoptosis itself has been firmly conserved through evolution. When is activated, it causes various changes in the cell condition including the morphology and characteristics (Fahy et al., 1999). The cell structural changes are imposed in two levels. It initiates with the nuclear contraction and cytoplasmic condensation. The cell shrinks and breaks into membrane-attached fragments. Then the second stage starts with separation of the epithelial-lined surfaces to form the apoptotic bodies which are mostly degraded via phagocytosis and autolysis within the ingesting cells (Kerr, 1971). There is a strong relation between the mechanism involved apoptosis and acidification in the cell undergoing it (Shamim et al., 2012). Regardless of the origin of apoptosis, in both mitochondria or death receptor-mediated activated pathways (Tait and Green, 2010) the pH of the cytosol tends to the acidic condition (Matsuyama and Reed, 2000).

In warm-blooded vertebrate species, an optimal cell pH is adjusted in each organelle by keeping the balance between active H^+ pumping and passive H^+ efflux. In the course of evolution, cells have developed a variety of specialized proton-translocation systems and most enzymes are pH sensitive (Demaurex, 2002). Cytosolic pH is one of the cell features which will be affected the most during apoptosis and its related pathways (Lagadic-Gossmann et al.,

2004). For example, in tumor cells, due to the high rate of lactic acid fermentation and glycolysis by imposed hypoxia, pH is lower than in regular tissues. Hence, controlling the pH gradient could be an efficient treatment against cancer (Shamim et al., 2012).

Besides apoptosis, pH maintenance and stability of ions is a critical cell feature which guarantees cells function. In case of any disorder, it causes cell malignancies. The translocation of ions in ATPase and their substrates is an effective target for therapeutic intervention in drug discovery practices. The class of enzymes, such as H^+, Na^+ or K^+ - ATPase serves as selective pH-related target for some therapeutic agents like omeprazole and digoxin, which are used for the treatments against ulcers or heart disease (Perlin, 1998). It has been shown that any change in intracellular pH modulates those signaling pathways which are controlling the cell fate. This modulation governs the cancer cells' metabolism and leads their survival (Aredia and Scovassi, 2014).

8.2 Lysosome modulates intracellular pH and is a possible target for anti-apoptotic properties of melanin

The most acidic cell compartment has been identified up to date, is lysosomes (Nilsson et al., 2003), (Hu et al., 2016). They are membrane- enclosed and morphologically diverse organelles containing digesting enzymes that are responsible for breaking any sort of bio molecules, from lipids to nucleic acids and their products. Decades ago, De Duve described the lysosomes as suicide bags which contain various hydrolyses (De Duve, 1965). Although in that time many facts about the intracellular organelles had not been discovered, any definition such as suicide bags needed to be linked to the death of cell. Now it is known that the proton release in lysosomes has a certain role in cytosolic acidification during apoptosis (Nilsson et al., 2003). They are highly dynamic organelles that will receive macromolecules from every endocytic, phagocytic or secretor membrane to degrade and digest them (Luzio et al., 2007). The digestion of absorbed macromolecules in lysosomes is being accomplished via its fusion to the phagosome as a transient cell activity. Regarding to its protective properties, most of the external pathogens that interfere with membrane-trafficking pathways to hijack the endocytic events, escape from lysosome (Demetriades et al., 2016).

The importance of lysosomes functions is better defined when it comes to lysosomal disorders. They are classically described as the abnormal accumulation of biomaterials due to the overlap in enzymes and their products (Suzuki and Vanier, 1999). Among these diseases some are more common, i.e. Krabbe's diseases (or Globoid cell leukodystrophy- abnormal digestion of sphingolipids in the myelin sheath), Niemann-pick diseases (deficiency of

lysosomal acid sphingomyelinase causing foamy cells in the bone marrow), Faber's lipogranulomatosis (abnormal accumulation of ceramide in lung and heart), etc.

Along with the caspases, some proteases i.e. lysosomal cathepsins are involved in programmed cell death. Inhibition of these substances prevents the release of cytochrome c from mitochondria, which it happens following the STS treatment. In other words, inhibition of lysosomal adapter molecules will inhibit caspases 9 and 3 as well as apoptosis (Johansson et al., 2003).This, highlights the key role of lysosome in modulating the mitochondrial function and cytochrome C secretion and verifies the mutual function of lysosome-mitochondria in governing the caspases during apoptosis (**Fig.** 26).

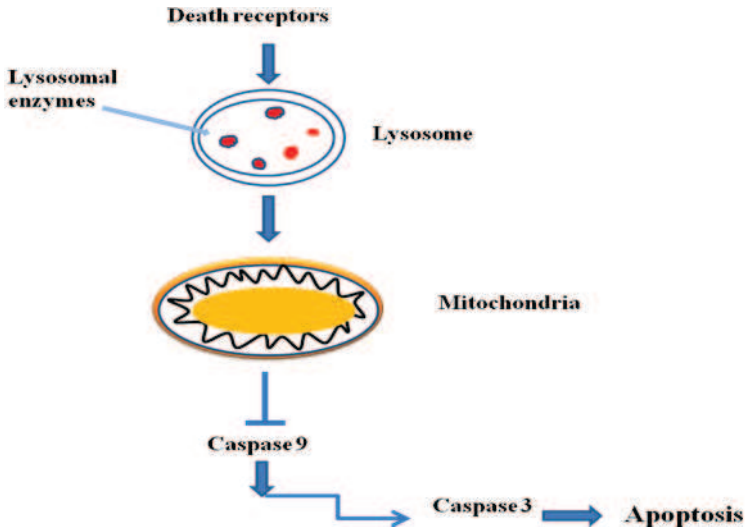

Figure 26. Main actors and compartments involved in mitochondria-derived apoptosis pathway. By the formation of cognate ligands of death receptors, lysosome components will be released into the cytosol and prompt mitochondrial dysfunction. The apoptotic factors will be activated following blockage of casp 9 and activation of casp 3.

In this study, tracing the cytosolic pH variation during apoptosis was aimed and it was noticed that as soon as apoptosis is accomplished, the cytosolic pH drops. This could be measured by labeling the cytosol with the probe pHrodo green and by recording the corresponding signals, quantify the outcome. When the cells were treated with STS and sorted the induced cells (Image 5), it was observed that the cytosol appears extremely acidic with a pH value less than 4, which indicates the known facts about lysosome and its function. The extreme lysosomal acidification has been known for a decade as one of the consequences of apoptosis. For example in the tumor cells due to the frequent proteases secretion in lysosome, the tumor makes it microenvironment more acidic to be able to spread (Victor and Sloane, 2007). Apart

from the specialized function of lysosomes in endocytosis, it has been also recognized that they function as an occasional storage for iron. Interestingly, lysosomes have been considered autophagic organelles which apparently have a certain role in degradation of iron-rich compounds (Kurz et al., 2008). Storing iron is an alternative plan for managing some special incidents. One of the most possible candidates for this hypothesis is oxidative stress. Since the oxidative stress is directly linked to apoptosis (Turk et al., 2002), it is not surprising that any phenomenon that modulates the function of lysosomes (from iron acquisition to proton secretion and infection-mediated events) will affect the apoptosis caspases via the lysosome-mitochondria interaction.

8.3 Role of staurosporine in mitochondrial and death-receptor apoptosis

The frequency of apoptosis-specific pathways is totally dependent on the cell type, time point of analysis and also on the stimuli that initiate apoptosis (Wlodkowic et al., 2011). For a long time and in various cell types, STS has been used to stimulate apoptosis *in vitro*, although its exact mechanism still remains elusive (Olguín-Albuerne et al., 2015). STS is a broad-spectrum microbial antiproliferative alkaloid, isolated from *Streptomyces*, which targets the protein kinase, inhibits its activity and blocks cell cycle proteins at the G2/M checkpoint (Antonsson and Persson, 2009).The treatment with STS causes the release of lysosomal proteases that interact with cytosolic targets and lead to apoptosis (Kågedal et al., 2005). When apoptosis is induced by STS, the permeability of the mitochondrial outer membrane changes, which causes a massive impulsive release of cytochrome c from this organelle (Duan et al., 2003).The actual mechanism of apoptosis induction by STS might be vary, according to the cell type or STS concentration but in general, STS activates the central components of the apoptosis machinery (Deshmukh and Johnson, 2000). To ensure that STS has been functioned properly, Annexin V was used for recognizing the already induced cells within the culture. Moreover, in order to differentiate the stages of apoptosis (from early phase to necrosis), the cells were exposed to propidium iodide as in the necrotic cell the DNA is fragmented and a fluorochrome label i.e. PI, would specifically binds to these fragments (Riccardi and Nicoletti, 2006). Thus, following the STS treatment, PI was used to verify the necrotic cells. Furthermore, for an accurate assessment of the STS treated cell, Annexin V was applied (Rieger et al., 2011). This way, any false positive apoptotic event was excluded. By using this combination through the cell sorting, only those cells that have been in their early phase of apoptosis were used (Image 5).

8.4 *A. fumigatus* conidia regulate apoptosis in monocytes by modulating phagolysosomal pH

In the innate immune system, monocytes are the motile white blood type cells (Goldman and Prabhakar, 1996), which are well known for their remarkable phagocytosis ability and intracellular killing for clearing the viral, bacterial, fungal and protozoal infections. They contribute to the pathogenesis of inflammatory immune responses and degenerative diseases. Therefore the host inflammatory responses during apoptosis, will regulate the number of monocytes and lead their function (Shi and Pamer, 2011). Considering the prominent role of monocytes in handling and further defeating infectious diseases, it becomes clear that studying their inner-cell events during infection or/and apoptosis as well as determining the condition and the range of surviving monocytes after infection are key to detect more possible and alternative treatments against different pathogens.
Berkova et al. discuss that *A.fumigatus*, has significant inhibitory effects on apoptosis which has been induced by either STS or TNF-α (Berkova et al., 2006). Besides the brown compound pyomelanin that is produced via oxidative polymerization of homogentisate through degradation of tyrosine, DHN-melanin is the main pigment which has an effective protective function against the host's anti-microbial defense and environmental stresses (Heinekamp et al., 2013).

It has been a while since *A. fumigatus* has been acknowledged for its capability of preventing the acidification of phagolysosomes to a certain extent (Wasylnka and Moore, 2003). This ability has been attributed to melanin. Since it is the main component in *A. fumigatus* which contributes to invade the host, the virulence of the fungus and its resistance against the host's immune system (Pihet et al., 2009). The complete melanized pigment specifically is responsible for the scavenging of the oxygen radicals which are generated through the host cell's metabolism and trickle from the cell membrane (Jacobson, 2000). Melanized conidia inhibit the apoptosis process when it is induced either intrinsically by STS or extrinsically with the Fas ligand (Volling et al., 2007), (Volling et al., 2011). Although the mechanisms of *A.fumigatus* interaction with human monocytes and its cell-related destruction in hyphal form have already been studied extensively (Diamond et al., 1983), the inner-apoptotic cell events including pH values post and during the infection have never been discussed. To determine if DHN-melanin governs fate of the monocyte undergoing apoptosis, the untreated monocytes were infected with: melanized wild-type conidia, intermediated melanized mutants (brown, red, yellow colored pigmented conidia) and with white *pksP* mutant conidia as controls. The

pH was measured every 15 min and the critical time points where the signal of pH had a drift at, were plotted (**Fig.** 14a). Volling et al., 2011 discovered that *A.fumigatus* prolonged their habitation in the host cell by activating the PI3K/Akt pathway, but only in the presence of melanin. Then they hypothesized that although this signaling pathway plays a key role in ruling apoptosis, there must still be an anti-apoptotic factor that contributes to this inhibitory function, since the inhibition of Akt applies only in the case of an infection with the wild-type.

Therefore, their results further were expanded here by examining different pigmented microorganisms that produce pigments of different nature and structure; i.e. *Aspergillus flavus:* ferric ion based pigment (Assante et al., 1981), *Aspergillus clavatus:* melanin-like brown pigment (HKI unpublished data collection) and *Lichtheimia brasiliensis*: sporopollenin.

Among all mentioned control samples, only those monocytes endure apoptosis that have been primarily infected with *A.clavatus.*

The major factor which determines either the susceptibility or resistance of the host cell towards *A.fumigatus* fungal infection is the ability of melanin to quench reactive oxygen species (Jackson et al., 2009). In other words, the prominent function of melanin consists in scavenging toxic oxygen radicals which are released during different ionic reactions or photodynamic activities in different cell compartments: mitochondria, cytoplasmic membrane and peroxisome (Sahnoun et al., 1997). This ability governs the response of the host cell to melanized fungi. The mutated proteins on the surface of *A.fumigatus* cause some considerable changes and make them look different from the wild-type. Consequently, the mutants are recognized more efficiently by the host cell and therefore, are taken better by the host. Furthermore, it has been shown the stronger phagocytosis of mutant conidia is unrelated to the lack of their quenching ability (Jahn et al., 1997). Accordingly, in the very first hours of conidia-host interaction, the number of incorporated mutant conidia is higher compared to the wild-type conidia. Furthermore, in the case of taking up the *pksP* mutant, the host cell is more acidic. Heinekamp et al. (**Fig.** 27) demonstrated how efficiently DHN-melanin can alter the phagocyte's function. Essentially, the fungus is able to establish its own microenvironment to survive. In comparison, the mutant lacks this ability.

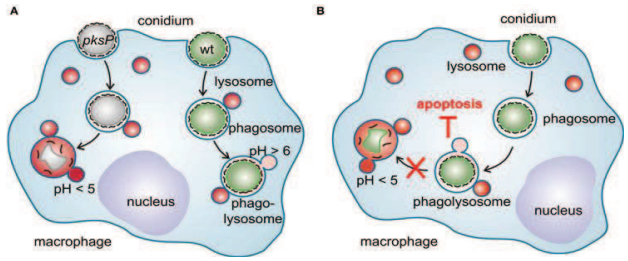

Figure 27. The cell events upon *A. fumigatus* conidia and macrophage interaction (Heinekamp et al., 2013). *A.fumigatus* interferes with the fate of cells and alters it after recognition and phagocytosis. Following the phagocytosis, the conidium should be localized into lysosome and after the phagolysosome formation; it imposes the inhibitory effect while the mutant does not interfere with apoptosis.

To investigate whether the induced apoptosis had progressed via the mitochondria-dependent pathway during infection, changes in phagolysosomes pH was measured by labeling the entire cytosol. The acidification in accordance to the cells shortened life cycle and shrinkage are the consequences of mitochondrial-driven apoptosis (Song et al., 2011). In parallel and again at 2011, Volling et al. stated that it was unknown whether only melanin could modulate the PI3K/Akt directly or if an additional factor was involved? The questions were pursued and expanded by tracing pH along the timeline of infection. By tracking the intracellular events in an undergoing apoptosis cell, pH was quantified over 35 hours. It was observed that once the apoptotic cell is infected with *A.fumigatus* wild-type, regardless of how far apoptosis preceded, the cell endured it. At the end of experiment, the final value of pH was ~ 6.2-6.5, while at the middle of apoptosis it had reached to the value of ~ 4 (**Fig.** 15). This result indicates that *A.fumigatus* manipulates the host cell by altering the outcome of apoptosis purposely phagolysosomal pH. Additionally, the generated data in this study provides a defined quantification analysis that verifies a previous study which mentioned that the fungus prevents the acidification of the host cell to a certain point (Thywißen et al., 2011). Although the observations in this study focused on the interaction between apoptotic cells and *A.fumigatus,* pH was also measured in the non-apoptotic controls where the infection only took around 8 h when the cell could digest the engulfed conidia (**Fig.** 12), and pH remained around ~ 5.8-6.

When comparing *A. fumigatus* to *A. clavatus* infection, no differences could be detected regarding the pattern of pH even though these two fungi are different in nature: *A.clavatus* is known as a cosmopolitan fungus, well adopted to malt-rich storages, responsible for extrinsic allergic reactions (Varga et al., 2007), it is known for the secondary metabolite secretion i.e.

putalin and kotanin (mycotoxins) (Suzuki et al., 1971), etc., and also it has a different morphology from *A.fumigatus* (mostly produce phototropic long conidiospores and prefer the growth at 20-23 ºC (Varga et al., 2007). But nevertheless, their effect on modulating pH and prolongation the cell's life cycle along with apoptosis was the same (**Fig.** 19). Surprisingly, the apoptotic monocytes that have been infected with the darkest color *A.fumigatus* mutant (brown mutant) also showed longer life cycle compared to light color mutants (red, yellow and white). It seems that the only molecular feature that these three subjects are sharing, is their pigment; melanin.

When the cell undergoes apoptosis, cellular ion homeostasis is lost. In fact, the first effect of apoptosis is suppression of Na^+/K^+ pump. The permeability of membrane upon suppression of the Na^+ pump causes the release of inflammatory mediators which are associated with extracellular acidification (Cao et al., 2015).This event, directly impacts the intracellular pH balance and causes a fast drop in pH (Austin and Wray, 1993).
Producing DHN-melanin is not limited to *Aspergillus* spp. For instance in *Cyptocossus neoformance*, melanin contributes to the organism's invasiveness and the host's death. Also, in *Fonsecaea pedrosoi,* melanin causes the oxidative burst of macrophages (Eisenman and Casadevall, 2012). Similarly, in *Paracoccidioides brasiliensis,* it inhibits phagocytosis (da Silva et al., 2006). So far, it is known that melanin has a determining role to control cell damage and consequently it mediates apoptosis. It is responsible for shielding the cells against the environmental stress i.e. UV radiation. In fact, the levels of melanin among different fungal species is related to the frequency of DNA damage which leads to apoptosis (Yamaguchi et al., 2008). Since during apoptosis and in the absence of melanin, the balance between the production of reactive oxygen radicals and the defense against their burden is disturbed, and in its presence, the cells showed more tolerance against the oxidative stress, it is suggested that melanin appears to contribute against the calamitous role of oxygen species (Betteridge, 2000). The up-regulation of anti-apoptotic genes could be the reason for the tolerance against STS-induced apoptosis. Melanin is a compound containing a mixture of hydrophobic macromolecules which are negatively charged; therefore any mutation in the melanin synthesis pathway can cause considerable alterations in the properties of the fungal cell wall, its properties and morphology. In *A.fumigatus*, the pigment is located in the outer section of the cell wall and mostly plays a protecting role, apart from being responsible for maintaining the integrity of the conidial structure (Jahn et al., 1997). Volling et al. 2011 showed that the cAMP/PKA cascade has an inhibitory effect on apoptosis which might be accomplished through alteration of the melanin synthesis pathway. Since mutation in the early

steps of melanin biosynthesis, causes the loss of *pksP* gene in the cluster (which produces white conidia with the reduced virulence factor) (Tsai et al., 1999), and from the generated fungus has no impact on apoptosis (**Fig.** 14). Besides the polyketide synthase gene (*pksP*), when a mutation occurs in the 6 genes cluster pathway of melanin biosynthesis, depending on the affected gene, different types of pigment would be generated. However, the darker pigments (which are the product of a later mutation within the cluster) resemble the more complete melanin molecular structure and function (Tsai et al., 2001) and expectedly, only the brown Δ*abr2* mutant, to some extend showed the similar effect on cell acidification as wild-type. The results show how the Δ*abr2* extends the apoptotic cell's lifespan with a final stabilized pH ~6 for over 28 h (**Fig.** 16). The same applies to the red mutant Δ*arp1* which prolonged the cell life cycle for 16h despite of the host cell having a more acidic intracellular pH (**Fig.** 17). Previously, it has been found that in *A.fumigatus* when the tyrosine or its assigned gene, were not degraded towards the mutation, the mutant strains appeared to be similar to the wild-type regarding the virulence (Sugareva et al., 2006), (Schmaler-Ripcke et al., 2009). Since in Δ*arp1* and Δ*abr2,* the mutation did not elevate the susceptibility of these mutants against reactive oxygen species, also the virulence of Δ*arp1* and Δ*abr2* assumedly remained the same (Dagenais and Keller, 2009). Considering the obtained results from *A.clavatus* and the fact this organism also contains melanin, the observation on pH recovery during apoptosis upon infection can be related to the presence of melanin and its ability to control oxidative stress and to reestablish the missing balance between the generating free radicals and their neutralization during apoptosis.

8.5 Vocoular ATPase appears to be a target for melanin to modulate cell acidification during apoptosis

When infectious material is ingested by the cell, there will be a relative contribution to pH regulation among proton pumps and V-ATPases. This phenomenon governs the fate of phagocytosis in favor of cell survival. If phagocytosis proceeds and cytosol acidification is sustained, apoptosis will be accelerated and proceeded to its late phases (Coakley et al., 2002). Phagosomes are the first organelles that guide the infectious particles to the further digestive organelles. They fuse their membranes and maturate to pump-in the hydrolytic enzymes needed to establish a lower pH, favoring the digestion of the particles (Scott et al., 2003). Many pathogens use this cell event in order to buy some time and expend their survival in the cell, (Gorvel, 2003), (Kumar et al., 2015). In the case of *A.fumigatus*, it has also been shown that the fungus uses the same strategy, which is basically associated with the *pksP*

gene function (Jahn et al., 2002). To expand the knowledge concerning pH behavior, two different chemical substances were applied to inhibit the phagosome-lysosome fusion and consequently altering the pH: chloroquine and bafilomycin A1. Whereas chloroquine has an inhibitory effect on autophagy; it prevents the formation of phagolysosome and thus the acidification of the organelles (Bijker et al., 2015), and bafilomycin as a macrolide; inhibits ATPases and by restricting the phagosome fusion and restrains the phagosomal further degradation (Bowman et al., 1988), (Palumbo et al., 2016). It could be observed that in an apoptotic cell treated with chloroquine and infected with the melanized conidia, the effect of melanin is annulled and phagolysosomes are not formed. Hence, the pH ~4.8 could not recover and the cell entered the death phase (**Fig.** 22). Alternatively in the presence bafilomycin, melanin was not affected by the substance and also recovered pH to around the neutral value (**Fig.** 23). The data is supported by the results obtained from other study (Thywißen et al., 2011) showing that *A.fumigatus* can inhibit the phagolysosomal acidification by possible targeting of an ATPase. Since the prevention of ATPase by bafilomycin, not only influenced on the function of melanin towards apoptosis, but also the inhibitory effect of melanin of cell acidification was accomplished faster. It can be concluded that additional mechanism of advance phagocytosis, such as modulation of oxidative reactions and distressing V-ATPase, could be the strategies of the fungus in governing pH and fate of cell.

8.6 Hyperspectral imaging in terms of comprehensiveness and real-time measurements, is not replaceable by other bulk detection techniques

If the cell populations that are used for apoptosis-related studies contain necrotic, apoptotic and viable cells at the same time, the result of this analysis will not be trustworthy. Since in standard routine techniques, i.e. western blot or DNA electrophoresis, the distinction between early and late stage of apoptosis among not induced cells is not possible and their detection requires various assays. However, this is still the regular practice in many experimental assignments. Such assays always require large amount of cells and therefore any assay on the single cell level cannot be performed through them. Alternative fluorescent staining methods, such as those use conjugating antibodies which depend on the specific band to apoptotic-related probes are not suited for the real-time monitoring. These methods reduce the background staining but since they are based on invasive approaches that lead to the cell membrane permeabilization (Brauchle et al., 2014), they appeared not sensible when the cell is considered as *in vivo* environment .

Alternative techniques which are commonly used to detect the fluorescent probes, are confocal microscopy and FACS (Wlodkowic et al., 2012).

Yet, to determine the different stages of apoptosis or any alteration in its process, other complementary assays, i.e. tracking caspases, should additionally be performed. Regardless of multi-color or monochrome labeling, the quality of imaging in confocal microscopy is regulated by spatial resolution. During long-term measurements if images become blurred, they will not suited for a reliable description of the event of interest.

However in this project, additional to the hyperspectral method, also functionalized beads were used. The beads that were applied as pH indicator bioparticles have been specifically designed for phagocytosis and endocytosis detection. The benefit of using the bioparticles comes from the reduced signal variability since the fluorescence particles are solid and stay intact. Thus, there will be no dye residue that might generate false signals. Moreover, the particles are rapidly taken up by the cells and the first signals are detectable within some minutes of the seeding. Nevertheless, as it is shown in the **Fig**. 25, there were some disadvantages in the application that made the probes not so suitable for specific purposes like single cell analysis.

When the cells engulf the bioparticles, pH drops abruptly. Although it does not impact the rate of phagocytosis of the conidia, it is hard to assess whether the pH reduction was caused by the uptake of beads or by the phagocyted conidia. Since the phagocytosis and acidification occur more or less simultaneously, it was not possible to accurately distinguish the cause of the first pH drop, regardless of its recovery afterwards. Interestingly, switching to dyes with the same fluorescence feature did not alter the first observed events and the same pH values in the same time frames were recorded. But since the latter option seemed more consistent, incorporating the bioparticles in further experiments was not feasible.

Hyperspectral imaging spectrometry (spectroscopy) provides the functional combination between spectroscopy and traditional two-dimensional imaging remote sensing technology, hence it is a first stone in remote sensing revolution (Plaza et al., 2004).

The hyperspectral analyzing method was developed on the basis of traditional spectral imaging technology, but has more effective bands than the latter and provides almost continuous spectral curves with a high spectral resolution.

Traditional classification methods of hyperspectral data mostly have two major features:

- Utilization of the abundant spetral information
- Providing stasistics of images from a multispectral data classifier section that is an algorithm which maps input data to a category(Tong et al., 2014), (Bioucas-Dias et al., 2012).

The emphasis on this system lies on its capacity as multispectral data analysis has the ability of simultaneously measure all events of interest within a sample in high time resolutions. HSI does not depend on the quality of a visual image. By elevating the spectral bands and making a fine division between the spectra from each compartment within object of interest, it adds up noticeable additional information from each spatial position of image (**Fig.** 28). Hence, concomitant advances in computer capacities are required. The method provides continuous data within one measurement and unlike the common laboratory techniques, it concurrently provides the statistics (Gaudi et al., 2014), (Lu and Fei, 2014).

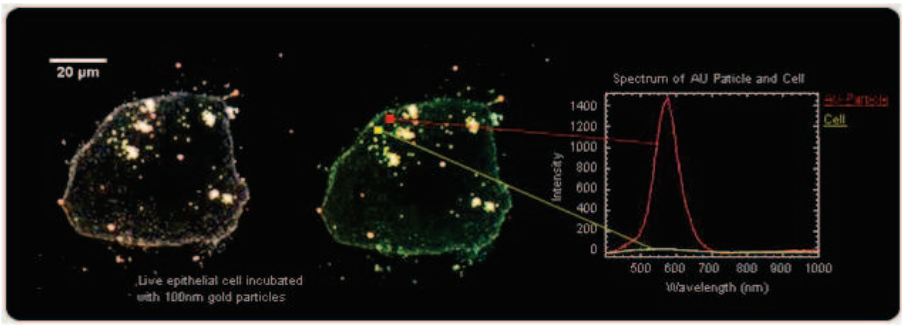

Figure 28. Hyperspectral image scan, from the optical image to the spectral plot. The image shows live cells which were incubated with nanoparticles and were imaged with a HSI System, as well as with a color digital camera. From each particle a unique spectrum is generated.
(Available at: http://www.scitech.com.au/index).

8.7 Selecting the most suitable methodology based on the outlines of this project

Regarding the similarity among the names and declarations of multispectral, hyperspectral or full-spectral imaging, usually there is confusion over the precise meanings and the definitions for each of these detecting systems, their capacities and application. Table 8 demonstrates the description of these three instrument modes. It should be noticed that the function of each imaging method as well as the range of a spectral system is determined by the instrument structure from the front-end designed optics to the back-end detection outcome (Chein-I Chang, 2000).

Mode	Numbest of spectral bands	Potential	Resolution
Imaging	None	Image brightness	None, sensitivity depends on the chosen detector
Multispectral	Tens	Detects either liquid or solid substances	Medium, many tens of nm
Hyperspectral	From hundreds to thousands	Detects liquid and solid substances	Narrow, few nm

Table 8. **Classification of the imaging systems.** Available at: http://www.photonics.com/EDU/Handbook.aspx?AID=25139

This project was conducted based on the HSI method. The applied HSI unit was gradually designed and customized to meet the aims of the assay and its requirements. Since all the assays focused on single cell analysis, by recording the data points in one-dimensional line and aligning them together, a two-dimensional image was acquired (**Fig.** 7b). Depending on the principle of its application, different probes were used to detect the sample or to report a specific event within the cell. The region of interest in the cell-based experiments, was not limited to one compartment within the cell while the entire cytosol as well as the core, phagosome, engulfed bioparticles or labeled conidia were detectable together using different filters. Therefore, the emitted spectra at the same time point could report some other events in the cell. From each probe, the signal intensity distribution, was equivalent to the fluorescence emission in space (vertically) and the related wavelength (horizontally).

This approach involves two steps. First, to find and follow the spectrally unique signals transmitted from the corresponding probes and the second, to alienate the unwanted signals which are found within the sample or in its environment.

Spectral shifts were identified in the two types of infection (wild-type vs. mutant) that reflect pH changes depending on the presence/absence of melanin during apoptosis. The main steps of the application have been demonstrated in **Fig.** 29.

a.

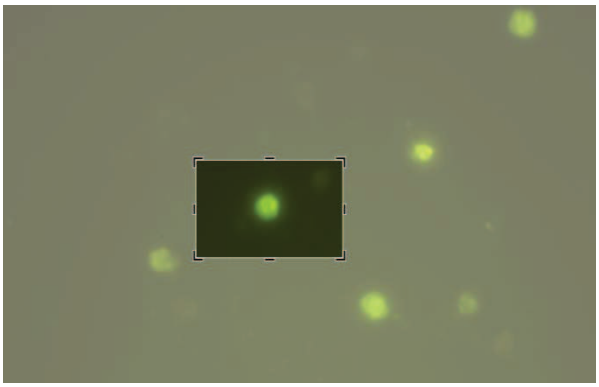

b.

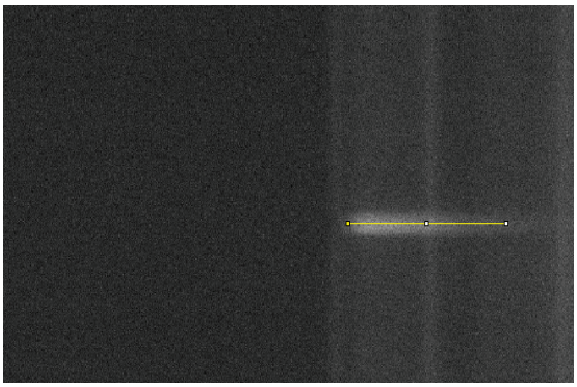

c.

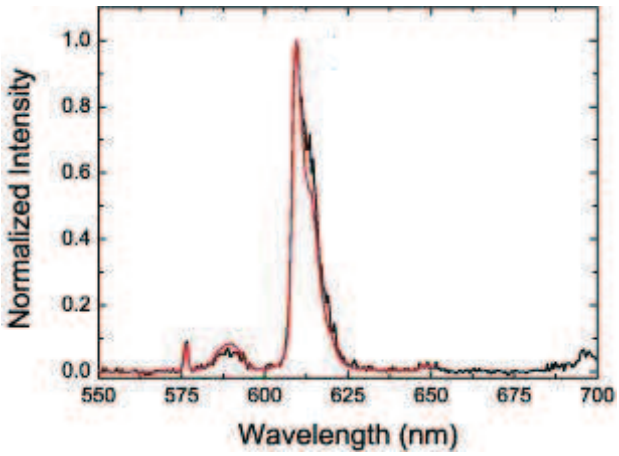

Figure 29. Scheme of HSI application in accordance with the experimental procedure. a. Image of the sample. The cell of interest contains a coated conidium which is already located in the phagolysosome. **b.** One – dimensional hyperspectral image recorded by using a pH sensitive fluorescent probe, incorporated into an apoptotic cell. Spatial resolution: ~0.8μ. **c.** Spectral plot of light scattering from the brightest green area of the sample, where conidium is visible. This spectral signature is consistent with previously measured spectra of the conidium.

8.8 Conclusion

This project was conducted based on a developed hyperspectral imaging to approach pH tracking and the fate of apoptosis in a level of single cell. Previously, it has been showed that *A. fumigatus* conidia can interfere with the acidification of phagolysosomes. Here, I extended this finding to human monocytes. I gained more-detailed information on host-melanized fungus interaction and I supported the results by examining variety of control samples. By using an endogenous data source any subtle pH changes have been detected in a living cell in the full morphological shape which made the possibility to determine survival cells from necrotic ones before, during and after the treatments. This data indicates that melanized *A. fumigatus* conidia have the ability to interfere with the apoptosis process in human monocytes as they enable the apoptotic cell to recover from mitochondrial acidification and to continue their life cycle. I also showed that, this ability of *A. fumigatus* is dependent on the presence of melanin but it is not limited to *A.fumigatus*, since neither a non-pigmented mutant nor any different sort of pigments could stop the progression of apoptosis while the Δ*abr2* mutant along with *A.clavatus* showed similar results. The applied quantification setup was sensitive enough to detect the standard pattern in pH variations out of one solitary cell. The statistical analysis was performed through the merging of at least three individual replicas to measure the sensitivity of the each assay and their results revealed no false-positive pH values nor any shift in the determined pattern of pH behavior.

As a general definition for HSI, it is a combined method for incorporating the classic imaging technique with optical spectroscopy. The method provides detailed information about a sample by recording the entire spectrum in each pixel of the whole image. Thus, in this project, the custom designed device made a new possibility to provide the real-time spectral and spatial data of single cells. In compare to HSI, there is no other non-invasive in-vivo detection method which is able to discriminate the different regions within the cell in long-term measurements, i.e. traditional fluorescence microscopy, confocal microscopy or FACS. Taken together, the presented work demonstrates that how hyperspectral imaging provides a new sensitive and non-invasive method of investigation the intracellular events in the level of single cell, with proper account of dynamic measurements. I applied HSI to quantify the constituent pH variation in a single infected apoptotic monocyte as a model system.

By conducting the current research I could measure the intracellular pH in a single apoptotic, infected human monocyte and show the pattern of pH variation during 35 h of measurements. In conclusion, I showed the pattern of pH changes and its importance in determining the fate

of apoptosis in the level of single cell and I measured the pH values during each apoptotic stage.

9 References

Abbas, H.K. (2005). Aflatoxin and food safety (Boca Raton, Fla.: CRC Press).

Aderem, A., and Underhill, D.M. (1999). Mechanisms of phagocytosis in macrophages. Annu. Rev. Immunol. *17*, 593–623.

Ahmad Sarji, S., Wan Abdullah, W., and Wastie, M. (2006). Imaging features of fungal infection in immuno-suppressed patients in a local ward outbreak. Biomed. Imaging Interv. J. *2*, e21.

Aimanianda, V., Bayry, J., Bozza, S., Kniemeyer, O., Perruccio, K., Elluru, S.R., Clavaud, C., Paris, S., Brakhage, A.A., Kaveri, S.V., et al. (2009). Surface hydrophobin prevents immune recognition of airborne fungal spores. Nature *460*, 1117–1121.

Alberts, B., Johnson, A., Lewis, J., Raff, M., Roberts, K., and Walter, P. (2002). Programmed Cell Death (Apoptosis).

Amin, S., Thywissen, A., Heinekamp, T., Saluz, H.P., and Brakhage, A.A. Melanin dependent survival of Apergillus fumigatus conidia in lung epithelial cells. Int. J. Med. Microbiol.

Antonsson, A., and Persson, J.L. (2009). Induction of Apoptosis by Staurosporine Involves the Inhibition of Expression of the Major Cell Cycle Proteins at the G2/M Checkpoint Accompanied by Alterations in Erk and Akt Kinase Activities. Anticancer Res. *29*, 2893–2898.

Aredia, F., and Scovassi, A.I. (2014). Multiple effects of intracellular pH modulation in cancer cells. Cancer Cell Microenviron.

Assante, G., Camarda, L., Locci, R., Merlini, L., Nasini, G., and Papadopoulos, E. (1981). Isolation and structure of red pigments from Aspergillus flavus and related species, grown on a differential medium. J. Agric. Food Chem. *29*, 785–787.

Austin, C., and Wray, S. (1993). Extracellular pH signals affect rat vascular tone by rapid transduction into intracellular pH changes. J. Physiol. *466*, 1–8.

Balasubramanian, D., Kumari, H., Jaric, M., Fernandez, M., Turner, K.H., Dove, S.L., Narasimhan, G., Lory, S., and Mathee, K. (2014). Deep sequencing analyses expands the Pseudomonas aeruginosa AmpR regulon to include small RNA-mediated regulation of iron acquisition, heat shock and oxidative stress response. Nucleic Acids Res. *42*, 979–998.

Barratt, R.W., Johnson, G.B., and Ogata, W.N. (1965). Wild-type and mutant stocks of Aspergillus nidulans. Genetics *52*, 233–246.

Behnsen, J., Hartmann, A., Schmaler, J., Gehrke, A., Brakhage, A.A., and Zipfel, P.F. (2008). The opportunistic human pathogenic fungus Aspergillus fumigatus evades the host complement system. Infect. Immun. *76*, 820–827.

Berkova, N., Lair-Fulleringer, S., Féménia, F., Huet, D., Wagner, M.-C., Gorna, K., Tournier, F., Ibrahim-Granet, O., Guillot, J., Chermette, R., et al. (2006). Aspergillus fumigatus conidia inhibit tumour necrosis factor- or staurosporine-induced apoptosis in epithelial cells. Int. Immunol. *18*, 139–150.

Berman, H.M., Westbrook, J., Feng, Z., Gilliland, G., Bhat, T.N., Weissig, H., Shindyalov, I.N., and Bourne, P.E. (2000). The Protein Data Bank. Nucleic Acids Res. *28*, 235–242.

Bernard, M., and Latgé, J.-P. (2001). Aspergillus fumigatus cell wall, composition and biosynthesis. Med. Mycol. *39*, 9–17.

Bertani, F.R., Botti, E., Costanzo, A., Ferrari, L., Mussi, V., D'Alessandro, M., and Selci, S. (2013). Label-free discrimination of cells undergoing apoptosis by hyperspectral confocual reflectance imaging. J. Eur. Opt. Soc. Rapid Publ. *8*.

Betteridge, D.J. (2000). What is oxidative stress? Metabolism, Clinical and Experimental: *49*, 3–8.

Bhat, M., and Hickey, A.J. (2000). Effect of chloroquine on phagolysosomal fusion in cultured guinea pig alveolar macrophages: implications in drug delivery. AAPS PharmSci *2*, E34.

Bijker, E.M., Nganou-Makamdop, K., van Gemert, G.-J., Zavala, F., Cockburn, I., and Sauerwein, R.W. (2015). Studying the effect of chloroquine on sporozoite-induced protection and immune responses in Plasmodium berghei malaria. Malar. J. *14*.

Bioucas-Dias, J.M., Plaza, A., Dobigeon, N., Parente, M., Du, Q., Gader, P., and Chanussot, J. (2012). Hyperspectral Unmixing Overview: Geometrical, Statistical, and Sparse Regression-Based Approaches. IEEE J. Sel. Top. Appl. Earth Obs. Remote Sens. *5*, 354–379.

Botha, C.J., Legg, M.J., Truter, M., and Sulyok, M. (2014). Multitoxin analysis of Aspergillus clavatus infected feed samples implicated in two outbreaks of neuromycotoxicosis in cattle in South Africa. Onderstepoort J Vet Res *81*.

Bowman, E.J., Siebers, A., and Altendorf, K. (1988). Bafilomycins: a class of inhibitors of membrane ATPases from microorganisms, animal cells, and plant cells. Proc. Natl. Acad. Sci. U. S. A. *85*, 7972–7976.

Brakhage, A.A., and Liebmann, B. (2005). Aspergillus fumigatus conidial pigment and cAMP signal transduction: significance for virulence. Med. Mycol. *43 Suppl 1*, S75–S82.

Brauchle, E., Thude, S., Brucker, S.Y., and Schenke-Layland, K. (2014). Cell death stages in single apoptotic and necrotic cells monitored by Raman microspectroscopy. Sci. Rep. *4*.

Busca, A., Saxena, M., Kryworuchko, M., and Kumar, A. (2009). Anti-Apoptotic Genes in the Survival of Monocytic Cells During Infection. Curr. Genomics *10*, 306–317.

Cagas, S.E., Jain, M.R., Li, H., and Perlin, D.S. (2011). The Proteomic Signature of Aspergillus fumigatus During Early Development. Mol. Cell. Proteomics *10*, M111.010108–M111.010108.

Calvo, A.M., and Cary, J.W. (2015). Association of fungal secondary metabolism and sclerotial biology. Front. Microbiol. *6*.

Cao, S., Liu, P., Zhu, H., Gong, H., Yao, J., Sun, Y., Geng, G., Wang, T., Feng, S., Han, M., et al. (2015). Extracellular Acidification Acts as a Key Modulator of Neutrophil Apoptosis and Functions. PLOS ONE *10*, e0137221.

Cary, J.W., Harris-Coward, P.Y., Ehrlich, K.C., Di Mavungu, J.D., Malysheva, S.V., De Saeger, S., Dowd, P.F., Shantappa, S., Martens, S.L., and Calvo, A.M. (2014). Functional characterization of a veA-dependent polyketide synthase gene in Aspergillus flavus necessary for the synthesis of asparasone, a sclerotium-specific pigment. Fungal Genet. Biol. *64*, 25–35.

Chein-I Chang (2000). An information-theoretic approach to spectral variability, similarity, and discrimination for hyperspectral image analysis. IEEE Trans. Inf. Theory *46*, 1927–1932.

Chen, Y.M., Lin, P., He, Y., He, J.Q., Zhang, J., and Li, X.L. (2016). Fast quantifying collision strength index of ethylene-vinyl acetate copolymer coverings on the fields based on near infrared hyperspectral imaging techniques. Sci. Rep. *6*, 20843.

Chi, M.-H., and Craven, K.D. (2016). RacA-Mediated ROS Signaling Is Required for Polarized Cell Differentiation in Conidiogenesis of Aspergillus fumigatus. PLOS ONE *11*, e0149548.

Coakley, R.J., Taggart, C., McElvaney, N.G., and O'Neill, S.J. (2002). Cytosolic pH and the inflammatory microenvironment modulate cell death in human neutrophils after phagocytosis. Blood *100*, 3383–3391.

Cotty, P.J. (1989). Virulence and Cultural Characteristics of Two Aspergillus flavus Strains Pathogenic on Cotton. Phytopathology *79*, 808.

Creagh, E.M., Conroy, H., and Martin, S.J. (2003). Caspase-activation pathways in apoptosis and immunity. Immunol. Rev. *193*, 10–21.

Cullen, S.P., and Martin, S.J. (2009). Caspase activation pathways: some recent progress. Cell Death Differ. *16*, 935–938.

Cunha, M.M., Franzen, A.J., Seabra, S.H., Herbst, M.H., Vugman, N.V., Borba, L.P., de Souza, W., and Rozental, S. (2010). Melanin in Fonsecaea pedrosoi: a trap for oxidative radicals. BMC Microbiol. *10*, 80.

Dagenais, T.R.T., and Keller, N.P. (2009). Pathogenesis of Aspergillus fumigatus in Invasive Aspergillosis. Clin. Microbiol. Rev. *22*, 447–465.

Daly, J.T., Bodkin, W.A., Schneller, W.J., Kerr, R.B., Noto, J., Haren, R., Eismann, M.T., and Karch, B.K. (2000). Tunable narrow-band filter for LWIR hyperspectral imaging. SPIE *3948*, 104–115.

Decan, N., Wu, D., Williams, A., Bernatchez, S., Johnston, M., Hill, M., and Halappanavar, S. (2016). Characterization of in vitro genotoxic, cytotoxic and transcriptomic responses following exposures to amorphous silica of different sizes. Mutat. Res. Genet. Toxicol. Environ. Mutagen. *796*, 8–22.

De Duve, C. (1965). The separation and characterization of subcellular particles. Harvey Lect. *59*, 49–87.

Degterev, A., and Yuan, J. (2008). Expansion and evolution of cell death programmes. Nat. Rev. Mol. Cell Biol. *9*, 378–390.

Demaurex, N. (2002). pH Homeostasis of cellular organelles. News Physiol. Sci. Int. J. Physiol. Prod. Jointly Int. Union Physiol. Sci. Am. Physiol. Soc. *17*, 1–5.

Demetriades, C., Plescher, M., and Teleman, A.A. (2016). Lysosomal recruitment of TSC2 is a universal response to cellular stress. Nat. Commun. *7*, 10662.

Deshmukh, M., and Johnson, E.M. (2000). Staurosporine-induced neuronal death: multiple mechanisms and methodological implications. Cell Death Differ. *7*, 250–261.

Desjardins, L.M., and MacManus, J.P. (1995). An adherent cell model to study different stages of apoptosis. Exp. Cell Res. *216*, 380–387.

Diamond, R.D., Huber, E., and Haudenschild, C.C. (1983). Mechanisms of destruction of Aspergillus fumigatus hyphae mediated by human monocytes. J. Infect. Dis. *147*, 474–483.

Dierckx, P. (1993). Curve and surface fitting with splines (Oxford; New York: Clarendon).

Di Napoli, C., Pope, I., Masia, F., Watson, P., Langbein, W., and Borri, P. (2014). Hyperspectral and differential CARS microscopy for quantitative chemical imaging in human adipocytes. Biomed. Opt. Express *5*, 1378–1390.

Duan, S., Hajek, P., Lin, C., Shin, S.K., Attardi, G., and Chomyn, A. (2003). Mitochondrial Outer Membrane Permeability Change and Hypersensitivity to Digitonin Early in Staurosporine-induced Apoptosis. J. Biol. Chem. *278*, 1346–1353.

van Duin, D., Casadevall, A., and Nosanchuk, J.D. (2002). Melanization of Cryptococcus neoformans and Histoplasma capsulatum Reduces Their Susceptibilities to Amphotericin B and Caspofungin. Antimicrob. Agents Chemother. *46*, 3394–3400.

Dyer, P.S., and Paoletti, M. (2005). Reproduction in Aspergillus fumigatus: sexuality in a supposedly asexual species? Med. Mycol. *43 Suppl 1*, S7–S14.

Eisenman, H.C., and Casadevall, A. (2012). Synthesis and assembly of fungal melanin. Appl. Microbiol. Biotechnol. *93*, 931–940.

Elmore, S. (2007). Apoptosis: A Review of Programmed Cell Death. Toxicol. Pathol. *35*, 495–516.

Ene, I.V., and Bennett, R.J. (2014). The cryptic sexual strategies of human fungal pathogens. Nat. Rev. Microbiol. *12*, 239–251.

Erl, W., Weber, C., Wardemann, C., and Weber, P.C. (1995). Adhesion properties of Mono Mac 6, a monocytic cell line with characteristics of mature human monocytes. Atherosclerosis *113*, 99–107.

Fackler, O.T., and Grosse, R. (2008). Cell motility through plasma membrane blebbing. J. Cell Biol. *181*, 879–884.

Fahy, R.J., Doseff, A.I., and Wewers, M.D. (1999). Spontaneous human monocyte apoptosis utilizes a caspase-3-dependent pathway that is blocked by endotoxin and is independent of caspase-1. J. Immunol. Baltim. Md 1950 *163*, 1755–1762.

Fass, E., Shvets, E., Degani, I., Hirschberg, K., and Elazar, Z. (2006). Microtubules Support Production of Starvation-induced Autophagosomes but Not Their Targeting and Fusion with Lysosomes. J. Biol. Chem. *281*, 36303–36316.

Feldmesser, M. (2006). Role of Neutrophils in Invasive Aspergillosis. Infect. Immun. *74*, 6514–6516.

Féménia, F., Huet, D., Lair-Fulleringer, S., Wagner, M.C., Sarfati, J., Shingarova, L., Guillot, J., Boireau, P., Chermette, R., and Berkova, N. (2009). Effects of conidia of various Aspergillus species on apoptosis of human pneumocytes and bronchial epithelial cells. Mycopathologia *167*, 249–262.

Finlayson, E.A., and Brown, P.D. (2011). Comparison of antibiotic resistance and virulence factors in pigmented and non-pigmented Pseudomonas aeruginosa. West Indian Med. J. *60*, 24–32.

Frisvad, J.C., and Larsen, T.O. (2016). Extrolites of Aspergillus fumigatus and Other Pathogenic Species in Aspergillus Section Fumigati. Front. Microbiol. *6*.

Fulda, S., and Debatin, K.-M. (2006). Extrinsic versus intrinsic apoptosis pathways in anticancer chemotherapy. Oncogene *25*, 4798–4811.

Gastebois, A., Clavaud, C., Aimanianda, V., and Latgé, J.-P. (2009). Aspergillus fumigatus: cell wall polysaccharides, their biosynthesis and organization. Future Microbiol. *4*, 583–595.

Gaudi, S., Meyer, R., Ranka, J., Granahan, J.C., Israel, S.A., Yachik, T.R., and Jukic, D.M. (2014). Hyperspectral Imaging of Melanocytic Lesions: Am. J. Dermatopathol. *36*, 131–136.

Geissler, A., Haun, F., Frank, D.O., Wieland, K., Simon, M.M., Idzko, M., Davis, R.J., Maurer, U., and Borner, C. (2013). Apoptosis induced by the fungal pathogen gliotoxin requires a triple phosphorylation of Bim by JNK. Cell Death Differ. *20*, 1317–1329.

Geissmann, F., Jung, S., and Littman, D.R. (2003). Blood monocytes consist of two principal subsets with distinct migratory properties. Immunity *19*, 71–82.

Goetz, A.F.H., Vane, G., Solomon, J.E., and Rock, B.N. (1985). Imaging Spectrometry for Earth Remote Sensing. Science *228*, 1147–1153.

Goldman, A.S., and Prabhakar, B.S. (1996). Immunology Overview. In Medical Microbiology, S. Baron, ed. (Galveston (TX): University of Texas Medical Branch at Galveston),.

Gordon, R.J., and Lowy, F.D. (2008). Pathogenesis of Methicillin-Resistant Staphylococcus aureus Infection. Clin. Infect. Dis. *46*, S350–S359.

Gorvel, J.-P. (2003). Intracellular pathogens in membrane interactions and vacuole biogenesis (Georgetown, Tex: Landes Bioscience).

Gosnell, M.E., Anwer, A.G., Cassano, J.C., Sue, C.M., and Goldys, E.M. (2016). Functional hyperspectral imaging captures subtle details of cell metabolism in olfactory neurosphere cells, disease-specific models of neurodegenerative disorders. Biochim. Biophys. Acta BBA - Mol. Cell Res. *1863*, 56–63.

Guobin, H., Congyi, Z., Sanfu, Q., and Yangbao, W. (1999). Studies on inhibitory effect of melanin on the apoptosis induced by influenza virus in host cells. Eur. PMC 140–146.

Hartmann, T., Baronian, G., Nippe, N., Voss, M., Schulthess, B., Wolz, C., Eisenbeis, J., Schmidt-Hohagen, K., Gaupp, R., Sunderkötter, C., et al. (2014). The Catabolite Control Protein E (CcpE) Affects Virulence Determinant Production and Pathogenesis of Staphylococcus aureus. J. Biol. Chem. *289*, 29701–29711.

Hedayati, M.T., Pasqualotto, A.C., Warn, P.A., Bowyer, P., and Denning, D.W. (2007). Aspergillus flavus: human pathogen, allergen and mycotoxin producer. Microbiol. Read. Engl. *153*, 1677–1692.

Heinekamp, T., Thywißen, A., Macheleidt, J., Keller, S., Valiante, V., and Brakhage, A.A. (2013). Aspergillus fumigatus melanins: interference with the host endocytosis pathway and impact on virulence. Front. Microbiol. *3*.

Heinekamp, T., Schmidt, H., Lapp, K., Pähtz, V., Shopova, I., Köster-Eiserfunke, N., Krüger, T., Kniemeyer, O., and Brakhage, A.A. (2015). Interference of Aspergillus fumigatus with the immune response. Semin. Immunopathol. *37*, 141–152.

Hernandez-Palacios, J., Haug, I.J., Grimstad, ø., and Randeberg, L.L. (2011). Hyperspectral characterization of fluorophore diffusion in human skin using a sCMOS based hyperspectral camera. N. Ramanujam, and J. Popp, eds. pp. 808717–808717 – 8.

Hill, H.Z. (1992). The function of melanin or six blind people examine an elephant. BioEssays News Rev. Mol. Cell. Dev. Biol. *14*, 49–56.

Hill, T., and Käefer, E. (2001). Improved protocols for Aspergillus minimal medium: trace element and minimal medium salt stock solutions. Fungal Genet. Newsl. 20–21.

Hochman, A. (1997). Programmed cell death in prokaryotes. Crit. Rev. Microbiol. *23*, 207–214.

Hoffmann, K., Discher, S., and Voigt, K. (2007). Revision of the genus Absidia (Mucorales, Zygomycetes) based on physiological, phylogenetic, and morphological characters; thermotolerant Absidia spp. form a coherent group, Mycocladiaceae fam. nov. Mycol. Res. *111*, 1169–1183.

Hohl, T.M., and Feldmesser, M. (2007). Aspergillus fumigatus: Principles of Pathogenesis and Host Defense. Eukaryot. Cell *6*, 1953–1963.

Holmgren, L., Szeles, A., Rajnavölgyi, E., Folkman, J., Klein, G., Ernberg, I., and Falk, K.I. (1999). Horizontal transfer of DNA by the uptake of apoptotic bodies. Blood *93*, 3956–3963.

Holt, D.C., Holden, M.T.G., Tong, S.Y.C., Castillo-Ramirez, S., Clarke, L., Quail, M.A., Currie, B.J., Parkhill, J., Bentley, S.D., Feil, E.J., et al. (2011). A Very Early-Branching Staphylococcus aureus Lineage Lacking the Carotenoid Pigment Staphyloxanthin. Genome Biol. Evol. *3*, 881–895.

Hospenthal, D.R., Kwon-Chung, K.J., and Bennett, J.E. (1998). Concentrations of airborne Aspergillus compared to the incidence of invasive aspergillosis: lack of correlation. Med. Mycol. *36*, 165–168.

Hu, Y., Carraro-Lacroix, L.R., Wang, A., Owen, C., Bajenova, E., Corey, P.N., Brumell, J.H., and Voronov, I. (2016). Lysosomal pH Plays a Key Role in Regulation of mTOR Activity in Osteoclasts: Lysosomal pH Plays a Key Role in Regulation. J. Cell. Biochem. *117*, 413–425.

Huang, S. (2009). Non-genetic heterogeneity of cells in development: more than just noise. Development *136*, 3853–3862.

Ibrahim-Granet, O., Philippe, B., Boleti, H., Boisvieux-Ulrich, E., Grenet, D., Stern, M., and Latge, J.P. (2003). Phagocytosis and Intracellular Fate of Aspergillus fumigatus Conidia in Alveolar Macrophages. Infect. Immun. *71*, 891–903.

Ip, W.K.E., Sokolovska, A., Charriere, G.M., Boyer, L., Dejardin, S., Cappillino, M.P., Yantosca, L.M., Takahashi, K., Moore, K.J., Lacy-Hulbert, A., et al. (2010). Phagocytosis and Phagosome Acidification Are

Required for Pathogen Processing and MyD88-Dependent Responses to Staphylococcus aureus. J. Immunol. *184*, 7071–7081.

Iqbal, A., Sun, D.-W., and Allen, P. (2014). An overview on principle, techniques and application of hyperspectral imaging with special reference to ham quality evaluation and control. Food Control *46*, 242–254.

Jackson, J.C., Higgins, L.A., and Lin, X. (2009). Conidiation Color Mutants of Aspergillus fumigatus Are Highly Pathogenic to the Heterologous Insect Host Galleria mellonella. PLoS ONE *4*, e4224.

Jacobson, E.S. (2000). Pathogenic Roles for Fungal Melanins. Clin. Microbiol. Rev. *13*, 708–717.

Jahn, B., Koch, A., Schmidt, A., Wanner, G., Gehringer, H., Bhakdi, S., and Brakhage, A.A. (1997). Isolation and characterization of a pigmentless-conidium mutant of Aspergillus fumigatus with altered conidial surface and reduced virulence. Infect. Immun. *65*, 5110–5117.

Jahn, B., Langfelder, K., Schneider, U., Schindel, C., and Brakhage, A.A. (2002). PKSP-dependent reduction of phagolysosome fusion and intracellular kill of Aspergillus fumigatus conidia by human monocyte-derived macrophages. Cell. Microbiol. *4*, 793–803.

Johansson, A.-C., Steen, H., Öllinger, K., and Roberg, K. (2003). Cathepsin D mediates cytochrome c release and caspase activation in human fibroblast apoptosis induced by staurosporine. Cell Death Differ. *10*, 1253–1259.

Johansson, A.-C., Appelqvist, H., Nilsson, C., Kågedal, K., Roberg, K., and Öllinger, K. (2010). Regulation of apoptosis-associated lysosomal membrane permeabilization. Apoptosis *15*, 527–540.

Kågedal, K., Johansson, A.-C., Johansson, U., Heimlich, G., Roberg, K., Wang, N.S., Jürgensmeier, J.M., and Öllinger, K. (2005). Lysosomal membrane permeabilization during apoptosis - involvement of Bax?: Bax-mediated lysosomal membrane permeabilization. Int. J. Exp. Pathol. *86*, 309–321.

Kerr, J.F. (1971). Shrinkage necrosis: a distinct mode of cellular death. J. Pathol. *105*, 13–20.

Kerr, J.F., Wyllie, A.H., and Currie, A.R. (1972). Apoptosis: a basic biological phenomenon with wide-ranging implications in tissue kinetics. Br. J. Cancer *26*, 239–257.

Kim, J.-M., Bae, H.R., Park, B.S., Lee, J.M., Ahn, H.B., Rho, J.H., Yoo, K.W., Park, W.C., Rho, S.H., Yoon, H.S., et al. (2003). Early Mitochondrial Hyperpolarization and Intracellular Alkalinization in Lactacystin-Induced Apoptosis of Retinal Pigment Epithelial Cells. J. Pharmacol. Exp. Ther. *305*, 474–481.

Kluytmans, J., van Belkum, A., and Verbrugh, H. (1997). Nasal carriage of Staphylococcus aureus: epidemiology, underlying mechanisms, and associated risks. Clin. Microbiol. Rev. *10*, 505–520.

Knetsch, R., Arnold, W., Erfurth, F., Scheibe, A., Nyuyki, B., and Schmidt, W.-D. (2009). Bildgebende optische Spektralsensorik zur automatischen Regelung von Gasbrennern für die Glas verarbeitende Industrie. 251–256.

Konforti, B. (1999). Picture story. How proton pumps make ATP. Nat. Struct. Biol. *6*, 1090.

Kornfeld, S., and Mellman, I. (1989). The biogenesis of lysosomes. Annu. Rev. Cell Biol. *5*, 483–525.

Kravchenko-Balasha, N., Mizrachy-Schwartz, S., Klein, S., and Levitzki, A. (2009). Shift from Apoptotic to Necrotic Cell Death during Human Papillomavirus-induced Transformation of Keratinocytes. J. Biol. Chem. *284*, 11717–11727.

Kriesel, J., Scriven, G., Gat, N., Nagaraj, S., Willson, P., and Swaminathan, V. (2012). Snapshot hyperspectral fovea vision system (HyperVideo). p. 83900T – 83900T – 6.

Kumar, S.K., Singh, P., and Sinha, S. (2015). Naturally produced opsonizing antibodies restrict the survival of Mycobacterium tuberculosis in human macrophages by augmenting phagosome maturation. Open Biol. *5*, 150171.

Kupfahl, C., Michalka, A., Lass-Flörl, C., Fischer, G., Haase, G., Ruppert, T., Geginat, G., and Hof, H. (2008). Gliotoxin production by clinical and environmental Aspergillus fumigatus strains. Int. J. Med. Microbiol. IJMM *298*, 319–327.

Kurz, T., Terman, A., Gustafsson, B., and Brunk, U.T. (2008). Lysosomes in iron metabolism, ageing and apoptosis. Histochem. Cell Biol. *129*, 389–406.

Kwon-Chung, K.J. (2012). Taxonomy of Fungi Causing Mucormycosis and Entomophthoramycosis (Zygomycosis) and Nomenclature of the Disease: Molecular Mycologic Perspectives. Clin. Infect. Dis. *54*, S8–S15.

Lagadic-Gossmann, D., Huc, L., and Lecureur, V. (2004). Alterations of intracellular pH homeostasis in apoptosis: origins and roles. Cell Death Differ. *11*, 953–961.

Langfelder, K., Jahn, B., Gehringer, H., Schmidt, A., Wanner, G., and Brakhage, A.A. (1998). Identification of a polyketide synthase gene (pksP) of Aspergillus fumigatus involved in conidial pigment biosynthesis and virulence. Med. Microbiol. Immunol. (Berl.) *187*, 79–89.

Langfelder, K., Streibel, M., Jahn, B., Haase, G., and Brakhage, A.A. (2003). Biosynthesis of fungal melanins and their importance for human pathogenic fungi. Fungal Genet. Biol. FG B *38*, 143–158.

Latge, J.-P. (1999). Aspergillus fumigatus and Aspergillosis. Clin. Microbiol. Rev. *12*, 310–350.

Ledda-Columbano, G.M., Coni, P., Curto, M., Giacomini, L., Faa, G., Oliverio, S., Piacentini, M., and Columbano, A. (1991). Induction of two different modes of cell death, apoptosis and necrosis, in rat liver after a single dose of thioacetamide. Am. J. Pathol. *139*, 1099–1109.

Levsky, J., and Singer, R. (2003). Gene expression and the myth of the average cell. Trends Cell Biol. *13*, 4–6.

Li, Q., Xue, Y., Xiao, G., and Zhang, J. (2008). Study on microscope hyperspectral medical imaging method for biomedical quantitative analysis. Chin. Sci. Bull. *53*, 1431–1434.

Litzka, O., Then Bergh, K., and Brakhage, A.A. (1996). The Aspergillus nidulans Penicillin-Biosynthesis Gene aat (penDE) is Controlled by a CCAAT-Containing DNA Element. Eur. J. Biochem. *238*, 675–682.

Liu, D. (2000). Caspase-8-mediated Intracellular Acidification Precedes Mitochondrial Dysfunction in Somatostatin-induced Apoptosis. J. Biol. Chem. *275*, 9244–9250.

Liu, G.Y. (2005). Staphylococcus aureus golden pigment impairs neutrophil killing and promotes virulence through its antioxidant activity. J. Exp. Med. *202*, 209–215.

Liu, C.-I., Liu, G.Y., Song, Y., Yin, F., Hensler, M.E., Jeng, W.-Y., Nizet, V., Wang, A.H.-J., and Oldfield, E. (2008). A Cholesterol Biosynthesis Inhibitor Blocks Staphylococcus aureus Virulence. Science *319*, 1391–1394.

Lu, G., and Fei, B. (2014). Medical hyperspectral imaging: a review. J. Biomed. Opt. *19*, 010901.

Luther, K., Torosantucci, A., Brakhage, A.A., Heesemann, J., and Ebel, F. (2007). Phagocytosis of Aspergillus fumigatus conidia by murine macrophages involves recognition by the dectin-1 beta-glucan receptor and Toll-like receptor 2. Cell. Microbiol. *9*, 368–381.

Luzio, J.P., Pryor, P.R., and Bright, N.A. (2007). Lysosomes: fusion and function. Nat. Rev. Mol. Cell Biol. *8*, 622–632.

Marvig, R.L., Dolce, D., Sommer, L.M., Petersen, B., Ciofu, O., Campana, S., Molin, S., Taccetti, G., and Johansen, H.K. (2015). Within-host microevolution of Pseudomonas aeruginosa in Italian cystic fibrosis patients. BMC Microbiol. *15*.

Matsuyama, S., and Reed, J.C. (2000). Mitochondria-dependent apoptosis and cellular pH regulation. Cell Death Differ. *7*, 1155–1165.

Mcfarland, J. (1907). The Nephelometer: an instrument for estimating the number of bacteria in suspensions used for calculating the opsonic index and for vaccins. JAMA J. Am. Med. Assoc. *XLIX*, 1176.

McIlwain, D.R., Berger, T., and Mak, T.W. (2013). Caspase functions in cell death and disease. Cold Spring Harb. Perspect. Biol. *5*, a008656.

Miao, Y., Liu, D., Li, G., Li, P., Xu, Y., Shen, Q., and Zhang, R. (2015). Genome-wide transcriptomic analysis of a superior biomass-degrading strain of A. fumigatus revealed active lignocellulose-degrading genes. BMC Genomics *16*, 459.

Michiels, B., Appelen, L., Franck, B., den Heijer, C.D.J., Bartholomeeusen, S., and Coenen, S. (2015). Staphylococcus aureus, Including Meticillin-Resistant Staphylococcus aureus, among General Practitioners and Their Patients: A Cross-Sectional Study. PLOS ONE *10*, e0140045.

Müllbacher, A., Waring, P., Tiwari-Palni, U., and Eichner, R.D. (1986). Structural relationship of epipolythiodioxopiperazines and their immunomodulating activity. Mol. Immunol. *23*, 231–235.

Nahrendorf, M., Swirski, F.K., Aikawa, E., Stangenberg, L., Wurdinger, T., Figueiredo, J.-L., Libby, P., Weissleder, R., and Pittet, M.J. (2007). The healing myocardium sequentially mobilizes two monocyte subsets with divergent and complementary functions. J. Exp. Med. *204*, 3037–3047.

Nanis G. Allam (2012). Protective role of Aspergillus fumigatus melanin against ultraviolet (UV) irradiation and Bjerkandera adusta melanin as a candidate vaccine against systemic candidiasis. Afr. J. Biotechnol. *11*.

Neustock, P., Brand, J.M., Kruse, A., and Kirchner, H. (1993). Cytokine production of the human monocytic cell line Mono Mac 6 in comparison to mature monocytes in peripheral blood mononuclear cells. Immunobiology *188*, 293–302.

Nilsson, C., Kågedal, K., Johansson, U., and Ollinger, K. (2003). Analysis of cytosolic and lysosomal pH in apoptotic cells by flow cytometry. Methods Cell Sci. Off. J. Soc. Vitro Biol. *25*, 185–194.

O'Gorman, C.M., Fuller, H.T., and Dyer, P.S. (2009). Discovery of a sexual cycle in the opportunistic fungal pathogen Aspergillus fumigatus. Nature *457*, 471–474.

Olguín-Albuerne, M., Ramos-Pittol, J.M., Coyoy, A., Martínez-Briseño, C.P., Domínguez, G., and Morán, J. (2015). Peroxynitrite is Involved in the Apoptotic Death of Cultured Cerebellar Granule Neurons Induced by Staurosporine, but not by Potassium Deprivation. Neurochem. Res.

Olivier, A.C., Lemaire, S., Van Bambeke, F., Tulkens, P.M., and Oldfield, E. (2009). Role of rsbU and Staphyloxanthin in Phagocytosis and Intracellular Growth of Staphylococcus aureus in Human Macrophages and Endothelial Cells. J. Infect. Dis. *200*, 1367–1370.

Olszewska-Słonina, D.M., Styczyński, J., Czajkowski, R., Drewa, T.A., and Musiałkiewicz, D. (2007). Cell cycle, melanin contents and apoptosis processes in B16 and Cloudman S91 mouse melanoma cells after exposure to cytostatic drugs. Acta Pol. Pharm. *64*, 469–478.

Osiewacz, H.D. (2002). Molecular biology of fungal development (New York: M. Dekker).

Palumbo, C., De Luca, A., Rosato, N., Forgione, M., Rotili, D., and Caccuri, A.M. (2016). c-Jun N-terminal kinase activation by nitrobenzoxadiazoles leads to late-stage autophagy inhibition. J. Transl. Med. *14*.

Park, H.J. (1995). Effects of intracellular pH on apoptosis in HL-60 human leukemia cells. Yonsei Med. J. *36*, 473–479.

Peña, M.D.P.S., Gottipati, A., Tahiliani, S., Neu-Baker, N.M., Frame, M.D., Friedman, A.J., and Brenner, S.A. (2016). Hyperspectral imaging of nanoparticles in biological samples: Simultaneous visualization and elemental identification: Hyperspectral Mapping in Biological Samples. Microsc. Res. Tech. n/a – n/a.

Perlin, D.S. (1998). Ion pumps as targets for therapeutic intervention: Old and new paradigms. Electron. J. Biotechnol. *1*, 55–64.

Philippe, B., Ibrahim-Granet, O., Prévost, M.C., Gougerot-Pocidalo, M.A., Perez, M.S., Meeren, A.V. der, and Latgé, J.P. (2003). Killing of Aspergillus fumigatus by Alveolar Macrophages Is Mediated by Reactive Oxidant Intermediates. Infect. Immun. *71*, 3034–3042.

Pihet, M., Vandeputte, P., Tronchin, G., Renier, G., Saulnier, P., Georgeault, S., Mallet, R., Chabasse, D., Symoens, F., and Bouchara, J.-P. (2009). Melanin is an essential component for the integrity of the cell wall of Aspergillus fumigatus conidia. BMC Microbiol. *9*, 177.

Pike, R., Patton, S.K., Lu, G., Halig, L.V., Wang, D., Chen, Z.G., and Fei, B. (2014). A Minimum Spanning Forest Based Hyperspectral Image Classification Method for Cancerous Tissue Detection. Proc. SPIE-- Int. Soc. Opt. Eng. *9034*, 90341W.

Plaza, A., Martinez, P., Perez, R., and Plaza, J. (2004). A Quantitative and Comparative Analysis of Endmember Extraction Algorithms From Hyperspectral Data. IEEE Trans. Geosci. Remote Sens. *42*, 650–663.

Pontecorvo, G., Roper, J.A., and Forbes, E. (1953). Genetic Recombination without Sexual Reproduction in Aspergillus niger. J. Gen. Microbiol. *8*, 198–210.

Reiter, M., Kirchner, B., Muller, H., Holzhauer, C., Mann, W., and Pfaffl, M.W. (2011). Quantification noise in single cell experiments. Nucleic Acids Res. *39*, e124–e124.

Rementeria, A., López-Molina, N., Ludwig, A., Vivanco, A.B., Bikandi, J., Pontón, J., and Garaizar, J. (2005). Genes and molecules involved in Aspergillus fumigatus virulence. Rev. Iberoam. Micol. *22*, 1–23.

Riccardi, C., and Nicoletti, I. (2006). Analysis of apoptosis by propidium iodide staining and flow cytometry. Nat. Protoc. *1*, 1458–1461.

Rieger, A.M., Nelson, K.L., Konowalchuk, J.D., and Barreda, D.R. (2011). Modified Annexin V/Propidium Iodide Apoptosis Assay For Accurate Assessment of Cell Death. J. Vis. Exp.

Saelens, X., Festjens, N., Vande Walle, L., van Gurp, M., van Loo, G., and Vandenabeele, P. (2004). Toxic proteins released from mitochondria in cell death. Oncogene *23*, 2861–2874.

Sahnoun, Z., Jamoussi, K., and Zeghal, K.M. (1997). [Free radicals and antioxidants: human physiology, pathology and therapeutic aspects]. Thérapie *52*, 251–270.

Samson, R.A., Visagie, C.M., Houbraken, J., Hong, S.-B., Hubka, V., Klaassen, C.H.W., Perrone, G., Seifert, K.A., Susca, A., Tanney, J.B., et al. (2014). Phylogeny, identification and nomenclature of the genus Aspergillus. Stud. Mycol. *78*, 141–173.

Sapmak, A., Boyce, K.J., Andrianopoulos, A., and Vanittanakom, N. (2015). The pbrB gene encodes a laccase required for DHN-melanin synthesis in conidia of Talaromyces (Penicillium) marneffei. PloS One *10*, e0122728.

Saral, R. (1991). Candida and Aspergillus infections in immunocompromised patients: an overview. Rev. Infect. Dis. *13*, 487–492.

Saravanan, M., and Nanda, A. (2010). Extracellular synthesis of silver bionanoparticles from Aspergillus clavatus and its antimicrobial activity against MRSA and MRSE. Colloids Surf. B Biointerfaces *77*, 214–218.

Schalk, I.J., and Guillon, L. (2013). Pyoverdine biosynthesis and secretion in Pseudomonas aeruginosa: implications for metal homeostasis. Environ. Microbiol. *15*, 1661–1673.

Schmaler-Ripcke, J., Sugareva, V., Gebhardt, P., Winkler, R., Kniemeyer, O., Heinekamp, T., and Brakhage, A.A. (2009). Production of Pyomelanin, a Second Type of Melanin, via the Tyrosine Degradation Pathway in Aspergillus fumigatus. Appl. Environ. Microbiol. *75*, 493–503.

Schumacher, J. (2016). DHN melanin biosynthesis in the plant pathogenic fungus *Botrytis cinerea* is based on two developmentally regulated key enzyme (PKS)-encoding genes: DHN melanogenesis in *Botrytis cinerea*. Mol. Microbiol. *99*, 729–748.

Schwartze, V.U., Hoffmann, K., Nyilasi, I., Papp, T., Vágvölgyi, C., de Hoog, S., Voigt, K., and Jacobsen, I.D. (2012). Lichtheimia Species Exhibit Differences in Virulence Potential. PLoS ONE *7*, e40908.

Schwartze, V.U., de A. Santiago, A.L.C.M., Jacobsen, I.D., and Voigt, K. (2014). The pathogenic potential of the Lichtheimia genus revisited: Lichtheimia brasiliensis is a novel, non-pathogenic species. Mycoses *57*, 128–131.

Scott, C.C., Botelho, R.J., and Grinstein, S. (2003). Phagosome maturation: a few bugs in the system. J. Membr. Biol. *193*, 137–152.

Serbina, N.V., Cherny, M., Shi, C., Bleau, S.A., Collins, N.H., Young, J.W., and Pamer, E.G. (2009). Distinct Responses of Human Monocyte Subsets to Aspergillus fumigatus Conidia. J. Immunol. *183*, 2678–2687.

Serranti, S., and Bonifazi, G. (2014). Hyperspectral imaging applied to end-of-life concrete recycling. R. Widenhorn, and A. Dupret, eds. p. 90220V.

Serranti, S., Gargiulo, A., and Bonifazi, G. (2012). Hyperspectral imaging for process and quality control in recycling plants of polyolefin flakes. J. Infrared Spectrosc. *20*, 573.

Seye, F., Faye, O., Ndiaye, M., Njie, E., and Marie Afoutou, J. (2009). Pathogenicity of the Fungus, Aspergillus clavatus , Isolated from the Locust, Oedaleus senegalensis , Against Larvae of the Mosquitoes Aedes aegypti, Anopheles gambiae and Culex quinquefasciatus. J. Insect Sci. *9*, 1–7.

Shamim, U., Hanif, S., Albanyan, A., Beck, F.W.J., Bao, B., Wang, Z., Banerjee, S., Sarkar, F.H., Mohammad, R.M., Hadi, S.M., et al. (2012). Resveratrol-induced apoptosis is enhanced in low pH environments associated with cancer. J. Cell. Physiol. *227*, 1493–1500.

Shapiro, R.S., Robbins, N., and Cowen, L.E. (2011). Regulatory Circuitry Governing Fungal Development, Drug Resistance, and Disease. Microbiol. Mol. Biol. Rev. *75*, 213–267.

Shi, C., and Pamer, E.G. (2011). Monocyte recruitment during infection and inflammation. Nat. Rev. Immunol. *11*, 762–774.

da Silva, M.B., Marques, A.F., Nosanchuk, J.D., Casadevall, A., Travassos, L.R., and Taborda, C.P. (2006). Melanin in the dimorphic fungal pathogen Paracoccidioides brasiliensis: effects on phagocytosis, intracellular resistance and drug susceptibility. Microbes Infect. Inst. Pasteur *8*, 197–205.

Skiada, A., Pagano, L., Groll, A., Zimmerli, S., Dupont, B., Lagrou, K., Lass-Florl, C., Bouza, E., Klimko, N., Gaustad, P., et al. (2011). Zygomycosis in Europe: analysis of 230 cases accrued by the registry of the European Confederation of Medical Mycology (ECMM) Working Group on Zygomycosis between 2005 and 2007. Clin. Microbiol. Infect. Off. Publ. Eur. Soc. Clin. Microbiol. Infect. Dis. *17*, 1859–1867.

Skouri-Gargouri, H., Jellouli-Chaker, N., and Gargouri, A. (2010). Factors affecting production and stability of the AcAFP antifungal peptide secreted by Aspergillus clavatus. Appl. Microbiol. Biotechnol. *86*, 535–543.

Slesiona, S., Gressler, M., Mihlan, M., Zaehle, C., Schaller, M., Barz, D., Hube, B., Jacobsen, I.D., and Brock, M. (2012). Persistence versus escape: Aspergillus terreus and Aspergillus fumigatus employ different strategies during interactions with macrophages. PloS One *7*, e31223.

Song, X., Zhang, J., Wang, M., Liu, W., Gu, X., and Lv, C.-J. (2011). Astaxanthin induces mitochondria-mediated apoptosis in rat hepatocellular carcinoma CBRH-7919 cells. Biol. Pharm. Bull. *34*, 839–844.

Stanzani, M., Orciuolo, E., Lewis, R., Kontoyiannis, D.P., Martins, S.L.R., St John, L.S., and Komanduri, K.V. (2005). Aspergillus fumigatus suppresses the human cellular immune response via gliotoxin-mediated apoptosis of monocytes. Blood *105*, 2258–2265.

Sturtevant, J., and Latgé, J.P. (1992). Participation of complement in the phagocytosis of the conidia of Aspergillus fumigatus by human polymorphonuclear cells. J. Infect. Dis. *166*, 580–586.

Sugareva, V., Härtl, A., Brock, M., Hübner, K., Rohde, M., Heinekamp, T., and Brakhage, A.A. (2006). Characterisation of the laccase-encoding gene abr2 of the dihydroxynaphthalene-like melanin gene cluster of Aspergillus fumigatus. Arch. Microbiol. *186*, 345–355.

Suzuki, K., and Vanier, M.T. (1999). Lysosomal Disease, Basic Neurochemistry: Molecular, Cellular and Medical Aspects. 6th edition (Philadelphia: Lippincott-Raven).

Suzuki, T., Takeda, M., and Tanabe, H. (1971). A new mycotoxin produced by Aspergillus clavatus. Chem. Pharm. Bull. (Tokyo) *19*, 1786–1788.

Tait, S.W.G., and Green, D.R. (2010). Mitochondria and cell death: outer membrane permeabilization and beyond. Nat. Rev. Mol. Cell Biol. *11*, 621–632.

Teutschbein, J., Albrecht, D., Pötsch, M., Guthke, R., Aimanianda, V., Clavaud, C., Latgé, J.-P., Brakhage, A.A., and Kniemeyer, O. (2010). Proteome profiling and functional classification of intracellular proteins from conidia of the human-pathogenic mold Aspergillus fumigatus. J. Proteome Res. *9*, 3427–3442.

Thau, N., Monod, M., Crestani, B., Rolland, C., Tronchin, G., Latgé, J.P., and Paris, S. (1994). rodletless mutants of Aspergillus fumigatus. Infect. Immun. *62*, 4380–4388.

Thornberry, N.A., and Lazebnik, Y. (1998). Caspases: enemies within. Science *281*, 1312–1316.

Thywißen, A., Heinekamp, T., Dahse, H.-M., Schmaler-Ripcke, J., Nietzsche, S., Zipfel, P.F., and Brakhage, A.A. (2011). Conidial Dihydroxynaphthalene Melanin of the Human Pathogenic Fungus Aspergillus fumigatus Interferes with the Host Endocytosis Pathway. Front. Microbiol. *2*.

Tolker-Nielsen, T., Chiodaroli, L., Bolognese, F., Orlandi, V.T., and Barbieri, P. (2015). Pigments influence the tolerance of Pseudomonas aeruginosa PAO1 to photodynamic induced oxidative stress. Microbiology.

Tong, Q., Xue, Y., and Zhang, L. (2014). Progress in Hyperspectral Remote Sensing Science and Technology in China Over the Past Three Decades. IEEE J. Sel. Top. Appl. Earth Obs. Remote Sens. *7*, 70–91.

Tredget, E.E., Shankowsky, H.A., Joffe, A.M., Inkson, T.I., Volpel, K., Paranchych, W., Kibsey, P.C., Alton, J.D., and Burke, J.F. (1992). Epidemiology of infections with Pseudomonas aeruginosa in burn patients: the role of hydrotherapy. Clin. Infect. Dis. Off. Publ. Infect. Dis. Soc. Am. *15*, 941–949.

Tsai, H.F., Chang, Y.C., Washburn, R.G., Wheeler, M.H., and Kwon-Chung, K.J. (1998). The developmentally regulated alb1 gene of Aspergillus fumigatus: its role in modulation of conidial morphology and virulence. J. Bacteriol. *180*, 3031–3038.

Tsai, H.F., Wheeler, M.H., Chang, Y.C., and Kwon-Chung, K.J. (1999). A developmentally regulated gene cluster involved in conidial pigment biosynthesis in Aspergillus fumigatus. J. Bacteriol. *181*, 6469–6477.

Tsai, H.-F., Fujii, I., Watanabe, A., Wheeler, M.H., Chang, Y.C., Yasuoka, Y., Ebizuka, Y., and Kwon-Chung, K.J. (2001). Pentaketide Melanin Biosynthesis in Aspergillus fumigatus Requires Chain-length Shortening of a Heptaketide Precursor. J. Biol. Chem. *276*, 29292–29298.

Turk, B., Stoka, V., Rozman-Pungercar, J., Cirman, T., Droga-Mazovec, G., Oreic, K., and Turk, V. (2002). Apoptotic Pathways: Involvement of Lysosomal Proteases. Biol. Chem. *383*.

Turra, G., Conti, N., and Signoroni, A. (2015). Hyperspectral image acquisition and analysis of cultured bacteria for the discrimination of urinary tract infections. (IEEE), pp. 759–762.

Upadhyay, S., Torres, G., and Lin, X. (2013). Laccases Involved in 1,8-Dihydroxynaphthalene Melanin Biosynthesis in Aspergillus fumigatus Are Regulated by Developmental Factors and Copper Homeostasis. Eukaryot. Cell *12*, 1641–1652.

VanHook, A.M. (2015). Intracellular pH gradient guides cells. Sci. Signal. *8*, ec106–ec106.

Varga, J., Due, M., Frisvad, J.C., and Samson, R.A. (2007). Taxonomic revision of Aspergillus section Clavati based on molecular, morphological and physiological data. Stud. Mycol. *59*, 89–106.

Victor, B.C., and Sloane, B.F. (2007). Cysteine cathepsin non-inhibitory binding partners: modulating intracellular trafficking and function. Biol. Chem. *388*, 1131–1140.

Vo-Dinh, T. (2004). A hyperspectral imaging system for in vivo optical diagnostics. IEEE Eng. Med. Biol. Mag. *23*, 40–49.

Volling, K., Brakhage, A.A., and Saluz, H.P. (2007). Apoptosis inhibition of alveolar macrophages upon interaction with conidia of Aspergillus fumigatus. FEMS Microbiol. Lett. *275*, 250–254.

Volling, K., Thywissen, A., Brakhage, A.A., and Saluz, H.P. (2011). Phagocytosis of melanized Aspergillus conidia by macrophages exerts cytoprotective effects by sustained PI3K/Akt signalling. Cell. Microbiol. *13*, 1130–1148.

Wagadarikar, A.A., Pitsianis, N.P., Sun, X., and Brady, D.J. (2009). Video rate spectral imaging using a coded aperture snapshot spectral imager. Opt. Express *17*, 6368.

Wasylnka, J.A., and Moore, M.M. (2003). Aspergillus fumigatus conidia survive and germinate in acidic organelles of A549 epithelial cells. J. Cell Sci. *116*, 1579–1587.

Wilson, S., and Latifi, S. (2014). Denoising HSI images for standoff target detection. M. Velez-Reyes, and F.A. Kruse, eds. p. 908812.

Wlodkowic, D., Telford, W., Skommer, J., and Darzynkiewicz, Z. (2011). Apoptosis and beyond: cytometry in studies of programmed cell death. Methods Cell Biol. *103*, 55–98.

Wlodkowic, D., Skommer, J., and Darzynkiewicz, Z. (2012). Cytometry of apoptosis. Historical perspective and new advances. Exp. Oncol. *34*, 255–262.

Wostemeyer, J. (1985). Strain-dependent variation in ribosomal DNA arrangement in Absidia glauca. Eur. J. Biochem. *146*, 443–448.

Wuren, T., Toyotome, T., Yamaguchi, M., Takahashi-Nakaguchi, A., Muraosa, Y., Yahiro, M., Wang, D.-N., Watanabe, A., Taguchi, H., and Kamei, K. (2014). Effect of serum components on biofilm formation by Aspergillus fumigatus and other Aspergillus species. Jpn. J. Infect. Dis. *67*, 172–179.

Yamaguchi, Y., Beer, J.Z., and Hearing, V.J. (2008). Melanin mediated apoptosis of epidermal cells damaged by ultraviolet radiation: factors influencing the incidence of skin cancer. Arch. Dermatol. Res. *300 Suppl 1*, S43–S50.

Yang, J., Zhang, L., Yu, C., Yang, X.-F., and Wang, H. (2014). Monocyte and macrophage differentiation: circulation inflammatory monocyte as biomarker for inflammatory diseases. Biomark. Res. *2*, 1.

10 Abbreviations

~	Approximately	/	Or
^0C	Degree Celsius	%	Percent
Δ	Deletion	®	Registered trademark
×	Fold magnification	™	Trademark
A		**I**	
Abr2	*Aspergillus* brown 2 mutant	**IA**	Invasive Aspergillosis
AMM	*Aspergillus minimal medium*	**IAP**	Inhibitor of apoptosis protein
Arp1	*Aspergillus* red 1 mutant	**i.e.**	That is
Ayg1	*Aspergillus* yellow1 mutant	**IFN**	Interferon
C		**IL**	Interleukin
cAMP	Cyclic AMP	**L**	
Casp	Caspase	**L**	Liter
CO_2	Carbon dioxide	**LPS**	Lipopolysaccharide
D		**M**	
Dapi	Deamino-phenylindole	**M**	Molar (mol/L)
DHN	Dihydroxynaphthalene	**m**	Mutant
DM	Diameter	**MAPK**	Mitogen-activated protein Kinase
DMSO	Dimethylsulfoxide	**µ**	Micro
DOPA	Dihydroxyphenylalanine	**µg**	Microgram
E		**min**	Minute (s)
Ex/ Em	Excitation/Emission	**ml**	Milliliter
EDTA	Ethylenediaminetetraacetic acid	**µl**	Microliter
e.g.	For example	**µm**	Micrometer
F		**mM**	Millimolare
FCS	Fatal calf serum	**MM6**	Monomac 6 cell line
FADD	Fas-associated death domain	**MOI**	Multiplicity of infection
Fig.	Figure	**N**	
FITC	Fluorescein isothiocyanate	**nM**	Nanomolar
G		**P**	
g	Gram (s)	**PBS**	Phosphate-buffered saline
H		**pHrodo**	pH-sensitive Molecular Probes
h	Hour (s)	**p.i.**	Post infection
HIV	Human Immunodeficiency Virus	**PI**	Propidium iodide
HSI	Hyperspectral imaging system	**pksP**	Polyketide synthase protein
R		**UV**	Ultraviolet
RT	Room temperature	**V**	
rpm	Rounds per minute	**v/v**	Volume/volume
RPMI	Roswell Park Memorial Institute medium	**V-ATPase**	Vacuolar-type H+ -ATPase
S		**ver.**	Version
SD	Standard deviation	**W**	
STS	Staurosporine	**wt**	wild-type
T		**w/v**	Weight/volume
TNF	Tumor necrosis factor		
U			

11 Publications Record and Presentations at National/International Conferences

2016	Hyperspectral imaging using intracellular spies: quantitative real-time measurement of intracellular parameters *in vivo* during interaction of the pathogenic fungus *Aspergillus fumigatus* with human monocytes. **Sara Mohebbi**, Florian Erfurth, Philipp Hennersdorf, Axel A. Brakhage & Hans Peter Saluz. PLOS ONE biology journal.2016. (in press).
2015	Hyperspectral imaging and quantitative measurement of pH *in vivo* during apoptosis using intracellular spies. **Sara Mohebbi**, Florian Erfurth, Axel Brakhage & Hans-Peter Saluz. 8th ILRS Symposium, Jena (Germany).
2014	In vivo monitoring the intracellular pH upon Aspergillus fumigatus infection in single apoptotic human monocytes. **Sara Mohebbi**, Florian Erfurth, Axel Brakhage & Hans-Peter Saluz. Life Science Conferences, Bacteriology - 2014, Chicago (USA).
2014	In vivo monitoring the intracellular pH variation upon Aspergillus fumigatus infection in single apoptotic human monocyte. **Sara Mohebbi**, Florian Erfurth, Axel Brakhage & Hans-Peter Saluz. 7th ILRS Symposium, Jena (Germany).
2013	Hyperspectral imaging to monitor specific conditions in single Aspergills-infected apoptotic cell. **Sara Mohebbi**, Berla Nyuki, Florian Erfurth, Axel Brakhage & Hans-Peter Saluz. BIOMICROWORLD, 2013, Madrid (Spain).
2013	Spying the intracellular pH during apoptosis induction and inhibition. **Sara Mohebbi** & Hans-Peter Saluz. 6th ILRS Symposium, Jena (Germany).

12 Financial Support

The experimental work for current thesis has been performed at the Department of Cell and Molecular Biology of the Leibniz Institute for Natural Product Research and Infection Biology – Hans Knöll Institute, Jena.

This work was financially supported by the International Leibniz Research School for Microbial and Bimolecular Interactions (ILRS) as part of the excellence graduate school: Jena School for Microbial Communication (JSMC).

13 Acknowledgement

First and foremost, I offer my sincerest gratitude to my first supervisor Prof. Dr. Hans Peter Saluz, who gave me the opportunity to work on an unique research topic, provided the required facilities throughout my thesis, arranged the collaborations and secured the project with his supervision.

I am certainly thankful to my second supervisor Prof. Dr. Axel Brakhage who has supported me with his knowledge and guidance. This thesis would not have been possible without his valuable feedback and wise discussions.

My special thanks to the international Leibniz Research School (ILRS) Jena and the Leibniz Association for funding my project and providing this precious opportunity for young researchers to expand their knowledge in a high-ranking scientific environment. Also I thank Dr. Christine Vogler for her assistance whenever I asked for her help.

I owe a debt of gratitude to our collaborators in the Department of Photonics and Sensorics (GMBU) Jena, specifically Mr. Florian Erfurth who modified the microscopy hardware and walked with me through the data analysis and publishing the results.

I also would like to thank the staff of Cell and Molecular Biology Department at Hans-Knöll Institute for creating the friendly atmosphere in the lab, specially Dr. Frank Hänel for reading my dissertation and giving me helpful comments.

My residence in Jena has been truly blessed with being among my cheerful friends. I thank the crew "*Die Kühle ☺ Gruppe vom Wochenende*" for all those good laughers that made me forget about the time or troubles. Felix and Tim, I highly appreciate your companionship for editing my thesis and paper. Also I thank Lorena, Federica, Reyna, Pol, Fernando, Matthias and Beng whom I always could highly trust and share my moments with. Surely, I will have a hard time to find myself again in such a compatible circle of friends like you guys.

Last but not least, my deepest thanks go to my family and my parents. I am grateful that during all years away from home, my family members in Iran especially my aunts and uncle have been emotionally so close and distinct to me. Above all, I thank my parents for their unconditional love, endless support, patience and encouragement. You have ensured me no matter of where I live and what I do; I always can come home where you are there for me. I would like to thank Arman for his love, friendship and help to complete my thesis and for standing by me to grow up together.

14 Curriculum Vitae

Career

2012-2016 PhD student and research fellow at Leibniz Institute for natural product resarch and infection biology- Hans -knöl-institute, HKI, Department of cell and molecular biology

2011-2012 Laboratory assistant at Marin biology/Department of Ecology and Evolution, Uppsala, Sweden

2006 – 2009 Part-time lecturer at Islamic Azad University of Rasht, Iran

2006 – 2009 Laboratory trainer on parasitology at Islamic Azad University of Rasht, Iran

2006 Translation of "Virgule Artistic Group's official web page from Persian to English

2005 Translation articles (English to Persian) on water resource management in aquaculture, Grogan University Of Agricultural Sciences And Natural Resources, Iran

2004 – 2006 Co-translation of text book: Laboratory Exercises in Microbiology by Robert A Polack et al.

Education

2012-2016 Measuring intercellular pH during the apoptosis induction and inhibition upon *Aspergillus fumigatus* infection (PhD project, Hans-knöll institute (HKI), Jena, Germany

2009 – 2011 Biology Diploma (MSc), Institutionen för biologisk grundutbildning (IBG) , Uppsala Universitet, Sweden

2011 Placement at Evolutionary Biology Center (EBC) for "*Sexually Antagonistic Fitness Variation*" Master thesis project, Uppsala, Sweden

2011 Placement at Evolutionary Biology Center (EBC) for "*The Genetic variation for sex-specific fitness in the fruit-fly Drosophila Melanogaster*" Research training project, Uppsala Sweden

2010 Placement at Rudbeck Department for Advanced techniques in Molecular Medicine, Uppsala, Sweden

2010 Placement at Angstrom Department for Molecular biotechnology for renewable sources, Uppsala , Sweden

2006 Training in Medical Microbiology Laboratory, Iran university of Medical Science, Tehran, Iran

2004-2006 Microbiology Diploma (MSc.), Azad University, Science and Researches Campus, Tehran, Iran (GPA out of 5: 4)

2003 *Microsoft Certified Systems Engineer* degree (MCSE), Tehran Institute of Technology, Rasht branch, Iran

2002 Microbiology Diploma, Lahijan, Iran.

Course Participation (With certification)

Scientific image processing and analysis, February 2015, Biovoxxel, Jena, Germany
Gene Technology, Biosafty and biosecurity, November 2013, Hannover, Germany
Fundamentals of mass spectrometr, July 2013, Maxplanc institute, Jena, Germany
Bioluminescent Reporter Gene Assay, December 2012, Jena, Germany
Image-based Systems Biology, September 2012, Jena, Germany

Publications

Hyperspectral imaging using intracellular spies: quantitative real-time measurement of intracellular parameters *in vivo* during interaction of the pathogenic fungus *Aspergillus fumigatus* with human monocytes. **Sara Mohebbi** ,Florian Erfurth, Philipp Hennersdorf, Axel A. Brakhage & Hans Peter Saluz, (2016). (PLOS ONE journal, in press).

Measuring the effect of inbreeding on reproductive success in a population of fruit flies (Raleigh lines), Master Thesis. **Sara Mohebbi**, (2012). Biology and Evolutionary Biology Center, Department of animal ecology, Uppsala University. Sweden.

Survey Genes And Species Of Non- Fermentative Gram Negative Bacilli Isolated From Hospitalized Patients, **Sara Mohebbi**, (2009). Master Thesis. Azad university, Science and research campus, Tehran, Iran.

Survey Genes And Species Of Non- Fermentative Gram Negative Bacilli Isolated From Hospitalized Patients . Noor Amir Mozafari, Homa Frouzesh Tehrani , **Sara Mohebbi**. Journal of Guilan University of Medical Science. Iran. 2008; 16(64):67-75.

Laboratory Exercises in Microbiology. Robert A. Polack, Lorraine Findlay, Walter Mondschein, R. Ronald Modesto, (2002). Translated by: Masoomeh Anvari, **Sara Mohebbi**, Ali Rafizadeh
Publisher: Azad University, Rasht branch. 2004. ISBN: 964-95210-3-8

15 Declaration of Independent Assignment

I declare in accordance with the conferral of the degree of doctor from the Faculty of Biology and Pharmacy of the Friedrich Schiller University, Jena, that the submitted thesis is written independently and only with the assistance and literature cited in the text.

This thesis has not been previously submitted either to the Friedrich Schiller University Jena or to any other university.

Jena, April 2016 **……**

Sara Mohebbi